Programa de Doctorado en Electrónica:

Sistemas Electrónicos Avanzados. Sistemas Inteligentes

ACTIVIDAD GAMMA DEL ELECTROENCEFALOGRAMA. MÉTODOS DE ANÁLISIS CON OBJETIVOS CLÍNICOS

Tesis Doctoral

Carlos Amo Usanos

Directores:

Dr. Luciano Boquete Vázquez

Dr. Rafael Barea Navarro

Alcalá de Henares, 2021

Resumen

Objetivos: El objetivo general de la presente tesis doctoral ha sido investigar la identificación de la actividad gamma [30-90 Hz] del electroencefalograma (EEG) utilizando un sistema monocanal, para posibles aplicaciones clínicas.

Métodos: Se ha obtenido la actividad gamma del EEG de las áreas motoras de la corteza cerebral en 25 sujetos sanos, con movimiento real e imaginario. Se analiza la señal mediante un método no lineal que utiliza transformaciones tiempo-frecuencia con wavelets. Posteriormente se añade un filtro, basado en la función matemática de descomposición en modo empírico (EMD: Empirical Mode Decomposition) y se comparan los resultados.

Resultados: Se identifica la actividad de la banda gamma de las áreas motoras cerebrales durante el movimiento voluntario real e imaginario. Se obtiene un método para cuantificar la plasticidad cerebral analizando la actividad gamma motora. Se demuestra que filtrando las señales EEG mediante EMD, se obtienen mejores resultados que con el análisis original de la señal.

Conclusiones: En esta tesis se demuestra que es posible obtener la actividad gamma del EEG de una forma simplificada, en relación a la adquisición y a la utilización de métodos relativamente sencillos de análisis de las señales.
Los resultados experimentales de la tesis, principalmente las variaciones de la actividad gamma de las áreas motoras cerebrales, se pueden utilizar desde un punto de vista práctico para proponer aplicaciones clínicas.

Palabras clave: Electroencefalografía, actividad gamma, áreas motoras, densidad espectral de potencia, aplicaciones clínicas, descomposición en modo empírico, plasticidad cerebral, tareas motoras reales, tareas motoras imaginarias.

Abstract

Objectives: The general objective of this doctoral thesis has been to investigate the identification of the gamma activity [30-90 Hz] of the electroencephalogram (EEG) using a single-channel system, for possible clinical applications.

Methods: EEG gamma activity was obtained from the motor areas of the cerebral cortex in 25 healthy subjects, with actual and imaginary movement. The signal is analyzed by a non-linear method that uses time-frequency transformations with wavelets. Subsequently, a filter is added, based on the empirical mode decomposition mathematical function (EMD: Empirical Mode Decomposition) and the results are compared.

Results: The gamma activity band of the cerebral motor areas is identified during the actual and imaginary voluntary movement. A method is obtained to quantify brain plasticity by analyzing gamma activity from motor areas. It is shown that filtering the EEG signals by EMD, better results are obtained than with the original analysis of the signal.

Conclusions: This thesis shows that it is possible to obtain the gamma activity of the EEG in a simplified way, in relation to the acquisition and use of relatively simple methods of signal analysis. The experimental results of the thesis, mainly the variations of the gamma activity of the cerebral motor areas, can be used from a practical point of view to propose clinical applications.

Keywords: Electroencephalography, Gamma Activity, Motor Areas, Power Spectral Density, Clinical Applications, Empirical Mode Decomposition, Brain Plasticity, Actual Motor Tasks, Imaginary Motor Tasks.

Agradecimientos

A mis directores de tesis, los catedráticos Luciano Boquete y Rafael Barea, y al Dr. Luis de Santiago por su trabajo, sus ideas y la ayuda prestada.

A todos los voluntarios participantes en los experimentos relacionados con esta tesis y a todas las personas que componen el grupo de investigación (Grupo de Ingeniería Biomédica del Departamento de Electrónica de la Universidad de Alcalá) que han colaborado en este trabajo.

Al proyecto de investigación del Ministerio de Ciencia, Innovación y Universidades: "Investigación de la técnica de potenciales evocados visuales multifocales. Aplicación en estudios de evolución de esclerosis múltiple y evaluación de medicamentos." (Ref. DPI2017-88438-R).

A la familia Rivas (de la empresa NSC Electromedicina) por su desinteresada ayuda y su eficaz apoyo técnico en el desempeño de la parte experimental de esta tesis.

A Michael Wibral, Cerisa Stawowsky, Georg-Friedrich Paasch y todo el equipo del Zentrum für Bildgebung in den Neurowissenschaften (MEG Laboratorium) des Max-Planck Institut in der Goethe Universität aus Frankfurt por sus enseñanzas y su paciencia.

In memoriam, a Felipe Quesney MD, PhD (Division of EEG and Clinical Neurophysiology, Montreal Neurological Institute, McGill University, Quebec, Canadá) que siempre creyó en la banda gamma.

Finalmente quiero agradecer a mi madre, a mis hermanos y demás familia y amigos su paciencia y apoyo prestados a lo largo de estos años de doctorado.

Preámbulo

La presente tesis doctoral, realizada en el "Programa de Doctorado en Electrónica: Sistemas Electrónicos Avanzados. Sistemas Inteligentes", del Departamento de Electrónica de la Universidad de Alcalá, se presenta bajo la modalidad de compendio de artículos. El artículo 5.4 del Reglamento de elaboración, autorización y defensa de la tesis doctoral de la Universidad de Alcalá establece que, si la Comisión Académica del Programa lo autoriza, la Tesis Doctoral podrá realizarse mediante el compendio de artículos del doctorando en publicaciones de reconocido prestigio. El número mínimo de artículos será de tres. La Tesis deberá incluir, además de los artículos, un resumen amplio que dé coherencia al conjunto de la investigación, en el que se muestre la línea argumental de la misma, así como un capítulo de conclusiones.

El "Programa de Doctorado en Electrónica: Sistemas Electrónicos Avanzados. Sistemas Inteligentes" acepta la presentación de tesis doctorales por compendio de artículos con las consideraciones recogidas en los siguientes puntos:

- Que los tres artículos estén como mínimo aceptados.
- Que el estudiante sea primer autor en todos los artículos.
- Que las publicaciones estén en el primer tercio (T1) del JCR.
- Que los artículos no sean previos a la matrícula de doctorado.

Las aportaciones realizadas se reflejan en cuatro artículos, siendo el doctorando el primer autor en todos los casos y tres de los artículos se han publicado en revistas incluidas en el primer tercio del JCR:

- "Induced Gamma-Band Activity During Voluntary Movement: EEG Analysis for Clinical Purposes", Carlos Amo Usanos, Miguel Ortiz del Castillo, Rafael Barea, Luis de Santiago, Alejandro Martínez-Arribas, Pedro Amo-López y Luciano Boquete, Motor Control, 2016, 20, 409 - 428, http://dx.doi.org/10.1123/mc.2015-0010.

  JCR año 2016: FI: 0,750. Posición: 65/81 (Q4 en el grupo de Sport Sciences). Número de citas (google citations, julio 2021): 9.

- “Induced gamma band activity from EEG as a possible index of training-related brain plasticity in motor tasks”, Carlos Amo Usanos, Luis de Santiago, Daniel Zarza Luciáñez, José Miguel León Alonso-Cortés, Miguel Alonso-Alonso, Rafael Barea, Luciano Boquete, PLoS ONE 2017, 12(10):e0186008, https://doi.org/10.1371/journal.pone.0186008.

  JCR año 2017: FI: 2,766. Posición: 15/64 (Q1 en el grupo de Multidisciplinary Sciences). Número de citas (google citations, julio 2021): 11.

- “Analysis of Gamma-Band Activity from Human EEG Using Empirical Mode Decomposition”, Carlos Amo Usanos, Luis de Santiago, Rafael Barea, Almudena López-Dorado y Luciano Boquete, Sensors 2017, 17(5), 989; https://doi.org/10.3390/s17050989

  JCR año 2017: FI: 2,475. Posición: 16/61 (Q2 en el grupo de Instruments and Instrumentation). Número de citas (google citations, julio 2021): 38.

- “Induced Gamma-Band Activity during Actual and Imaginary Movements: EEG Analysis”, Carlos Amo Usanos, Luciano Boquete, Luis de Santiago, Rafael Barea Navarro y Carlo Cavaliere, Sensors 2020, 20(6), 1545; https://doi.org/10.3390/s20061545

  JCR año 2020: FI: 3,576. Posición: 14/64 (Q1 en el grupo de Instruments and Instrumentation). Número de citas (google citations, julio 2021): 5.

Tabla de contenido

Presentación

El objetivo general de la presente tesis doctoral ha sido investigar la identificación de la actividad gamma del electroencefalograma utilizando un sistema monocanal, para posibles aplicaciones clínicas de la técnica.

Con el fin de dar coherencia al conjunto de la investigación realizada, se presenta un ***resumen*** estructurado en los siguientes capítulos:

- Introducción.
- Objetivos e Hipótesis.
- Metodología y Resultados.
- Discusión general.
- Conclusiones.
- Trabajos futuros.
- Referencias.
- Anexos (Aprobación del Comité de Ética, Artículos Publicados).

1 INTRODUCCIÓN

En este capítulo se describe brevemente el electroencefalograma (EEG) y se presentan las principales características de la denominada banda gamma del EEG. También se comenta con más detalle la actividad gamma producida en las áreas motoras cerebrales, que son el objeto de estudio de esta investigación. Por último, se describen brevemente los métodos de análisis y las dificultades técnicas de la obtención de la banda gamma mediante el EEG convencional.

1.1 ACTIVIDAD GAMMA DEL ELECTROENCEFALOGRAMA

Aspectos históricos y técnicos del EEG

La actividad eléctrica del cerebro se registra actualmente a diferentes escalas, cada una de las cuales exhibe una actividad oscilatoria correlacionada con la activación funcional. Los diferentes tipos de registros utilizados en investigación básica y en aplicaciones clínicas (Canolty and Knight, 2010) son, de menor a mayor escala:

- Los registros realizados mediante microelectrodos profundos (implantados directamente en la corteza cerebral) que detectan no solo picos de neuronas individuales, sino también actividad poblacional sincronizada como el potencial de campo local (local field potential: LFP) que refleja la actividad de varias decenas de miles de células nerviosas.
- Los registros realizados mediante el electrocorticograma subdural (ECoG) - registrado desde macroelectrodos clínicos, utilizados para detectar la actividad de varios millones de células.
- Los registros no invasivos realizados mediante el electroencefalograma (EEG) y magnetoencefalograma (MEG), que detectan a gran escala la actividad simultánea de múltiples áreas corticales.

El electroencefalograma fue descrito por primera vez en Liverpool en el siglo XIX por el médico Richard Caton, quien en sus primeros experimentos registró mediante un galvanómetro la actividad oscilatoria eléctrica del cerebro de diferentes animales (conejos, gatos y monos) (‘Forty-Third Annual Meeting of the British Medical Association’, 1875).

Desde finales del siglo XIX hasta principios del siglo XX, diferentes neurofisiólogos europeos continuaron avanzando en los registros EEG en animales (Coenen and Zayachkivska, 2013). Pero fue ya en 1929 cuando el neurólogo alemán de la Universidad de Jena, Hans Berger, obtuvo los primeros registros de electroencefalograma de humanos (Berger, 1929). El objetivo de Berger era demostrar que los campos electromagnéticos del cerebro humano podrían usarse para generar la telepatía.

Berger usó electrodos de aguja de platino, unidos en un extremo al cuero cabelludo de su hijo Klaus de 15 años, y en el otro extremo a un galvanómetro de Siemens de doble bobina. Colocó los electrodos en los polos frontal y occipital de la cabeza, registrando así amplias diferencias de voltaje que genera prácticamente todo el cerebro.

Berger también fue el primero en describir los ritmos básicos de las oscilaciones del EEG en vigilia con sus diferentes rangos de frecuencia. En particular, observó un ritmo de 8-12 Hz mientras su hijo estaba sentado, relajado y con los ojos cerrados. Dado que este fue el primer y más prominente ritmo que observó, lo llamó ritmo “alfa”.

También notó una supresión del ritmo alfa, cuando sus sujetos abrían los ojos; este ritmo alfa era reemplazado por una amplitud más baja, a una frecuencia más alta, en un rango de frecuencias de 14-30 Hz, que denominó ritmo “beta”. También reemplazó el antiguo término híbrido greco-latino "electrocerebrograma" por el nombre enteramente griego, “electroencefalograma” (Brazier, 1961). Por todos sus hallazgos se considera a Hans Berger como “*el padre de la electroencefalografía humana*” (Ahmed and Cash, 2013).

En la actualidad el EEG es una herramienta diagnóstica de uso común en todo el mundo. Se utiliza preferentemente en el ámbito de la neurología y su aplicación más frecuente es en diagnóstico de la epilepsia, dada su gran utilidad para clasificar las crisis epilépticas y localizar anatómicamente su inicio (foco epiléptico) en la corteza cerebral (Rayi and Murr, 2021). Esto permite el tratamiento quirúrgico de determinadas epilepsias refractarias al tratamiento farmacológico.

Los electrodos del EEG se colocan sobre la superficie del cuero cabelludo para medir los potenciales eléctricos generados por las neuronas de la corteza cerebral. Estos potenciales son debidos a la descarga síncrona de las células piramidales de las capas III y V (DeFelipe and Fariñas, 1992); se requieren al menos 10 cm^2 de corteza cerebral para producir una señal significativa en el registro del EEG. La señal se detecta mejor cuando un grupo de neuronas próximas se activan de forma sincrónica, o "spiking" neuronal. También se ha comprobado que la amplitud de la señal EEG aumenta cuantas más neuronas estén sincronizadas y cuanto mayor grado de sincronía presenten simultáneamente (Herrmann and Demiralp, 2005).

El equipo básico del EEG incluye electrodos (los electrodos de plata/cloruro de plata son los más utilizados), un amplificador y un sistema de adquisición, proceso de datos y visualizador de los resultados. En la práctica clínica actual, un sistema EEG estándar tiene la capacidad de obtener información de al menos 128 canales, con una frecuencia de muestreo superior a 10 kHz y con una resolución de 24 bits en cada uno de los canales. Antes de iniciar el registro debe medirse la impedancia de contacto de todos los electrodos y asegurarse de que sea inferior a 5 KΩ (Rayi and Murr, 2021).

1.2 LA ACTIVIDAD GAMMA DEL CEREBRO HUMANO

Historia

Los ritmos cerebrales son fluctuaciones de actividad eléctrica compartidas en poblaciones de neuronas, y se hacen más evidentes como fluctuaciones de voltaje extracelular. Estos ritmos surgen de la suma de la actividad eléctrica (principalmente señales de entrada o aferencias, aunque no exclusivamente) en poblaciones de neuronas, y están moldeados por la geometría y alineación de esas neuronas (Buzsaki, 2006).

Las oscilaciones rítmicas de la actividad eléctrica del cerebro humano registradas mediante el EEG se pueden dividir en cinco bandas de frecuencia diferentes; estas son nombradas mediante letras del alfabeto griego, siguiendo la nomenclatura establecida por Hans Berger en sus primeras descripciones. Las bandas de frecuencias son (Uhlhaas *et al.*, 2008):

- Delta (δ): 0–3 Hz.
- Theta (θ): 4–7 Hz.
- Alpha (α): 8–12 Hz.
- Beta (β): 13–30Hz.
- Gamma (γ): 30–200 Hz.

Dentro del rango de frecuencias de la banda gamma, se puede distinguir entre banda gamma baja [30-60 Hz] (oscilaciones de la banda gamma baja) y banda gamma alta [60-200 Hz] (oscilaciones de la banda gamma alta) (Uhlhaas *et al.*, 2011) (Combrisson *et al.*, 2017).

La primera descripción del ritmo gamma aparece en un artículo de Herbert Jasper y Howard Andrews en 1938 (Jasper and Andrews, 1938). Jasper también fue uno de los primeros en señalar explícitamente una relación entre la amplitud y la frecuencia de las distintas señales del EEG: "*Parece como regla general, la amplitud de los potenciales cerebrales disminuye con su frecuencia*" (Jasper, 1936). En los años

siguientes, cuando el análisis de Fourier se aplicó más comúnmente a las señales de EEG para generar espectros de potencia, esta disminución en la amplitud o potencia con el aumento de la frecuencia se conoció como la relación 1/f (Ahmed and Cash, 2013).

Ya en los años 80, se observó oscilación gamma en células del tracto olfatorio en respuesta a diferentes estímulos olfatorios (Freeman, 1978), (Viana Di Prisco and Freeman, 1985). Estas oscilaciones también se observaron en áreas visuales en respuesta a diferentes estímulos visuales (Gray and Singer, 1989).

Características de la banda gamma

En estudios de potencial de campo local se observa que siguiendo la relación entre la amplitud y la frecuencia de las distintas señales del EEG, las fluctuaciones gamma son las más pequeñas, aproximadamente de 10 a 20 µV de promedio en registros realizados mediante microelectrodos (esta amplitud disminuye hasta < 5 µV en el registro de EEG de superficie).

También se sabe que la potencia relativa de cada componente de frecuencia disminuye al aumentar la frecuencia, por ello la banda gamma representa solo el 0,5% - 10% de la potencia total en el LFP (Jia and Kohn, 2011).

En redes neuronales inactivas, la mayor parte de la potencia en el LFP se encuentra en frecuencias bajas, lo que indica que ritmos como delta y theta contribuyen de manera más significativa que los de alta frecuencia. Pero cuando las redes están activadas, la potencia en las frecuencias más altas (beta y gamma) aumenta, mientras que en las frecuencias más bajas se suprimen. También se ha comprobado que la potencia en la banda gamma aumenta con la intensidad del estímulo externo (input) que activa esa red neuronal (Jia and Kohn, 2011).

La actividad gamma espontánea puede ser registrada con el sujeto en reposo, sin necesidad de ninguna activación ni tarea. Además, se supone que representa un reflejo del nivel de consciencia (Herrmann and Demiralp, 2005).

Mecanismos celulares y bioquímicos

Los mecanismos celulares subyacentes responsables de las oscilaciones gamma aún no han sido completamente dilucidados, pero se cree que las interacciones recíprocas entre las neuronas piramidales excitatorias y las interneuronas inhibitorias GABAérgicas, particularmente las células en cesto (parvalbumin positive fast-spiking basket cells) probablemente desempeñan un papel clave (Cardin *et al.*, 2009). De este modo se considera a la actividad gamma como un producto de una entrada balanceada de sinapsis excitatorias e inhibitorias (Hirase *et al.*, 2014).

Desde un punto de vista bioquímico, la generación de actividad de banda gamma depende fundamentalmente de varios sistemas de neurotransmisores (GABA, noradrenalina, glutamato y acetilcolina). Las redes de neuronas GABAérgicas acopladas química y eléctricamente juegan un papel fundamental en la generación primaria de oscilaciones de alta frecuencia y sincronización local, mientras que las conexiones glutamatérgicas de mayor alcance parecen controlar su intensidad, duración y sincronización de largo alcance (Uhlhaas *et al.*, 2008).

Mecanismos fisiológicos de acción en los circuitos neuronales

Se cree que las interneuronas inhibitorias de descarga rápida (Fast-spiking inhibitory interneurons) juegan un papel fundamental en la excitación de las células piramidales en el rango de las frecuencias gamma. La descarga rítmica y sincrónica de las interneuronas proporciona a las células piramidales inhibidas periódicamente una ventana de tiempo muy estrecha para disparar una descarga (potencial de acción) en

cada ciclo, después de terminar la inhibición anterior, y justo antes de que llegue la siguiente señal de inhibición (Ahmed and Cash, 2013).

Estudios in vitro han probado que la inhibición mutua entre las neuronas inhibitorias Fast-spiking puede ser suficiente para originar las oscilaciones gamma (Wang and Buzsáki, 1996). Estas interneuronas serían estimuladas por señales externas (de otras áreas cerebrales), y a su vez inhibirían a otras interneuronas, estableciendo un circuito una vez recuperadas de su inhibición, que mantendría en ritmo de las oscilaciones gamma. Por tanto, la inhibición sincroniza los tiempos de pico de las células piramidales, dando lugar a una sincronía de banda gamma entre ambos tipos de células (Ahmed and Cash, 2013).

Se usa el término «oscilación o actividad oscilatoria» para referirse a las fluctuaciones rítmicas de los potenciales postsinápticos de un grupo neuronal (potenciales de campo local, LFP) o de una región cortical (EEG, electrocorticografía) y también al patrón de descarga rítmico de los potenciales de acción de una neurona o un grupo neuronal. La actividad oscilatoria posibilita la sincronización entre grupos neuronales de la misma área cortical o de áreas distantes entre sí que intervienen en una acción motora, tarea cognitiva o perceptiva (Artieda *et al.*, 2009).

Estas interacciones neuronales producen diferentes tipos de actividad en la banda gamma que pueden ser agrupados en las siguientes categorías: **Oscilaciones gamma espontáneas** (Spontaneous gamma oscillations), **oscilaciones gamma inducidas** (Induced gamma oscillations) y **respuestas evocadas gamma** (Evoked gamma responses) (Herrmann and Demiralp, 2005).

Las oscilaciones gamma espontáneas, corresponden a la actividad neuronal basal, que puede encontrarse en el estado de reposo, cuando no hay una actividad específica (Herrmann and Demiralp, 2005).

Por otro lado, los cambios que ocurren en relación con un estímulo o evento, pueden clasificarse como actividad inducida o actividad evocada, dependiendo de la relación de la fase de la actividad con el inicio del estímulo o evento que la producen.

Las oscilaciones gamma inducidas, presentan una fase variable en relación con el evento y por ello desaparecen con la promediación. Un ejemplo de estas oscilaciones gamma inducidas sería la actividad inducida en las áreas motoras debida al movimiento voluntario, que son objeto de esta tesis (Amo *et al.*, 2016).

Sin embargo, las oscilaciones o respuestas evocadas guardan la relación constante de fase de la respuesta con el estímulo. Por ello mediante el promediado es posible obtener estas señales. Un ejemplo de estas respuestas gamma evocadas sería la respuesta oscilatoria evocada de ≈ 40 Hz que aparece 100 ms después de un estímulo auditivo (Tallon-Baudry and Bertrand, 1999).

Distribución y funciones fisiológicas

La actividad de la banda gamma está ampliamente distribuida en todas las estructuras cerebrales además de en la retina y en el tracto olfatorio. Está mediada por los neurotransmisores GABA, glutamato y acetilcolina, y participa en varias funciones cerebrales cognitivas como la percepción, atención, memoria, conciencia, plasticidad sináptica y control motor (Uhlhaas *et al.*, 2008).

Parece ser que la actividad gamma inducida se incrementa durante las tareas complejas o que exigen atención, por ello ha sido interpretada como el substrato neuronal de los procesos cognitivos (Tallon-Baudry and Bertrand, 1999).

El ritmo gamma está modulado por información sensorial y procesos internos como la memoria de trabajo y la atención.

Un ritmo gamma prominente proporciona una certeza de redes neuronales activadas. Se ha observado actividad en la banda gamma en varias áreas corticales, así como en estructuras subcorticales, en numerosas especies. En la corteza sensorial, la potencia gamma aumenta con el impulso sensorial (Adrian, 1942) (Henrie and Shapley, 2005) y con una amplia serie de fenómenos cognitivos, incluidos el agrupamiento perceptivo (Tallon-Baudry and Bertrand, 1999) y la atención (Fries, 2001).
En la corteza superior, la potencia gamma se eleva durante la activación de la memoria de trabajo (Pesaran *et al.*, 2002) y durante el aprendizaje (Bauer, Paz and Pare, 2007).

Mecanismos de acoplamiento neuronal.

Para realizar todas sus funciones fisiológicas, los ritmos gamma están relacionados con otros ritmos para conseguir comunicación entre áreas próximas o distantes de la corteza cerebral. Los modelos de red (network) sugieren que estas conexiones se basan en interacciones con neuronas excitadoras, y que las redes locales generadoras de actividad gamma pueden acoplarse mediante conexiones horizontales de largo alcance.

La sincronización de corta distancia tiende a ocurrir a frecuencias más altas (banda gamma) que la sincronización de larga distancia, que a menudo se manifiesta no solo en rango beta, sino también en theta y alfa.

La mayoría de estos acoplamientos dependen de una relación entre la actividad inhibitoria gamma y el momento de la actividad excitatoria (de despolarización) en las neuronas cercanas.

Es importante destacar que, si bien la actividad cerebral de alta frecuencia refleja los dominios locales del procesamiento cortical, los ritmos cerebrales de baja frecuencia se propagan dinámicamente a través de las regiones cerebrales distribuidas tanto por información sensorial externa como por eventos cognitivos internos.

Diversos estudios sugieren que el acoplamiento de frecuencia cruzada (cross-frequency coupling CFC) puede desempeñar un papel funcional en la computación, la comunicación y el aprendizaje neuronales (Canolty and Knight, 2010). El fenómeno de acoplamiento de frecuencia cruzada (CFC), se refiere a un mecanismo regulador complejo formado por las interacciones entre los distintos grupos neuronales con sus diferentes frecuencias de oscilación (Canolty and Knight, 2010).

Existen diferentes variedades de CFC: Fase-fase, amplitud-amplitud y fase-amplitud. En particular, la intensidad de la CFC de fase-amplitud difiere en cada área del cerebro de una manera relevante para cada tarea, cambia rápidamente en respuesta a eventos sensoriales, motores y cognitivos y se correlaciona con el desempeño de las tareas de aprendizaje.

Por lo tanto, el CFC puede servir como un mecanismo para transferir información desde redes cerebrales a gran escala en el procesamiento cortical local rápido requerido para el cálculo efectivo y la modificación sináptica, integrando así sistemas funcionales en múltiples escalas espacio-temporales.

Hay diferentes teorías que intentan explicar este acoplamiento de frecuencias (CFC) en las redes neuronales (Jia and Kohn, 2011):

1. La actividad gamma no se propaga activamente. Es un componente de un potencial de campo extracelular (LFP) que refleja principalmente la entrada sináptica a una colección de neuronas. Debido a esto, la actividad gamma solo puede desempeñar un papel en el procesamiento si está relacionada con la actividad de picos (spiking) de manera significativa.

   Podría surgir un acoplamiento entre la actividad gamma y la temporización del pico “spiking” debido a que las neuronas inhibidoras locales, que contribuyen en gran medida a la actividad gamma, se activan preferentemente en el valle del ciclo gamma. Esto hace que sea más probable que el pico de las neuronas

de proyección excitadoras ocurra en una fase de compensación, cuando la inhibición es más débil (Hasenstaub *et al.*, 2005).

2. Las oscilaciones en la banda gamma pueden influir en la comunicación entre poblaciones neuronales. Es decir, cuando los potenciales de campo y la actividad de picos en dos grupos de neuronas son coherentes en fase, la comunicación entre ellos será máxima (Fries, 2009) (Womelsdorf *et al.*, 2007).

3. La hipótesis de "unión por sincronía" (‘binding by synchrony’’), sugiere que la actividad gamma puede vincular la representación de una única entrada sensorial (por ejemplo, un objeto visual) cuyas características son procesadas por diferentes grupos de neuronas (Singer, 1999).

Ritmos gamma en procesos patológicos. Aplicaciones clínicas

En diferentes estudios se ha observado una actividad gamma irregular en trastornos neurológicos como la enfermedad de Alzheimer, la enfermedad de Parkinson, la esquizofrenia y la epilepsia (Uhlhaas and Singer, 2006).

Estas irregularidades varían en cada patología estudiada (Herrmann and Demiralp, 2005). Incluso en sujetos sanos, la actividad gamma muestra una variación interindividual significativa que se correlaciona con los parámetros cognitivos:

- La enfermedad de Alzheimer se acompaña de una reducción de la sincronización gamma.

- En la enfermedad de Parkinson hay un aumento de la sincronía neuronal en los ganglios basales y también entre estructuras cortico-subcorticales.

- Para la esquizofrenia, está bien documentado un aumento de la actividad gamma en relación a los síntomas positivos de la enfermedad, especialmente

para las alucinaciones, y una reducción de la actividad gamma en relación a los síntomas negativos.

- En la epilepsia, se ha observado que un nivel extremadamente alto de actividad gamma puede provocar ataques epilépticos a través de la hiperexcitación de la corteza. En consecuencia, los estados con mayor actividad gamma presentan un riesgo de tales convulsiones.

Todos estos hallazgos podrían contribuir al mejor diagnóstico y seguimiento de estas patologías.

1.3 ACTIVIDAD GAMMA DE LAS ÁREAS MOTORAS CEREBRALES

En relación con la actividad motora del cerebro humano, la actividad gamma inducida ha sido observada en respuesta a estímulos sensoriales y durante tareas motoras en varios experimentos con EEG y MEG, antes o durante el movimiento voluntario. Estas oscilaciones gamma no estaban en fase con el inicio del movimiento (Tallon-Baudry and Bertrand, 1999).

Algunos estudios describen oscilaciones gamma en el rango de 40 Hz, pero otros estudios neurofisiológicos han mostrado que la actividad de la banda gamma alta en el rango de frecuencias de 30-90 Hz puede ser registrada en amplias áreas cerebrales durante el reposo o durante el desarrollo de tareas motoras (Cheyne and Ferrari, 2013).

Además, estas oscilaciones gamma relacionadas con el movimiento parecen corresponderse con la organización somatotópica de las áreas primarias sensitivo-motoras, y por ello se ha propuesto la actividad gamma como la integración de los procesos sensitivos y motores durante la preparación y el control del movimiento. También se ha observado que el mapeo de la respuesta gamma en tareas motoras

sugiere un área cortical de activación más bien restringida (Tallon-Baudry and Bertrand, 1999).

La actividad gamma también está relacionada con el movimiento imaginario. Se define como movimiento imaginario (Motor imagery), el estado dinámico del pensamiento durante el cual las representaciones de un acto motor dado se ensayan internamente en la memoria de trabajo sin ningún acto motor (Decety, 1996). En esta tarea mental (preparación del movimiento), se instruye a los sujetos para que se imaginen moviéndose sin realizar ese movimiento y sin activación muscular. La evidencia disponible indica que los movimientos reales e imaginarios comparten una superposición sustancial de circuitos funcionales comunes (Hardwick *et al.*, 2018).

En relación a la actividad gamma producida durante el movimiento imaginario, hay varios ejemplos de esta actividad registrada mediante métodos invasivos como la electrocorticografía (ECoG) (Miller *et al.*, 2010) (Leuthardt *et al.*, 2004).

Existen pocos ejemplos de experimentos que registren la actividad gamma producida durante el movimiento imaginario con EEG convencional de superficie. En ellos se ha observado que hay un aumento significativo de la potencia de la banda gamma durante el movimiento imaginario (Smith *et al.*, 2014), y que esta actividad es similar durante la preparación y la ejecución del movimiento tanto con el movimiento real como con el imaginario (Veslin *et al.*, 2019) y que están implicadas áreas sensoriales, motoras y asociativas de ambos hemisferios tanto con el movimiento real como con el imaginario (Lazurenko *et al.*, 2018).

1.4 ANÁLISIS DE LA ACTIVIDAD GAMMA

Adquisición de la señal. Problemas técnicos.

La obtención de señales en la banda gamma en registros de superficie del EEG es técnicamente muy difícil debido a que la amplitud de la señal es muy pequeña (≈ 1 µV),

mientras que el ruido de fondo basal es del orden de 0,5 µV (Ruido de fondo de la señal adquirida ≈ 0,5 µV para una impedancia (resistencia de entrada) < 10 kΩ).
Además, el ruido más común, el producido por el artefacto muscular, se superpone en el rango de las frecuencias gamma. Por ello se piensa que los cambios obtenidos en el rango de 30-100 Hz en los registros eléctricos de EEG de superficie son casi completamente debidos a artefactos de la señal del electromiograma (EMG) (Whitham *et al.*, 2008). Técnicamente, registrando en los electrodos centrales del EEG (Fz, Cz, Pz, Oz) y en el rango inferior de frecuencias gamma (30 – 45 Hz), el artefacto de EMG es lo suficientemente bajo como para poder detectar actividad gamma en forma de cambios significativos en el EEG convencional (Whitham *et al.*, 2008).

Por ello, en el experimento de esta tesis sólo utilizamos datos del canal Cz por ser el electrodo más libre de artefacto EMG (Fitzgibbon *et al.*, 2013) (Whitham *et al.*, 2008).

Hasta hace unos años, la limitación técnica del ruido y los artefactos de registro, había impedido que se obtuvieran resultados concluyentes para el diagnóstico de patologías analizando la banda gamma. Sin embargo, debido al avance de los sistemas de captura de registros (electrodos, amplificadores,…) y especialmente a los avances en el procesado de señales mediante algoritmos matemáticos novedosos (filtrado, separación de componentes independientes, procesado tiempo-frecuencia, etc.), actualmente es posible analizar la actividad gamma con resultados más concluyentes.

Adquisición de la señal. Requerimientos técnicos.

Para registrar oscilaciones de frecuencias de hasta 80 Hz, el filtro anti-aliasing (paso bajo) del hardware de adquisición debe establecerse en un valor superior, es decir, 100 Hz. Esto al mismo tiempo requiere una frecuencia de muestreo de al menos 200 Hz (como mínimo del doble de la frecuencia máxima registrada, como establece el teorema de muestreo de Nyquist). La resolución de amplitud del amplificador debe

establecerse en valores inferiores a las diferencias que se van a resolver, es decir, por debajo de 0,1 mV si es posible (Herrmann and Demiralp, 2005).

Hay que tener en cuenta el entorno para el registro del EEG, porque las tomas de corriente, monitores y lámparas de techo, funcionan con corriente alterna (AC), que oscila a 50 Hz. Una cámara blindada eléctricamente (jaula de Faraday) puede reducir la cantidad de energía que inducen estos campos en los cables del EEG.
Solamente se deben utilizar dispositivos que funcionen con baterías. Incluso el amplificador de EEG debe funcionar con baterías recargables en lugar de adaptadores de alimentación de AC (convertidores AC/DC) que producen oscilaciones residuales de la línea de alimentación (Herrmann and Demiralp, 2005).

Adquisición de la señal. Actividad gamma basal

La actividad gamma basal, también denominada de reposo o espontánea, se puede registrar durante la vigilia con los ojos abiertos o cerrados, estando el sujeto en reposo, sin realizar ninguna de tarea en ese momento. Esta actividad supone una pequeña fracción (0,5 - 10%) de la potencia total de la señal EEG/MEG (Jia and Kohn, 2011) y puede ser explicada por interacciones sinápticas resonantes tálamo-corticales. Además, se supone que representa un reflejo del nivel de consciencia (Herrmann and Demiralp, 2005).

Para la obtención de actividad basal el trazado EEG generalmente se separa en épocas de 1 segundo, que luego se transforman en el dominio de frecuencia mediante una transformada de Fourier u otros métodos matemáticos. Normalmente, esto produce una resolución de frecuencia de 1 Hz. Los espectros de frecuencia múltiple de tales ventanas de 1 s se pueden promediar después de la transformación (Herrmann and Demiralp, 2005).

Adquisición de la señal. Actividad gamma inducida.

Para obtener una respuesta gamma provocada o inducida por un estímulo, es necesario asignar una tarea a los pacientes. La actividad gamma inducida, es decir, relacionada con el estímulo sólo alcanza un pico brevemente después de la estimulación. Es este caso hay que dividir el trazado adquirido en épocas, cuyo inicio se corresponde con el trigger o señal de disparo del estímulo utilizado. Las épocas individuales se transforman primero en el dominio de frecuencia mediante una transformada de Fourier rápida o utilizando modelos de ondas pequeñas (de baja amplitud y alta frecuencia) denominadas "wavelets" y después se promedian las magnitudes de la transformación (los valores de densidad espectral de potencia). Los resultados se expresan habitualmente en representaciones de tiempo-frecuencia. Debido a la pequeña amplitud de las respuestas gamma evocadas e inducidas, preferiblemente se deben promediar más de 100 ensayos (Herrmann and Demiralp, 2005).

Adquisición de la señal. Experimento.

En esta tesis se estudia la actividad gamma espontánea y la inducida a través de tareas motoras. La actividad gamma inducida ha sido interpretada como un elemento integrador de la información sensorial y de la actividad motora. Pero hay evidencias de que ambas, espontánea e inducida, pueden estar generadas por los mismos circuitos neuronales (Herrmann and Demiralp, 2005). Por ello en nuestro estudio, estaría justificado comparar las oscilaciones gamma espontáneas (basal) e inducidas (actividad motora), porque de esta forma podemos comparar el funcionamiento de las mismas áreas corticales del cerebro tanto en reposo como durante el movimiento. Dicha comparación es uno de los objetivos de esta tesis.

Procesado de la señal. Bases

Los registros de actividad gamma tienen una pobre relación señal a ruido, debido a su baja amplitud en comparación con otras bandas de frecuencia, otras señales fisiológicas y al ruido electrónico (interferencias). La amplitud del ruido puede ser mayor que la amplitud de la señal y la información queda enmascarada. Por ello requieren métodos especiales de análisis.

Durante los procesos sensoriales, cognitivos y motores se pueden producir dos tipos de cambios en la actividad eléctrica de la corteza cerebral: el primero es la **actividad evocada**, la cual está asociada al estímulo en tiempo y fase (time-and phase locked). Esta actividad evocada puede ser extraída de la actividad de fondo del EEG mediante métodos lineales como la promediación. El segundo cambio es la **actividad inducida**, que está asociada al estímulo en tiempo pero no en fase (time-locked but non phase-locked). La actividad inducida solo puede ser extraída de la actividad de fondo del EEG mediante métodos no lineales como el análisis espectral de potencia (power spectral analysis).

Estos métodos no lineales utilizan transformaciones tiempo-frecuencia (por ejemplo Morlet wavelets o Trasformada de Fourier de tiempo reducido) sobre cada trial de forma individual antes de promediar todos los trials (Tan, Lana and Uhlhaas, 2013).

Procesado de la señal. Experimento

En este estudio se obtuvo la actividad gamma inducida y se expresó en términos de densidad espectral de potencia (DEP, power spectrum density (PSD)) para un rango de frecuencia determinado [30-90 Hz].

También se cuantificaron las variaciones de la actividad gamma inducida mediante la tarea motora (gamma motora) en relación a la actividad cortical basal (gamma basal).

Los incrementos de la actividad gamma motora con respecto a la basal, son denominados event-related synchronization (ERS). La ERS, puede considerarse debida a cambios en la sincronía de las poblaciones neuronales subyacentes (Pfurtscheller and Lopes da Silva, 1999).

Para el análisis tiempo-frecuencia de señales de EEG, en el caso concreto de esta tesis, se utilizó el modelo de descomposición de wavelets.

El problema de la cuantificación de la actividad gamma es que dado su pequeña amplitud y su mala relación señal/ruido, no se puede cuantificar con los métodos clásicos de análisis en frecuencia como la trasformada de Fourier. Tampoco se puede dividir la señal en intervalos y promediarla porque ni las ondas gamma de la actividad basal ni las de la actividad inducida están en fase y se perdería la información.

Por lo tanto se precisa dividir la señal en intervalos o ventanas de un tiempo T, y extraer de cada uno de ellos la información espectral de los componentes de frecuencia y posteriormente promediar esos valores de frecuencia.

2 OBJETIVOS E HIPÓTESIS

2.1 OBJETIVOS

El objetivo general de la presente tesis doctoral ha sido investigar la identificación de la actividad gamma del electroencefalograma utilizando un sistema monocanal, para posibles aplicaciones clínicas de la técnica.

Se señalan dos sub-objetivos, el primero relativo a la aplicación clínica y en investigación y el segundo relacionado con el procesamiento de los registros:

- Objetivo de aplicación clínica e investigación: Obtener un método sencillo de adquisición y análisis de la señal EEG en la banda gamma para la práctica clínica habitual. Se plantean varios ejemplos como la actividad de la banda gamma en áreas motoras durante el movimiento real e imaginario y el análisis de la plasticidad cerebral.
- Objetivo de análisis de la señal. Comparar los resultados de dos métodos de análisis: usando la transformada wavelet directamente y utilizando la misma transformada agregando un filtro, basado en la función matemática de descomposición en modo empírico (EMD).

2.2 HIPÓTESIS

Se plantean dos hipótesis en función de los objetivos:

- Se puede obtener la actividad en la banda gamma inducida en la corteza motora, mediante el EEG, utilizando un método sencillo de adquisición y procesamiento de los registros.

- Mediante técnicas avanzadas de tratamiento digital de la señal, es posible disponer de alternativas que mejoran los resultados originales.

3 METODOLOGÍA Y RESULTADOS

Tanto la metodología como los resultados de esta tesis quedan expuestos en el conjunto de los cuatro artículos publicados:

1. Amo C, Del Castillo MO, Barea R, de Santiago L, Martínez-Arribas A, Amo-López P, Boquete L. Induced Gamma-Band Activity During Voluntary Movement: EEG Analysis for Clinical Purposes. **Motor Control 2016** Oct;20(4):409-28. doi: 10.1123/mc.2015-0010. Epub 2016 Aug 19. PMID: 26284500.

2. Amo C, de Santiago L, Barea R, López-Dorado A, Boquete L. Analysis of Gamma-Band Activity from Human EEG Using Empirical Mode Decomposition. **Sensors (Basel) 2017** Apr 29;17(5):989. doi: 10.3390/s17050989. PMID: 28468250; PMCID: PMC5469342.

3. Amo C, De Santiago L, Zarza Luciáñez D, León Alonso-Cortés JM, Alonso-Alonso M, Barea R, Boquete L. Induced gamma band activity from EEG as a possible index of training-related brain plasticity in motor tasks. **PLoS One 2017** Oct 5;12(10):e0186008. doi: 10.1371/journal.pone.0186008. PMID: 28982173; PMCID: PMC5628939.

4. Amo Usanos C, Boquete L, de Santiago L, Barea Navarro R, Cavaliere C. Induced Gamma-Band Activity during Actual and Imaginary Movements: EEG Analysis. **Sensors (Basel) 2020** Mar 11;20(6):1545. doi: 10.3390/s20061545. PMID: 32168747; PMCID: PMC7146111.

3.1 ASPECTOS COMUNES AL TRABAJO REALIZADO

Los experimentos realizados en esta tesis han sido autorizados por el Comité de Ética de Investigación y Experimentación Animal (CEI-EA) de la Universidad de Alcalá, con fecha de 22 de abril de 2013 (Código CEI: 2013/013/20130422).

Muestra

En la parte experimental participaron 31 sujetos de los cuales 6 fueron excluidos durante el análisis de los datos (usando la función FieldTrip ft_RejectArtifact) debido a la presencia de un alto número de artefactos en el registro EEG (parpadeo, artefacto de músculo, etc.). Todos los sujetos de la muestra eran sanos, sin enfermedad médica, neurológica (incluido traumatismo craneoencefálico y epilepsia) ni psiquiátrica.

Ninguno de ellos tomaba medicamentos ni tenía antecedentes de abuso o dependencia de alcohol o tóxicos. Antes del inicio del experimento se requirió a los sujetos participantes la firma de un consentimiento informado.

Finalmente fueron incluidos en el estudio 25 sujetos, 9 mujeres y 16 hombres (edad media= 25,16 años, rango = 18-47). Los sujetos fueron clasificados según la escala Edinburgh Handedness Inventory (EHI) de lateralidad manual (Oldfield, 1971) resultando 19 diestros (EHI medio = 79,47), 3 zurdos (EHI medio = -73,33) y 3 ambidiestros (EHI medio = 20,00).

Adquisición de señales

En el experimento se utilizó un equipo de EEG Micromed de 32 canales modelo Handy EEG SD32 y el software de adquisición SystemPlus Evolution (Micromed SpA, Treviso, Italy). Las condiciones de registro fueron las siguientes: conversor A/D: 22 bits sigma-delta, frecuencia de muestreo (Fs) de 2048 Hz, filtros antisolapamiento paso banda de 0,15 a 537,53 Hz y un filtro notch de 50 Hz e impedancias de los electrodos menores

de 10 kΩ (que aseguran que el ruido de fondo de la señal adquirida es < 0,5 µV). Se utilizaron 3 canales de EEG, 2 de electrooculograma (EOG) y 2 de electromiograma (EMG).

El EEG (canales C3, C4 y Cz) fue registrado en modo continuo utilizando un gorro elástico con electrodos de Ag/AgCl situados según el sistema 10/20. Los canales FPz y Pz fueron referencia y tierra respectivamente.

El electrooculograma fue registrado para monitorizar los movimientos oculares verticales y horizontales, mediante un electrodo situado por encima del canto ocular externo del ojo derecho y otro por debajo del canto ocular externo del ojo izquierdo.

La señal de EMG se obtuvo mediante dos electrodos de superficie (uno activo y otro de referencia) situados en cada uno de los antebrazos sobre el músculo extensor radial largo del carpo (extensor carpi radialis).

Durante todos los registros se apagaron las luces del laboratorio y se utilizaron baterías recargables para el equipo de adquisición.

Experimento

Los participantes se sentaron en una silla, en situación cómoda y delante de una pantalla de ordenador (distancia: 0,8 metros) con las palmas de ambas manos reposando hacia abajo sobre una mesa.

El experimento se ha dividido en dos partes, realizadas en la misma sesión por cada participante.

Primera parte (actividad basal): cada participante mantenía sus ojos abiertos y la mirada fija en el centro de la pantalla del ordenador durante 18 minutos, con el fin de registrar su actividad basal, en tres segmentos de 6 minutos cada uno, con un

descanso entre ellos de 1 minuto aproximadamente. El objetivo era obtener las oscilaciones gamma espontáneas (actividad basal).

Segunda parte (experimento motor): Los participantes realizaban una actividad motora (real o imaginaria dependiendo del experimento) después de recibir un estímulo en la pantalla del ordenador, lo que permitía obtener la actividad gamma inducida a partir de los registros de EEG.

La actividad motora consistió en flexionar la muñeca. Los voluntarios fueron entrenados previamente en esta actividad antes del experimento. Durante el ejercicio, mantenían la vista fija en el centro de la pantalla para evitar movimientos oculares y minimizar el parpadeo y en definitiva, evitar otros movimientos diferentes al movimiento de sus manos.

Cada trial se iniciaba visualizando en el centro de la pantalla (150 ms) una cruz y el movimiento duraba aproximadamente 2 segundos. A continuación la pantalla quedaba en negro hasta el inicio del siguiente trial. Por cada mano se realizaron 5 runs, cada uno de 100 trials. Se alternaban los runs de la mano derecha y de la mano izquierda para prevenir la fatiga muscular. La duración total de la actividad motora era aproximadamente de 40 minutos, tanto en la actividad imaginaria como en la real.

En primer lugar se realizó la actividad motora imaginaria y después de un descanso de aproximadamente 30 minutos, la actividad motora real.

Análisis de las señales

Las señales de EEG, EMG y EOG fueron analizadas offline utilizando el programa Matlab 2009b (The MathWorks Inc. Natick, MA, USA https://es.mathworks.com/) y el software específico de análisis para señales de EEG y MEG FieldTrip (Oostenveld *et al.*, 2011) (https://www.fieldtriptoolbox.org/), trabajando con datos en formato EDF (European Data Format).

En primer lugar se fraccionó la señal de cada run (adquirida en modo continuo) en 100 trials de 2 segundos de duración a partir de los triggers correspondientes a cada señal de inicio del trial (cue).

Para el análisis de la señal de EEG se utilizó un filtro paso banda (1 Hz, 100 Hz) y un filtro notch (banda eliminada 49-51 Hz). Mediante la función ft_RejectArtifact de FieldTrip se eliminaron los trials que contenían artefactos de EMG y EOG, utilizando los parámetros estándar de la función y los filtros correspondientes (EMG 30-100 Hz, EOG: 1-70 Hz).

Posteriormente se realiza la inspección de cada trial visualmente utilizando la función ft_RejectVisual de FieldTrip con el fin de eliminar saltos de amplitud, parpadeo y artefactos musculares no suprimidos previamente en el análisis automático (ft_RejectArtifact). El último paso del pre-procesamiento de las señales consiste en la eliminación del error de tendencia lineal (Linear trend) (función ft_Detrend de FieldTrip).

Después de estos pasos de procesado resulta la señal “limpia” para obtener mediante diferentes rutinas de análisis automático (Matlab) los diferentes parámetros EMG y EEG necesarios para el método diagnóstico propuesto.

El análisis de frecuencias (30-90Hz) se realizó mediante la función ft_freqanalisys de Fieldtrip basada en multitapers (multi-taper FFT). La función utiliza una ventana de tiempo deslizante para la que se calcula la potencia para una frecuencia determinada. Antes de calcular la potencia mediante transformadas discretas de Fourier, a los datos (x(t)) se les aplica la convolución con multitapers (wavelets). Se pueden usar varios tapers ortogonales para cada ventana de tiempo. La potencia se calcula para cada segmento de datos correspondiente a un taper. Los datos finales de actividad gamma se obtienen promediando los valores de cada ventana temporal.

Los resultados fueron expresados para cada banda de frecuencias como el valor medio de la densidad espectral de potencia (DEP) en (μV^2) ya que la DEP refleja la amplitud de las oscilaciones neuronales calculadas mediante las trasformaciones tiempo-frecuencia (Uhlhaas and Singer, 2013).

En el caso concreto del análisis con EMD, antes de realizar el análisis de frecuencias, se descompuso la señal "limpia" en las diferentes funciones de modo intrínseco (IMFs) mediante el programa Matlab 2009b.

3.2 RESUMEN DE CADA UNO DE LOS ARTÍCULOS

Actividad en la banda Gamma inducida durante el movimiento voluntario: Análisis EEG para aplicaciones clínicas.

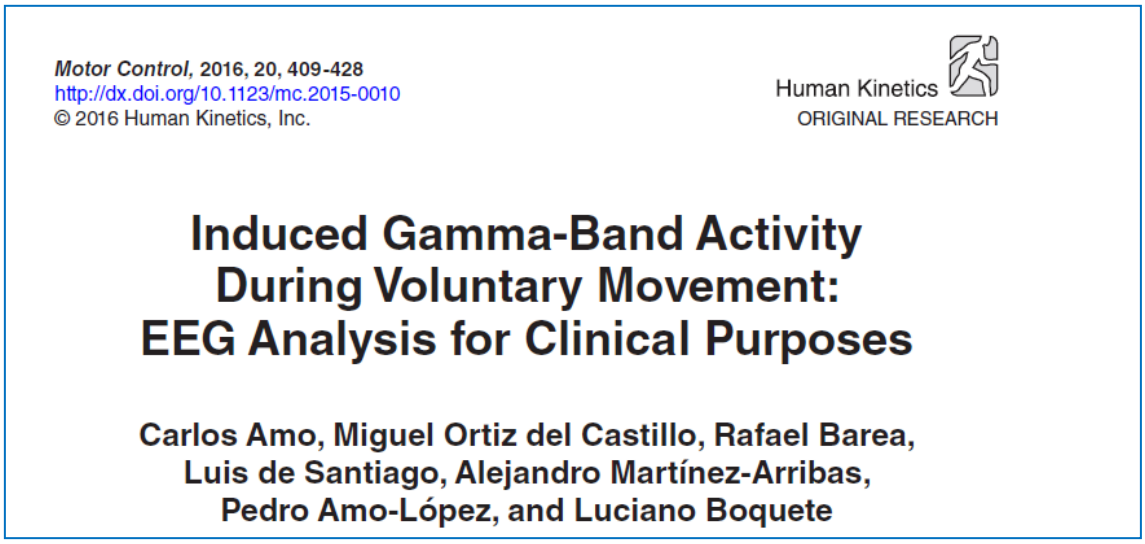

En este trabajo, publicado en la revista Motor Control en 2016, se expone principalmente la metodología básica utilizada para la obtención de la banda gamma de las áreas motoras cerebrales durante el movimiento voluntario. También se calcula la actividad gamma motora en 25 sujetos sanos.

En este primer artículo se explica la metodología de manera muy detallada porque tanto las tareas motoras como los métodos de adquisición y de análisis de la señal EEG son aplicables a los cuatro artículos de la tesis.

Objetivos: El objetivo de este estudio es proponer un método simplificado basado en el EEG aplicable en la práctica clínica cotidiana, que sirva para evaluar la actividad de la banda gamma (GBA) inducida en áreas motoras cerebrales en el rango de frecuencias de [30-90 Hz].

Este método diagnóstico debe ser sencillo en su ejecución tanto para el examinador como para el paciente, aplicable en la práctica clínica cotidiana, eficaz en el análisis de los datos y obtención de los resultados, y útil para la valoración de la patología de las áreas corticales motoras. Por supuesto debe ser no invasivo, barato y disponible en cualquier centro médico. Para ello utilizamos el EEG, que tiene una distribución prácticamente universal.

Métodos: Se registró mediante EEG la actividad cerebral de 25 voluntarios sanos, tanto de la actividad basal como durante una tarea motora. A partir de la señal EEG se obtuvo la actividad de la banda gamma (GBA) como densidad espectral de potencia (PSD) para las bandas de frecuencia (30-60Hz, 60-90Hz, 30-90Hz) y fueron calculadas con multi-taper FFT, utilizando ft_freqanalysis del programa FieldTrip.
La GBA fue definida como event-related synchronization (ERS) y fue calculada a partir de los valores de PSD de la GBA basal y la GBA obtenida durante el movimiento.

Resultados: Los valores medios del ERS fueron del 30% para la mano derecha y del 22% para la mano izquierda. La lateralidad manual se correlacionó con los incrementos de la ERS.

Conclusión: Los valores de ERS de la banda gamma del EEG obtenidos durante la actividad motora en sujetos sanos proporcionan una forma útil de comprobar indirectamente el funcionamiento de los circuitos neuronales motores al ser activados. Este método podría aplicarse en el diagnóstico de patologías de las áreas motoras y en el seguimiento de los procesos de rehabilitación. Del mismo modo, la GBA podría permitir la evaluación de la capacidad motora, el entrenamiento físico y la lateralidad manual en medicina deportiva.

Análisis de la actividad de la banda gamma del EEG en humanos utilizando descomposición en modo empírico (EMD)

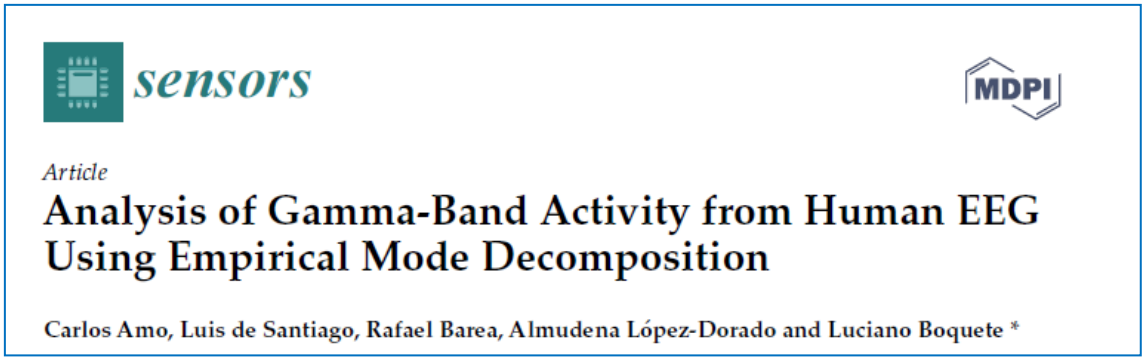

La motivación principal de este trabajo ha sido investigar la eficacia de procesar la señal de EEG mediante un filtro basado en la descomposición en modo empírico para mejorar la capacidad de detección de la actividad en la banda gamma.

Objetivos: El propósito de este artículo es determinar si la detección de actividad de banda gamma mejora cuando se agrega un filtro, basado en la función matemática de descomposición en modo empírico (EMD), al bloque de preprocesamiento de señales de electroencefalografía monocanal (EEG). Para ello se utilizan como ejemplo las señales de EEG obtenidas en el experimento inicial del artículo primero *"Actividad en la banda Gamma inducida durante el movimiento voluntario: Análisis EEG para aplicaciones clínicas".*

Métodos: EMD descompone la señal original EEG de los 25 sujetos de control en un número finito de funciones de modo intrínseco (IMF).
Posteriormente se realizó un reanálisis de las señales IMF obtenidas con el fin de obtener la actividad gamma con el mismo procedimiento que las del experimento del artículo inicial, calculando la densidad del espectro de potencia en el rango de 30 a 60 Hz y la ERS (event-related synchronization).

Resultados: Para evaluar el rendimiento del nuevo método basado en EMD, se calculó ERS a partir de la señal básica del experimento original (sin aplicar EMD) y a partir de

las IMF (obtenidas aplicando EMD). El ERS obtenido con IMF mejora, del 31,00% al 73,86%, del ERS original para la mano derecha y del 22,17% al 47,69% para la mano izquierda.

Conclusión: La aplicación del filtro de descomposición en modo empírico (EMD) mejora la capacidad de detección de la actividad de la banda gamma con respecto al método simple sin filtro. El análisis de la actividad gamma aplicando EMD podría mejorar la evaluación funcional de la corteza motora. A medida que se mejore el procesamiento de EEG, se podrían expandir las aplicaciones clínicas de la actividad de la banda gamma.

Actividad de la banda gamma del EEG inducida como un posible índice de plasticidad cerebral relacionada con el movimiento en tareas motoras

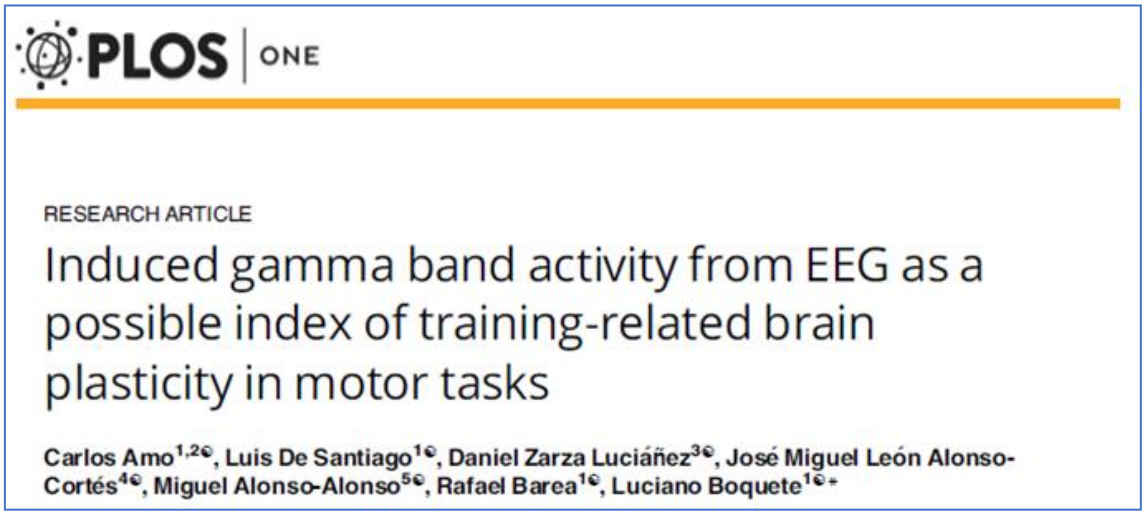
PLOS ONE

RESEARCH ARTICLE

Induced gamma band activity from EEG as a possible index of training-related brain plasticity in motor tasks

Carlos Amo[1,2☯], Luis De Santiago[1☯], Daniel Zarza Luciáñez[3☯], José Miguel León Alonso-Cortés[4☯], Miguel Alonso-Alonso[5☯], Rafael Barea[1☯], Luciano Boquete[1☯*]

En este estudio se expone una posible aplicación de la obtención de la actividad gamma EEG en las áreas motoras. Se calcula un índice de plasticidad cerebral comparando la actividad gamma obtenida al principio y al final de cada tarea motora.

Objetivo: El objetivo de este estudio es proponer un método eficaz para cuantificar los efectos del entrenamiento físico en la práctica deportiva habitual midiendo los cambios plásticos de la corteza cerebral.

Métodos: Muestra (16 sujetos sanos). Registro EEG de la actividad cerebral de la banda gamma (GBA, 30-60 Hz) obtenida como la densidad espectral de potencia (DEP) en reposo (basal) y durante una tarea motora. Se define el índice de plasticidad (IP) como la relación entre la GBA al final de la tarea motora (GBAm_fin), dividida por la GBA al inicio (GBAm_ini) para los movimientos de ambas manos.

Resultados: Se obtiene un incremento significativo ($p < 0,05$) de la GBA final comparada con la GBA inicial en ambas manos para la tarea motora (GBAm_fin > GBAm_ini), mientras que no hay diferencias significativas en la GBA basal (GBAb_fin ≈

GBAb_ini). Además se puede establecer una correlación positiva (r = 0,624) y significativa (p < 0,01) del IP con la lateralidad manual de los sujetos.

Conclusión: El parámetro IP podría medir de forma indirecta pero objetiva la plasticidad cerebral asociada al entrenamiento físico, así como la lateralidad manual en cada individuo. El IP puede tener utilidad tanto en el entrenamiento físico y en la medicina deportiva como en el diagnóstico de la patología de las áreas cerebrales motoras, así como en el seguimiento de los procesos de rehabilitación tras una lesión traumática o vascular.

Actividad gamma inducida durante el movimiento real e imaginario: Análisis de EEG

En este artículo se propone otra posible aplicación de la obtención de la actividad gamma EEG en las áreas motoras. En esta ocasión se comparan los resultados obtenidos en el artículo tercero con los obtenidos en otra tarea motora consistente en realizar movimientos imaginarios generados en las áreas premotoras de la corteza frontal.

Objetivo: Detectar y analizar la actividad de la banda gamma (GBA) inducida en áreas motoras cerebrales en el rango de frecuencias de [30-60 Hz] durante el movimiento imaginario y su compararlo con la actividad obtenida en las mismas áreas durante el movimiento real.

Métodos: Registro de EEG (12 sujetos sanos) de la actividad cerebral (basal, tarea motora imaginaria y tarea motora real). La GBA se obtuvo como densidad espectral de potencia (PSD). La GBA definida como event related synchronization (ERS) fue calculada a partir de los valores de PSD de la GBA basal (GBA_B) y la GBA del movimiento imaginario (GBA_{IM}) y del movimiento real (GBA_{RE}).

Resultados: Los valores medios de GBA durante el movimiento imaginario y el movimiento real (G_{IM} = 0,0180 μV^2, G_{RE} = 0,0185 μV^2) no presentan diferencias significativas ($p > 0,01$).

Los valores medios del ERS del movimiento imaginario (ERS_{IM} = 1,25) y del movimiento real (ERS_{RE} = 1,27) no presentan diferencias significativas ($p > 0,01$).

Conclusión: Se ha obtenido GBA de movimiento imaginario con un registro EEG simplificado y fácil de llevar a la práctica clínica. El ERS podría proporcionar una forma útil de comprobar indirectamente el funcionamiento de los circuitos neuronales motores al ser activados mediante el movimiento voluntario, tanto imaginario (ERS_{IM}) como real (ERS_{RE}). Esta información podría aplicarse en un futuro en el estudio de la fisiología y en el diagnóstico de la patología de las áreas motoras.

4 DISCUSIÓN GENERAL

En esta tesis se ha descrito un método sencillo y eficaz de adquisición de la señal EEG en el rango de la banda gamma [30 – 90 Hz] y análisis de la señal obtenida mediante un método no lineal que utiliza transformaciones tiempo-frecuencia. Y en segundo lugar se evidencia el método mediante un experimento capaz de analizar la actividad gamma de la corteza cerebral motora y proponer diversas aplicaciones clínicas.

En cuanto a la metodología utilizada, se pueden destacar las siguientes observaciones:

- El registro mediante EEG convencional de la actividad gamma proporciona una reducida relación señal-ruido (SNR) que hace que la adquisición en la práctica clínica sea difícil y no siempre posible. Una alternativa para obtener la actividad gamma de forma no invasiva sería la adquisición con un equipo de MEG (Magnetoencefalografía) que mejoraría notablemente la SNR. Pero el hecho de que la MEG sea una técnica demasiado cara y muy poco disponible en hospitales y centros sanitarios, la alejan de su uso clínico en la actualidad.

- Nuestra muestra es muy reducida y no está homogéneamente distribuida en nuestro experimento, ni en edad (rango: 18-47), ni en lateralidad manual (19 diestros, 3 zurdos, 3 ambidiestros). Sería necesario introducir sujetos de más edad y equilibrar el número de zurdos y ambidiestros.

- Dadas las dificultades técnicas de la adquisición de la actividad gamma con EEG de superficie, en el experimento de esta tesis sólo utilizamos datos del canal Cz por ser el electrodo más libre de artefacto EMG (Fitzgibbon *et al.*, 2013) (Whitham *et al.*, 2008). Además, durante todos los registros se apagaron las luces del laboratorio para evitar interferencias inducidas por la corriente alterna, y se utilizaron baterías recargables para el equipo de adquisición.

En cuanto a los resultados:

- En el primer experimento (Amo et al., 2016) se demostró que es posible obtener valores de actividad gamma de la corteza cerebral motora (frontal) inducidos por el movimiento voluntario. Los resultados obtenidos en este primer experimento son equiparables cuantitativamente a los de otros experimentos similares publicados previamente. Se observó un incremento de ≈ 27% de actividad gamma inducida por el movimiento en relación a la actividad gamma basal. Mientras que en los estudios publicados previamente se obtuvieron valores entre el 10 y el 20% de incremento (Shibata *et al.*, 1999) (Ball *et al.*, 2008).

- En el segundo experimento (Amo, de Santiago, *et al.*, 2017) se comprobó que la detección de la actividad de banda gamma mejora cuando se agrega un filtro, basado en la descomposición en modo empírico (EMD), al bloque de preprocesamiento de señales de EEG monocanal. En este caso, el incremento de actividad gamma inducida por el movimiento (ERS, Event-Related Synchronization) mejora desde una media ≈ 27%, hasta ≈ 60%, es decir, mejora el doble la detección inicial de actividad gamma, eliminando artefactos de la señal adquirida. Esto podría mejorar las aplicaciones clínicas, aumentado la sensibilidad en los diagnósticos relacionados con lesiones de las áreas motoras cerebrales, y facilitar los estudios de neurofisiología.

- En el tercer experimento (Amo, De Santiago, *et al.*, 2017) se demostró que debido a los cambios plásticos, la potencia de la actividad gamma inducida por el movimiento es significativamente mayor al final de una tarea motora que al principio de ella. Este método obtiene la actividad gamma a través del EEG y define el índice de plasticidad (IP). Los resultados obtenidos son significativos y coherentes con la neurofisiología. Sin embargo, en este experimento, realizado con EEG de superficie no es posible comprobar directamente qué áreas se activan con la tarea motora, pero sí se puede medir el aumento de la actividad gamma (ERS), por lo que de forma indirecta se mide la activación de nuevas

áreas y su progreso en el tiempo con la repetición del ejercicio, es decir, se pueden medir los cambios plásticos.

- En el cuarto experimento (Amo Usanos *et al.*, 2020) se detecta y analiza la actividad gamma inducida en áreas motoras cerebrales durante el movimiento imaginario y se compara con la actividad obtenida en las mismas áreas durante el movimiento real. No se observan diferencias significativas entre la densidad espectral de potencia de la actividad gamma durante el movimiento imaginario y el movimiento real. Los valores medios del ERS del movimiento imaginario indican un incremento ≈ 25%, y los del movimiento real ≈ 27%, y no presentan diferencias significativas ($p > 0.01$). Estos resultados son coherentes con la neurofisiología, teniendo en cuenta que durante los movimientos reales e imaginarios se activan las mismas áreas corticales y ambos tipos de movimiento comparten mecanismos de preparación y programación (Decety, 1996). Otros estudios similares a esta tesis también han demostrado que durante el movimiento imaginario de la mano, hay un aumento en la potencia de las bandas gamma en relación con el estado de reposo (ERS), activando las mismas áreas corticales que se activan con el movimiento real (Miller *et al.*, 2010). El ERS podría proporcionar una forma útil de comprobar indirectamente el funcionamiento de los circuitos neuronales motores al ser activados mediante el movimiento voluntario, tanto imaginario (ERS-IM) como real (ERS-RE). Esta información podría aplicarse en un futuro en el estudio de la fisiología y en el diagnóstico de patologías de las áreas motoras.

5 CONCLUSIONES

La actividad investigadora desarrollada en esta tesis ha permitido cumplir los objetivos planteados:

- Objetivo de aplicación clínica e investigación: se ha obtenido un método de sencillo de adquisición y análisis de la señal EEG en la banda gamma para la práctica clínica habitual. Se ha comprobado la viabilidad experimental de obtener la actividad de la banda gamma en áreas motoras durante el movimiento real e imaginario y se ha propuesto un nuevo método para la cuantificación de la plasticidad cerebral en entornos clínicos.

- Se ha implementado un nuevo método de análisis de los registros de EEG, basado en la descomposición en modo empírico, que mejora el proceso de detección de la banda gamma.

Se enumeran a continuación posibles aplicaciones de la investigación desarrollada:

- La actividad gamma inducida en áreas motoras (movimiento real o imaginario) podría ser una forma útil de comprobar indirectamente el funcionamiento de los circuitos motores al ser activados.

- En algunas enfermedades (lesiones por patología vascular, traumática y degenerativa) existe un daño de las neuronas piramidales excitatorias y de las interneuronas inhibitorias GABAérgicas responsables de las oscilaciones gamma; por lo tanto este método podría ser útil para la valoración de patología de las áreas motoras y como seguimiento en los procesos de rehabilitación.

- Otra posible aportación de este trabajo es la valoración de la lateralidad manual de los sujetos mediante las diferencias en la activación cerebral al mover una mano u otra, ya que debido a la plasticidad cerebral (Pascual-Leone

et al., 2005), se observan mejores resultados de plasticidad al mover la mano más utilizada de forma cotidiana.

- Del mismo modo, este método podría permitir la evaluación de la capacidad motora, los efectos del entrenamiento físico y la lateralidad manual en la medicina deportiva.

6 TRABAJOS FUTUROS

En cuanto al método, se podrían introducir mejoras en futuros estudios:

- Hacer el experimento con los ojos cerrados (utilizando un estímulo auditivo o haciendo un movimiento continuo de las manos sin señal de aviso (cue)) para evitar el frecuente artefacto de parpadeo.

- Hacer la prueba más cómoda para el sujeto, reduciendo el tiempo total de registro (acortando el tiempo de cada trial), utilizando un solo cable de EEG (canal Cz) y no el gorro con todos los canales, etc.

- Utilizar métodos más complejos de análisis matemático de la señal que podrían mejorar los resultados de nuestro estudio.

Dado lo reducido de nuestra muestra, los datos obtenidos de este experimento deberían ser confirmados en futuros estudios con muestras más amplias. También sería necesario introducir sujetos de más edad y equilibrar el número de zurdos y ambidiestros.

A nivel de procesamiento de señales, sería conveniente implementar algún método para la identificación y eliminación de artefactos fisiológicos en los registros de EEG (Mannan, Kamran and Jeong, 2018). En consecuencia, se debería evaluar la capacidad de detección de la actividad gamma utilizando técnicas de reducción de artefactos en sistemas de adquisición monocanal, diseñadas para eliminar algún tipo particular de interferencia como los movimientos oculares (Saini, Payal and Satija, 2020) o más generalistas (Chavez *et al.*, 2018).

Otra posible vía de futura investigación sería la implementación de un sistema de Brain Computer Interface (BCI) monocanal. La ventaja de un BCI se puede centrar en la implementación de un sistema de comunicación (Han *et al.*, 2019) para el control en

tiempo real de periféricos como robots (Edelman *et al.*, 2019). Muchas de las BCI actuales basadas en la detección de movimientos imaginarios de EEG (Padfield *et al.*, 2019) analizan la banda de EEG alfa / beta, generalmente utilizando varios canales. El éxito de las imágenes motoras BCI en aplicaciones traslacionales se establece en tres pilares de aprendizaje: a nivel de máquina, sujeto y aplicación (Perdikis *et al.*, 2018). Existen algunos trabajos multicanal de BCI que analizan la banda gamma: (Ahn *et al.*, 2013) (19 canales EEG) (Szczuko, 2017) (21 canales), o (Van Benthem *et al.*, 2018) (128 canales). En nuestro caso, al ser más simplificado (monocanal), podría tener aplicaciones más sencillas de valoración funcional en sujetos sanos o en procesos de rehabilitación.

7 REFERENCIAS

Adrian, E. D. (1942) 'Olfactory reactions in the brain of the hedgehog', *The Journal of Physiology*, 100(4), pp. 459–473. doi: 10.1113/jphysiol.1942.sp003955.

Ahmed, O. J. and Cash, S. S. (2013) 'Finding synchrony in the desynchronized EEG: the history and interpretation of gamma rhythms', *Frontiers in Integrative Neuroscience*, 7. doi: 10.3389/fnint.2013.00058.

Ahn, M. *et al.* (2013) 'Gamma band activity associated with BCI performance: simultaneous MEG/EEG study.', *Frontiers in human neuroscience*, 7, p. 848. doi: 10.3389/fnhum.2013.00848.

Amo, C. *et al.* (2016) 'Induced Gamma-Band Activity During Voluntary Movement: EEG Analysis for Clinical Purposes.', *Motor control*, 20(4), pp. 409–28. doi: 10.1123/mc.2015-0010.

Amo, C., de Santiago, L., *et al.* (2017) 'Analysis of Gamma-Band Activity from Human EEG Using Empirical Mode Decomposition', *Sensors*, 17(5), p. 989. doi: 10.3390/s17050989.

Amo, C., De Santiago, L., *et al.* (2017) 'Induced gamma band activity from EEG as a possible index of training-related brain plasticity in motor tasks', *PLOS ONE*. Edited by T. Yuan, 12(10), p. e0186008. doi: 10.1371/journal.pone.0186008.

Amo Usanos, C. *et al.* (2020) 'Induced Gamma-Band Activity during Actual and Imaginary Movements: EEG Analysis', *Sensors*, 20(6), p. 1545. doi: 10.3390/s20061545.

Artieda, J. *et al.* (2009) '[Brain oscillations: pathophysiological and potentially therapeutic role in some neurological and psychiatric diseases].', *Anales del sistema sanitario de Navarra*, 32 Suppl 3, pp. 45–60. doi: 10.23938/ASSN.0150.

Ball, T. *et al.* (2008) 'Movement related activity in the high gamma range of the human EEG.', *NeuroImage*, 41(2), pp. 302–310. doi: 10.1016/j.neuroimage.2008.02.032.

Bauer, E. P., Paz, R. and Pare, D. (2007) 'Gamma Oscillations Coordinate Amygdalo-Rhinal Interactions during Learning', *Journal of Neuroscience*, 27(35), pp. 9369–9379.

doi: 10.1523/JNEUROSCI.2153-07.2007.

Van Benthem, K. D. *et al.* (2018) 'An EEG Brain–Computer Interface Approach for Classifying Vigilance States in Humans: A Gamma Band Focus Supports Low Misclassification Rates', *International Journal of Human–Computer Interaction*, 34(3), pp. 226–237. doi: 10.1080/10447318.2017.1342942.

Berger, H. (1929) 'Über das Elektrenkephalogramm des Menschen', *Archiv für Psychiatrie und Nervenkrankheiten*, 87(1), pp. 527–570. doi: 10.1007/BF01797193.

Brazier, M. A. B. (1961) *A history of the electrical activity of the brain: The first half-century*. Macmillan.

Buzsaki, G. (2006) *Rhythms of the Brain*. Oxford University Press.

Canolty, R. T. and Knight, R. T. (2010) 'The functional role of cross-frequency coupling', *Trends in Cognitive Sciences*, 14(11), pp. 506–515. doi: 10.1016/j.tics.2010.09.001.

Cardin, J. A. *et al.* (2009) 'Driving fast-spiking cells induces gamma rhythm and controls sensory responses', *Nature*, 459(7247), pp. 663–667. doi: 10.1038/nature08002.

Chavez, M. *et al.* (2018) 'Surrogate-Based Artifact Removal From Single-Channel EEG', *IEEE Transactions on Neural Systems and Rehabilitation Engineering*, 26(3), pp. 540–550. doi: 10.1109/TNSRE.2018.2794184.

Cheyne, D. and Ferrari, P. (2013) 'MEG studies of motor cortex gamma oscillations: evidence for a gamma "fingerprint" in the brain?', *Frontiers in human neuroscience*, 7, p. 575. doi: 10.3389/fnhum.2013.00575.

Coenen, A. and Zayachkivska, O. (2013) 'Adolf Beck: A pioneer in electroencephalography in between Richard Caton and Hans Berger.', *Advances in cognitive psychology*, 9(4), pp. 216–21. doi: 10.2478/v10053-008-0148-3.

Combrisson, E. *et al.* (2017) 'From intentions to actions: Neural oscillations encode motor processes through phase, amplitude and phase-amplitude coupling', *NeuroImage*, 147, pp. 473–487. doi: 10.1016/j.neuroimage.2016.11.042.

Decety, J. (1996) 'The neurophysiological basis of motor imagery.', *Behavioural brain research*, 77(1–2), pp. 45–52.

DeFelipe, J. and Fariñas, I. (1992) 'The pyramidal neuron of the cerebral cortex: Morphological and chemical characteristics of the synaptic inputs', *Progress in Neurobiology*, 39(6), pp. 563–607. doi: 10.1016/0301-0082(92)90015-7.

Edelman, B. J. *et al.* (2019) 'Noninvasive neuroimaging enhances continuous neural tracking for robotic device control.', *Science robotics*, 4(31). doi: 10.1126/scirobotics.aaw6844.

Fitzgibbon, S. P. *et al.* (2013) 'Surface Laplacian of central scalp electrical signals is insensitive to muscle contamination.', *IEEE transactions on bio-medical engineering*, 60(1), pp. 4–9. doi: 10.1109/TBME.2012.2195662.

'Forty-Third Annual Meeting of the British Medical Association' (1875) *BMJ*, 2(765), pp. 257–279. doi: 10.1136/bmj.2.765.257.

Freeman, W. J. (1978) 'Models of the dynamics of neural populations.', *Electroencephalography and clinical neurophysiology. Supplement*, (34), pp. 9–18. Available at: http://www.ncbi.nlm.nih.gov/pubmed/285858.

Fries, P. (2001) 'Modulation of Oscillatory Neuronal Synchronization by Selective Visual Attention', *Science*, 291(5508), pp. 1560–1563. doi: 10.1126/science.1055465.

Fries, P. (2009) 'Neuronal Gamma-Band Synchronization as a Fundamental Process in Cortical Computation', *Annual Review of Neuroscience*, 32(1), pp. 209–224. doi: 10.1146/annurev.neuro.051508.135603.

Gray, C. M. and Singer, W. (1989) 'Stimulus-specific neuronal oscillations in orientation columns of cat visual cortex.', *Proceedings of the National Academy of Sciences*, 86(5), pp. 1698–1702. doi: 10.1073/pnas.86.5.1698.

Han, C.-H. *et al.* (2019) 'Electroencephalography-based endogenous brain–computer interface for online communication with a completely locked-in patient', *Journal of NeuroEngineering and Rehabilitation*, 16(1), p. 18. doi: 10.1186/s12984-019-0493-0.

Hardwick, R. M. *et al.* (2018) 'Neural correlates of action: Comparing meta-analyses of imagery, observation, and execution', *Neuroscience & Biobehavioral Reviews*, 94, pp. 31–44. doi: 10.1016/j.neubiorev.2018.08.003.

Hasenstaub, A. *et al.* (2005) 'Inhibitory Postsynaptic Potentials Carry Synchronized

Frequency Information in Active Cortical Networks', *Neuron*, 47(3), pp. 423–435. doi: 10.1016/j.neuron.2005.06.016.

Henrie, J. A. and Shapley, R. (2005) 'LFP Power Spectra in V1 Cortex: The Graded Effect of Stimulus Contrast', *Journal of Neurophysiology*, 94(1), pp. 479–490. doi: 10.1152/jn.00919.2004.

Herrmann, C. S. and Demiralp, T. (2005) 'Human EEG gamma oscillations in neuropsychiatric disorders.', *Clinical neurophysiology : official journal of the International Federation of Clinical Neurophysiology*, 116(12), pp. 2719–33. doi: 10.1016/j.clinph.2005.07.007.

Hirase, H. *et al.* (2014) 'Volume transmission signalling via astrocytes', *Philosophical Transactions of the Royal Society B: Biological Sciences*, 369(1654), p. 20130604. doi: 10.1098/rstb.2013.0604.

Jasper, H. H. (1936) 'CORTICAL EXCITATORY STATE AND VARIABILITY IN HUMAN BRAIN RHYTHMS', *Science*, 83(2150), pp. 259–260. doi: 10.1126/science.83.2150.259.

Jasper, H. H. and Andrews, H. L. (1938) 'ELECTRO-ENCEPHALOGRAPHY', *Archives of Neurology & Psychiatry*, 39(1), p. 96. doi: 10.1001/archneurpsyc.1938.02270010106010.

Jia, X. and Kohn, A. (2011) 'Gamma Rhythms in the Brain', *PLoS Biology*, 9(4), p. e1001045. doi: 10.1371/journal.pbio.1001045.

Lazurenko, D. M. *et al.* (2018) 'Electrographic Properties of Movement-Related Potentials', *Neuroscience and Behavioral Physiology*, 48(9), pp. 1078–1087. doi: 10.1007/s11055-018-0670-9.

Leuthardt, E. C. *et al.* (2004) 'A brain-computer interface using electrocorticographic signals in humans.', *Journal of neural engineering*, 1(2), pp. 63–71. doi: 10.1088/1741-2560/1/2/001.

Mannan, M. M. N., Kamran, M. A. and Jeong, M. Y. (2018) 'Identification and Removal of Physiological Artifacts From Electroencephalogram Signals: A Review', *IEEE Access*, 6, pp. 30630–30652. doi: 10.1109/ACCESS.2018.2842082.

Miller, K. J. *et al.* (2010) 'Cortical activity during motor execution, motor imagery, and

imagery-based online feedback.', *Proceedings of the National Academy of Sciences of the United States of America*, 107(9), pp. 4430–4435. doi: 10.1073/pnas.0913697107.

Oldfield, R. C. (1971) 'The assessment and analysis of handedness: the Edinburgh inventory.', *Neuropsychologia*, 9(1), pp. 97–113.

Oostenveld, R. *et al.* (2011) 'FieldTrip: Open source software for advanced analysis of MEG, EEG, and invasive electrophysiological data.', *Computational intelligence and neuroscience*, 2011, p. 156869. doi: 10.1155/2011/156869.

Padfield, N. *et al.* (2019) 'EEG-Based Brain-Computer Interfaces Using Motor-Imagery: Techniques and Challenges.', *Sensors (Basel, Switzerland)*, 19(6). doi: 10.3390/s19061423.

Pascual-Leone, A. *et al.* (2005) 'The plastic human brain cortex.', *Annual review of neuroscience*, 28, pp. 377–401. doi: 10.1146/annurev.neuro.27.070203.144216.

Perdikis, S. *et al.* (2018) 'The Cybathlon BCI race: Successful longitudinal mutual learning with two tetraplegic users', *PLOS Biology*. Edited by K. Ganguly, 16(5), p. e2003787. doi: 10.1371/journal.pbio.2003787.

Pesaran, B. *et al.* (2002) 'Temporal structure in neuronal activity during working memory in macaque parietal cortex', *Nature Neuroscience*, 5(8), pp. 805–811. doi: 10.1038/nn890.

Pfurtscheller, G. and Lopes da Silva, F. H. (1999) 'Event-related EEG/MEG synchronization and desynchronization: basic principles.', *Clinical neurophysiology : official journal of the International Federation of Clinical Neurophysiology*, 110(11), pp. 1842–57. Available at: http://www.ncbi.nlm.nih.gov/pubmed/10576479.

Rayi, A. and Murr, N. (2021) *Electroencephalogram*, *StatPearls [Internet]. Treasure Island (FL): StatPearls Publishing; 2021 Jan-.* Available at: https://www.ncbi.nlm.nih.gov/books/NBK563295/.

Saini, M., Payal and Satija, U. (2020) 'An Effective and Robust Framework for Ocular Artifact Removal From Single-Channel EEG Signal Based on Variational Mode Decomposition', *IEEE Sensors Journal*, 20(1), pp. 369–376. doi: 10.1109/JSEN.2019.2942153.

Shibata, T. *et al.* (1999) 'Event-related dynamics of the gamma-band oscillation in the human brain: information processing during a GO/NOGO hand movement task.', *Neuroscience research*, 33(3), pp. 215–22.

Singer, W. (1999) 'Neuronal Synchrony: A Versatile Code for the Definition of Relations?', *Neuron*, 24(1), pp. 49–65. doi: 10.1016/S0896-6273(00)80821-1.

Smith, M. M. *et al.* (2014) 'Non-invasive detection of high gamma band activity during motor imagery.', *Frontiers in human neuroscience*, 8, p. 817. doi: 10.3389/fnhum.2014.00817.

Szczuko, P. (2017) 'Real and imaginary motion classification based on rough set analysis of EEG signals for multimedia applications', *Multimedia Tools and Applications*, 76(24), pp. 25697–25711. doi: 10.1007/s11042-017-4458-7.

Tallon-Baudry, C. and Bertrand, O. (1999) 'Oscillatory gamma activity in humans and its role in object representation.', *Trends in cognitive sciences*, 3(4), pp. 151–162.

Tan, H.-R. M., Lana, L. and Uhlhaas, P. J. (2013) 'High-frequency neural oscillations and visual processing deficits in schizophrenia', *Frontiers in Psychology*, 4. doi: 10.3389/fpsyg.2013.00621.

Uhlhaas, P. J. *et al.* (2008) 'The role of oscillations and synchrony in cortical networks and their putative relevance for the pathophysiology of schizophrenia.', *Schizophrenia bulletin*, 34(5), pp. 927–943. doi: 10.1093/schbul/sbn062.

Uhlhaas, P. J. *et al.* (2011) 'A new look at gamma? High- (>60 Hz) γ-band activity in cortical networks: function, mechanisms and impairment.', *Progress in biophysics and molecular biology*, 105(1–2), pp. 14–28. doi: 10.1016/j.pbiomolbio.2010.10.004.

Uhlhaas, P. J. and Singer, W. (2006) 'Neural Synchrony in Brain Disorders: Relevance for Cognitive Dysfunctions and Pathophysiology', *Neuron*, 52(1), pp. 155–168. doi: 10.1016/j.neuron.2006.09.020.

Uhlhaas, P. J. and Singer, W. (2013) 'High-frequency oscillations and the neurobiology of schizophrenia', *Dialogues in Clinical Neuroscience*, 15(3), pp. 301–313. doi: 10.31887/DCNS.2013.15.3/puhlhaas.

Veslin, E. Y. *et al.* (2019) 'Lower gamma band in the classification of left and right

elbow movement in real and imaginary tasks', *Journal of the Brazilian Society of Mechanical Sciences and Engineering*, 41(2), p. 91. doi: 10.1007/s40430-019-1585-2.

Viana Di Prisco, G. and Freeman, W. J. (1985) 'Odor-related bulbar EEG spatial pattern analysis during appetitive conditioning in rabbits.', *Behavioral Neuroscience*, 99(5), pp. 964–978. doi: 10.1037/0735-7044.99.5.964.

Wang, X. J. and Buzsáki, G. (1996) 'Gamma oscillation by synaptic inhibition in a hippocampal interneuronal network model.', *The Journal of neuroscience : the official journal of the Society for Neuroscience*, 16(20), pp. 6402–13. Available at: http://www.ncbi.nlm.nih.gov/pubmed/8815919.

Whitham, E. M. *et al.* (2008) 'Thinking activates EMG in scalp electrical recordings', *Clinical Neurophysiology*, 119(5), pp. 1166–1175. doi: 10.1016/j.clinph.2008.01.024.

Womelsdorf, T. *et al.* (2007) 'Modulation of Neuronal Interactions Through Neuronal Synchronization', *Science*, 316(5831), pp. 1609–1612. doi: 10.1126/science.1139597.

8 ANEXOS

8.1 AUTORIZACIÓN DEL COMITÉ DE ÉTICA DE LA UAH

Universidad de Alcalá

(A rellenar por la Secretaría)
Cód. CEI: 2013/013/20130422

Proyecto:

COMITÉ DE ÉTICA DE LA INVESTIGACIÓN

INFORME

UNIVERSIDAD DE ALCALÁ, PATRIMONIO DE LA HUMANIDAD

El Comité de Ética de la Investigación de la Universidad de Alcalá, en su reunión del 22 de abril de 2013, ha evaluado el proyecto de investigación titulado ***"Caracterización de la actividad gamma eeg en áreas corticales motoras en sujetos controles"***, dirigido por el Dr. D. Luciano Boquete del Departamento de Electrónica de esta Universidad.

Analizados los extremos acreditados en el expediente, el Comité considera que el proyecto de investigación y el procedimiento evaluado son correctos desde el punto de vista ético y metodológico, y por lo tanto da su informe **FAVORABLE.**

Y para que conste, se firma este informe en Alcalá de Henares, a 22 de abril de 2013.

UNIVERSIDAD DE ALCALÁ VICERRECTORADO DE INVESTIGACIÓN

María Luisa Marina Alegre
Presidenta del CEI

el Dr. D. Luciano Boquete
Departamento de Electrónica

8.2 ARTÍCULOS PUBLICADOS

8.2.1 Induced Gamma-Band Activity During Voluntary Movement: EEG Analysis for Clinical Purposes

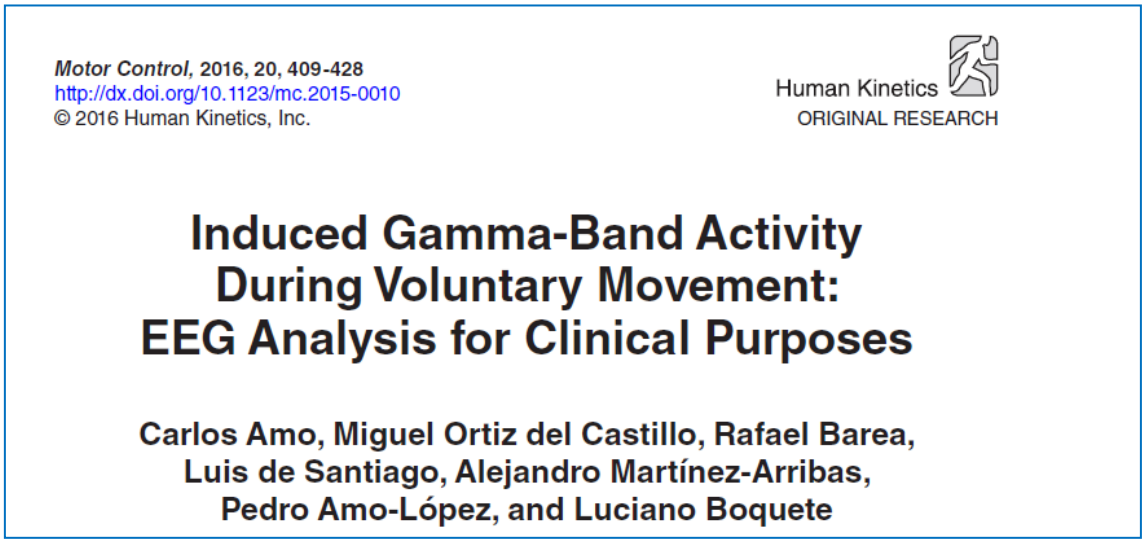

Motor Control, 2016, 20, 409-428
http://dx.doi.org/10.1123/mc.2015-0010

Human Kinetics
ORIGINAL RESEARCH

Induced Gamma-Band Activity During Voluntary Movement: EEG Analysis for Clinical Purposes

Carlos Amo, Miguel Ortiz del Castillo, Rafael Barea, Luis de Santiago, Alejandro Martínez-Arribas, Pedro Amo-López, and Luciano Boquete

Motor Control, 2016, 20, 409-428
http://dx.doi.org/10.1123/mc.2015-0010

Human Kinetics
ORIGINAL RESEARCH

Induced Gamma-Band Activity During Voluntary Movement: EEG Analysis for Clinical Purposes

Carlos Amo, Miguel Ortiz del Castillo, Rafael Barea, Luis de Santiago, Alejandro Martínez-Arribas, Pedro Amo-López, and Luciano Boquete

Objective: Propose a simplified method applicable in routine clinical practice that uses EEG to assess induced gamma-band activity (GBA) in the 30–90 Hz frequency range in cerebral motor areas. ***Design***: EEG recordings (25 healthy subjects) of cerebral activity (at rest, motor task). GBA was obtained as power spectral density (PSD). GBA — defined as the gamma index (Iγ) — was calculated using the basal GBA (γ_B) and motor GBA (γ_{MOV}) PSD values. ***Results***: The mean values of Iγ were ($I\gamma_R$ (right hand) = 1.30, $I\gamma_L$ (left hand) = 1.22). Manual laterality showed a correlation with Iγ. ***Conclusions:*** Iγ may provide a useful way of indirectly assessing operation of activated motor neuronal circuits. It could be applied to diagnosis of motor area pathologies and as follow up in rehabilitation processes. Likewise, Iγ could enable the assessment of motor capacity, physical training and manual laterality in sport medicine.

Keywords: electroencephalography, gamma rhythm, motor area, motor tasks, cortical synchronization, power spectral density

Gamma Activity

Rhythmic electroencephalogram (EEG) activity is commonly subdivided into 5 frequency bands: delta (0–3 Hz), theta (4–7 Hz), alpha (8–12 Hz), beta (13–30 Hz), and gamma (30–200 Hz) (Uhlhaas, Haenschel, Nikolić, & Singer, 2008).

Gamma band activity (GBA) is distributed widely throughout the cerebral structures, as well as throughout the retina and olfactory tract. It is generated by GABA, glutamate and acetylcholine neurotransmitters and participates in various cerebral functions such as perception, attention, memory, consciousness, synaptic plasticity and motor control (Uhlhaas et al., 2008).

Amo, del Castillo, Barea, Luis de Santiago, Martínez-Arribas and Boquete are with the Dept. de Electrónica, Biomedical Engineering, University of Alcalá, Alcalá de Henares, Spain. Amo-López is with the Dept. of Signal Theory and Communications, University of Alcalá, Alcalá de Henares, Spain. Address author correspondence to Luciano Boquete at luciano.boquete@uah.es.

Within the gamma-band frequency range, it is possible to differentiate between low gamma-band oscillations (30–60 Hz) and high gamma-band oscillations (60–200 Hz) (Uhlhaas, Pipa, Neuenschwander, Wibral, & Singer, 2011).

The underlying cellular mechanisms responsible for gamma oscillations (GBA) have not yet been completely elucidated, but it is believed that reciprocal interaction between the excitatory pyramidal neurons and the GABAergic inhibitory interneurons, particularly the parvalbumin positive fast-spiking basket cells, probably plays a key role (Cardin et al., 2009). The GBA is therefore considered a product of balanced excitatory and inhibitory synaptic input (Hirase, Iwai, Takata, Shinohara, & Mishima, 2014).

These neuronal interactions produce different types of GBA that can be grouped in the following categories: spontaneous gamma oscillations, induced gamma oscillations, evoked gamma responses and steady-state gamma oscillations (Herrmann & Demiralp, 2005).

From a functional standpoint, neuronal gamma-band synchronization is induced by various stimuli and tasks and is related to several cognitive capacities (Fries, 2009). A characteristic common to these cognitive processes appears to be that induced gamma activity increases during complex tasks or during tasks that require attention. Consequently, it has been interpreted as being the neuronal substrate of cognitive processes (Tallon-Baudry, & Bertrand, 1999).

Gamma Activity Recorded During Motor Tasks

In relation to motor activity in the human brain, induced gamma-band activity has been observed in response to sensory stimuli and during motor tasks in a variety of experiments employing EEG and magnetoencephalography (MEG), before or during voluntary movement. These gamma oscillations were not phase-locked to movement onset (Tallon-Baudry & Bertrand, 1999).

Some of these studies describe gamma oscillations in the 40 Hz range, but others electrophysiological studies have shown that high gamma-band activity in the frequency range of 30–90 Hz can be recorded from a wide range of brain regions during rest or the performance of motor tasks (Cheyne, & Ferrari, 2013).

Furthermore, these movement-related gamma oscillations appear to correspond to the somatotopic organization of the primary sensory–motor areas. Consequently, gamma activity has been proposed as the integrator of sensory and motor processes during movement preparation and control. It has also been observed that the mapping of the gamma response in motor tasks suggests that the cortical area of activation is rather restricted (Tallon-Baudry & Bertrand, 1999).

Gamma Activity Analysis Methods

During sensory, cognitive and motor processes two types of change may be produced in the electrical activity in the cerebral cortex. The first of these is evoked activity, which is associated with stimulus and is time- and phase-locked. This evoked activity can be extracted from background activity in the EEG by linear methods such as averaging. The second change is induced activity, which is associated

with stimulus and is time-locked but not phase-locked. Induced activity can only be extracted from background activity in the EEG by nonlinear methods such as power spectral analysis (Pfurtscheller, & Lopez da Silva, 2011).

These nonlinear methods use time–frequency transformations (e.g., Morlet wavelets or short-time Fourier transforms) on each individual trial before averaging across all trials (Tan, Lana, & Uhlhaas, 2013).

This paper obtains the induced GBA expressed as power spectral density (PSD) for a selected frequency range (30–90 Hz). In addition, the results are broken down into low GBA (30–60 Hz) and high GBA (60–90 Hz).

Finally, this study quantifies the variations in GBA induced by the motor task (motor GBA) in relation to basal cortical activity (basal GBA). The decreases or increases of the motor GBA in relation to basal are known as event-related desynchronization (ERD) and event-related synchronization (ERS), respectively. Both changes, ERD and ERS, may be considered attributable to changes in synchrony in underlying neuronal populations (Pfurtscheller, & Lopes da Silva, 1999).

Spontaneous gamma activity is recorded with the subject at rest without the need for activation or for performance of a task. This activity constitutes a small fraction (0.5–10%) of total EEG/MEG signal power (Jia, & Kohn, 2011) and can be explained by thalamocortical resonant synaptic interactions. It is also assumed to reflect level of consciousness (Herrmann & Demiralp, 2005).

Meanwhile, induced gamma activity has been interpreted as an integrator of sensory information and motor activity. However, there is evidence that both spontaneous and induced activity, as well as the other types (evoked gamma responses and steady-state gamma oscillations), may be generated by the same neuronal circuits (Herrmann & Demiralp, 2005). Therefore, this paper's proposal of comparing the spontaneous gamma oscillations (basal GBA) against the induced ones (motor GBA) to obtain the ERS values is justified, as it compares function of the same areas of the cerebral cortex at rest and during movement.

In this study we obtain GBA using EEG because is the technique most applicable in the clinical practice. Other methods are invasive (intracerebral recordings and ECoG) or too much expensive (MEG).

Study Objectives

Analysis of cerebral GBA has been described in many neurophysiological papers but mainly oriented to the research.

The objective of this study is to propose a simplified method of using the EEG in clinical applications to evaluate the increase in induced GBA in cerebral motor areas. This diagnostic method needs to be simple to perform for both practitioners and patients; applicable in routine clinical practice; effective at analyzing data and obtaining results; and useful for assessing pathology in cortical motor areas.

Likewise, it must be noninvasive, low-cost and viable at any health center. To achieve these objectives, this method uses the EEG, which is practically universally available.

This method could be simplified by future improvements explained at the end of this paper in the discussion.

Material and Methods

This study protocol was approved by the Ethics Committee of the University of Alcalá de Henares (Madrid, Spain). Subjects participating in the study were required to sign an informed consent form before the start of the experiment.

Sample

The sample for this experiment comprised 31 subjects, 6 of which were excluded during the analysis of the data (using the FieldTrip ft_RejectArtifact function) due to the presence of a high number of artifacts in their EEG recordings (blinking, muscle artifacts, etc.). All sample subjects were healthy and free of medical, neurological (including craniocerebral trauma and epilepsy) and psychiatric disease. None of the subjects were taking drugs and none had a record of alcohol or drug abuse or dependency.

The final sample comprised 9 females and 16 males (mean age = 25.16; range = 18–47). The subjects were classified by manual laterality according to the Edinburgh Handedness Inventory (EHI) (Oldfield, 1971) identifying 19 right-handed subjects (mean EHI = 79.47), 3 left-handed subjects (mean EHI = -73.33) and 3 ambidextrous subjects (mean EHI = 20.00).

Experiment

Each subject sat in a comfortable chair facing a computer monitor placed 0.8 m away from them. They rested their forearms on a table with the palms of their hands facing downward.

The experiment comprised two parts conducted in a single session per subject. In the first part (basal experiment), the subjects kept their eyes open and their gaze fixed on the center of the computer screen. A total of 18 min of basal activity were recorded, divided into 3 parts (each 6 min long) with a rest of approximately 1 min between each. The objective of this first part was to obtain basal GBA (spontaneous gamma oscillations) from the EEG trace.

In the second part (motor experiment), the subjects performed a motor task immediately after receiving an on-screen cue, thereby obtaining motor GBA induced by that movement (induced gamma oscillations) from the EEG trace. The task consisted of rapidly bending the wrist upwards and then briefly relaxing (rather than voluntarily flexing it). The subjects practiced this exercise in a training session held before the experiment. Throughout the experiment, the subjects kept their gaze fixed on a constant point on the screen to prevent eye movement and were instructed to avoid blinking, swallowing or any other movement other than that required with their hand.

Each trial lasted 2 s and started (at t = 0 s) with display (for 150 ms) of the cue in the center of the computer screen. This was followed by a white screen that remained in place until the start of the next trial (t = 2 s). The cue was the order to start the motor task. The motor experiment comprised 5 runs per hand. Each run comprised 100 trials. Runs alternated between the right and left hands to prevent muscle fatigue. Total motor task duration was approximately 40 min.

Data Acquisition

The equipment used in this experiment comprised a 32-channel Micromed EEG (Handy EEG SD32) and the SystemPlus Evolution (Micromed SpA, Treviso, Italy) acquisition software. The recordings were obtained using a 22-bit sigma-delta A/D converter, a sampling frequency (Fs) of 2048 Hz, an antialiasing band-pass filter set at 0.15–537.53 Hz, and a notch filter (50 Hz). Electrode impedances were kept below 10 kΩ to ensure background noise in the acquired signal was < 0.5 μV. The number of channels employed was, 3 for EEG, 2 for electrooculogram (EOG) and 2 for electromyogram (EMG).EEG (C3, C4, and Cz) was continuously recorded using an elastic cap fitted with Ag/AgCl-positioned electrodes as per the 10/20 system. FPz and Pz were the reference and ground electrode, respectively.

To monitor horizontal and vertical eye movements, the EOG signal was obtained via two electrodes, one placed above the outer canthus of the right eye and the other placed below the outer canthus of the left eye.

The EMG signal was obtained via two surface electrodes (one active electrode and one reference electrode) located on each forearm above the extensor carpi radialis longus muscle.

During all recordings the laboratory lights were turned off and rechargeable batteries were used in the acquisition equipment to minimize potential AC induction at 50 Hz in the EEG power cables (Herrmann, & Demiralp, 2005).

Data Analysis

The EEG, EMG and EOG signals were analyzed offline using Matlab 2009b (The MathWorks Inc. Natick, MA, USA) and FieldTrip (Oostenveld, Fries, Maris, & Schoffelen, 2011), and the data were processed in European Data Format (EDF).

First, each run's signal (acquired in continuous mode) was split into 100 two-second trials based on the signal's cue triggers.

The EEG signal was analyzed using a band-pass filter (1 Hz, 100 Hz) and a narrow-band notch filter (which eliminated the 49–51 Hz band).

Using the FieldTrip ft_RejectArtifact function (applying the function's standard parameters and the corresponding EMG (30–100 Hz) and EOG (1–70 Hz) filters), trials containing EMG and EOG artifacts were discarded.

Each trial was then inspected visually using the FieldTrip ft_RejectVisual function to eliminate amplitude jumps, eye blink and muscle movements not previously eliminated by automatic analysis (ft_RejectArtifact). In the final signal preprocessing step, the linear trend error (FieldTrip function ft_Detrend) was eliminated.

A mean of 388 trials (77.7%) per subject and motor task (right or left hand) were qualified as valid for the following analysis (see Table 1).

Figure 1 shows an example of a valid trial, corresponding to movement of the right hand by subject no. 1.

Automatic analysis routines (Matlab) were then applied to the clean signal produced by these preprocessing steps to obtain the different EMG and EEG parameters necessary for the proposed diagnosis method.

Table 1 Elimination of Artifacts and Qualification of Valid Trials (77.7%), Right Hand, and Left Hand

Total (25 Subjects)	Average (25 Subjects)
Total Valid Trials	Valid Trials (500 = 100%)
RH: 9,609 trials	384 (76.8%)
LH: 9,824 trials	393 (78.6%)
Mean (RH, LH): 9,716 trials	**388 (77.7%)**

Note. RH = right hand, LH = left hand.

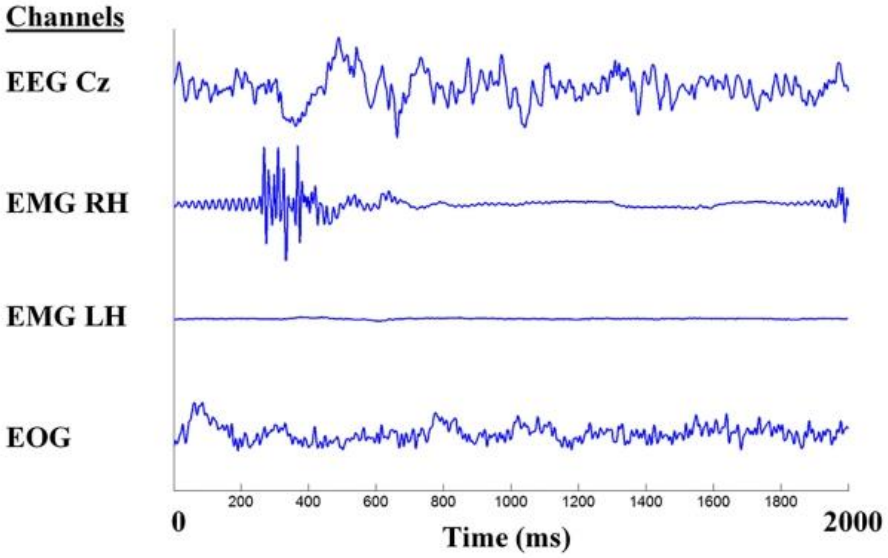

Figure 1 — Example of a valid trial in the motor experiment (right hand) conducted on subject 1. EEG Cz channel (-15, 15 μV), EMG channel (-300, 300 μV) and EOG channel (-40, 40 μV). RH (Right Hand) and LH (Left Hand).

EMG Parameters

For the EMG signals, the onset latency (EMG_{LAT}), mean amplitude (EMG_{MED}) and maximum amplitude (EMG_{MAX}) was calculated in each trial. Also the peak-average ratio (EMG_{PAR}) was defined as:

$$EMG_{PAR} = EMG_{MAX} / EMG_{MED}.$$

When calculating the EMG_{LAT}, onset was considered to occur on the first instance of EMG ≥ 200 μV in each trial's interval (150–750 ms). The maximum amplitude was taken as the EMG signal's peak-to-peak value while the mean amplitude was calculated from the rectified EMG signal.

Finally, the mean values of all the EMG parameters were calculated for each subject before calculating the grand average for all subjects.

EEG Parameters

Characterization of the Event-Related Potential (ERP). To analyze the EEG signal, only the Cz channel signals were used, as this channel was the least contaminated by movement and EMG artifacts (Fitzgibbon, Lewis, Powers, Whitham, Willoughby, & Pope, 2013). Figure 2 shows a schematic representation of the averaging method used to obtain the evoked activity (time-locked responses), in the form of ERP, from the artifact-free EEG trials. The average for the signals recorded from each subject was obtained and these data were then averaged to

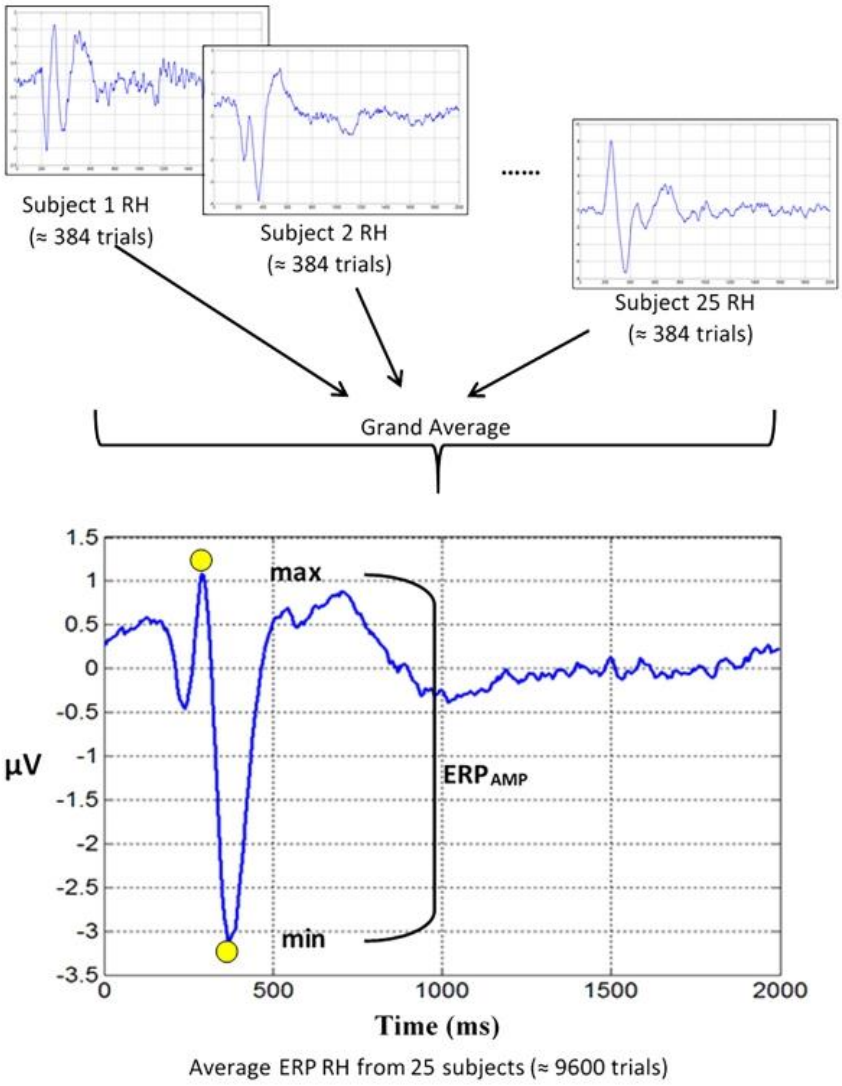

Figure 2 — Example of ERP graphs. Obtained from the EEG Cz channel for the right-hand (RH) motor task for each subject (averaging a mean of 384 trials per subject) and from the average for all subjects (grand average of the 25 subjects, averaging a total of ≈ 9,600 trials). Maximum, minimum and ERP_{AMP} values expressed in µV.

produce the grand average. This process was applied to both the left- and right-hand responses. The peak-to-peak ERP amplitude was defined from the trace of the averaged signal: ERP_{AMP} = maximum value—minimum value.

Calculation of GBA. The induced GBA was obtained as power spectral values for the three frequency bands (30–60 Hz, 60–90 Hz and 30–90 Hz) and was estimated using a multitaper Fast-Fourier transform (FFT) (FieldTrip ft_freqanalysis function). The results were expressed for each frequency band as the mean PSD value (in μV^2), as the PSD reflects the amplitude of the neuronal oscillations calculated using the time–frequency transformations (Uhlhaas, & Singer, 2013).

Based on the GBA's mean PSD values, the following parameters were defined:

- Basal GBA (γ_B) = GBA during the basal experiment = spontaneous gamma oscillations.
- Motor GBA = GBA during motor activity of the right (γ_R) or left hand (γ_L) = induced gamma oscillations.
- Mean motor GBA (γ_{MOV}) = mean value of γ_R and γ_L.

These GBA parameters were calculated for each single trial and averaged for each hand and for each frequency band. At the end, the grand average was calculated for all subjects.

Each value of γ expresses the mean PSD value in a selected frequency band and its value is given in μV^2. For example, γ_R (30–60) indicates the mean PSD value obtained from the right-hand movement in the 30–60 Hz range (Figure 3).

Calculation of GBA ERS. Once the basal GBA (γ_B) and motor GBA values were obtained for the right (γ_R) and left (γ_L) hands, the ERS was defined by normalizing the values in relation to basal gamma activity (γ_B). This established the ERS in terms of gamma index ($I\gamma$) as:

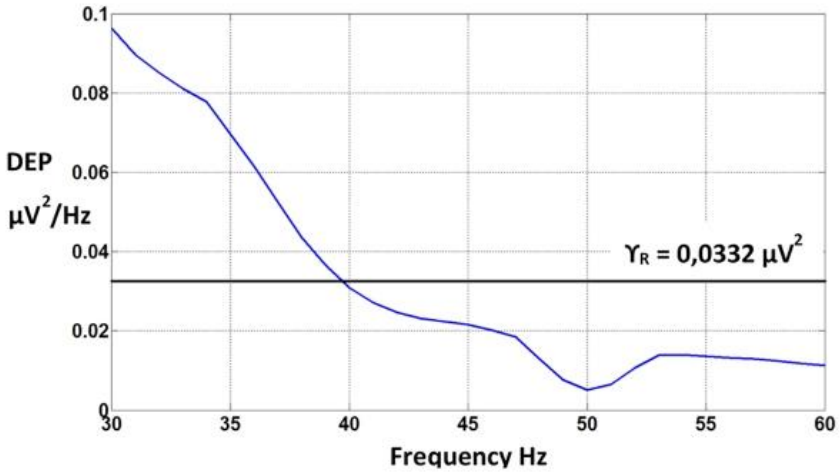

Figure 3 — Example of calculation of γ_R in subject 1. The horizontal line indicates the mean PSD value (μV^2) in the 30–60 Hz frequency band.

- Right-hand gamma index ($I\gamma_R$) = ERS during right-hand motor activity:

$$I\gamma_R = \frac{\gamma_R}{\gamma_B}$$

- Left-hand gamma index ($I\gamma_L$) = ERS during left-hand motor activity:

$$I\gamma_L = \frac{\gamma_L}{\gamma_B}$$

- Motor gamma index ($I\gamma_{MOV}$) = mean value of $I\gamma_R$ and $I\gamma_L$:

$$I\gamma_{MOV} = \frac{I\gamma_R + I\gamma_L}{2}$$

- Index difference ($I\gamma_{DIF}$) = ERS difference between both sides: $I\gamma_{DIF} = I\gamma_R — I\gamma_L$.

Statistical Analysis

All statistical analyses were performed using the SPSS 22.0 program (SPSS Inc. Chicago, Illinois, USA). Student's *t* test was used to compare the means and Pearson's linear correlation was used to compare quantitative variables. The results are expressed as mean and confidence interval (CI 95%). The significance value for the differences was set at $p < .05$.

Results

Table 2 shows the mean values (grand average of the 25 subjects) for the EMG parameters and ERP response. No significant differences were found (*t* test) between the right- and left-hand values for any of the parameters included in the table.

Table 3 shows the mean values (grand average of the 25 subjects) for the PSD of the GBA (γ_B, γ_R, γ_L and γ_{MOV}) for the three frequency bands calculated.

Table 2 Average Values (Mean; CI 95%) of the EMG Parameters (Latency) and Amplitude (Expressed as EMG_{PAR}, EMG_{MED} and EMG_{MAX}) and of the ERP (ERP_{AMP})

Parameters	Left Hand	Right Hand	Mean (Left and Right)
EMG_{LAT} (ms)	328 (303–352)	315 (295–336)	322 (300–343)
EMG_{PAR} (*)	12.1 (10.5–13.8)	12.1 (10.9–13.2)	12.1 (10.9–13.3)
EMG_{MED} (μV)	70.3 (62–78.6)	77.5 (64.5–90.5)	73.9 (65.4–82.4)
EMG_{MAX} (μV)	807.1 (709–905)	912.6 (757.3–1068)	859 (745–974.7)
ERP_{AMP} (μV)	6 (4.8–7.3)	6.2 (5–7.5)	6.1 (4.9–7.4)

Note. Amplitude is expressed as EMGPAR, EMGMED, and EMGMAX. EMG_{LAT} = latency, ERP_{AMP} = ERP.

*EMG_{PAR} is a unitless index (μV/μV).

Table 3 Average GBA Values (PSD in μV²)

f (Hz)	Υ_B	Υ_L	Υ_R	Υ_{MOV}
[30–60]	**0.0151** (0.0121–0.0179)	**0.0186** (0.0146–0.0225)	**0.0194** (0.0156–0.0232)	**0.0190** (0.0151–0.0228)
[60–90]	**0.0044** (0.0033–0.0053)	**0.0055** (0.0041–0.0068)	**0.0057** (0.0042–0.0071)	**0.0056** (0.0042–0.0069)
[30–90]	**0.0097** (0.0078–0.0116)	**0.0120** (0.0094–0.0146)	**0.0126** (0.0100–0.0152)	**0.0123** (0.0098–0.0149)

Note. Values are expressed as mean (CI 95%).

The PSD values of the basal GBA (γ_B) were compared against those of the motor GBA (γ_R, γ_L and γ_{MOV}) and those of γ_R were compared against γ_L for the three frequency ranges using Student's *t* test. Significant differences were observed between basal GBA and motor GBA in all the frequency ranges. No significant differences were found between the right-hand motor GBA (γ_R) and the left-hand motor GBA (γ_L) (Figure 4).

The ERS ($I\gamma_R$, $I\gamma_L$ and $I\gamma_{MOV}$) of the GBA was calculated for the three frequency ranges (Figure 5). No significant differences were found (*t* test) between $I\gamma_R$ and $I\gamma_L$ in any of the frequency bands analyzed. Neither were significant differences found between $I\gamma_{R\,[30–60]}$ and $I\gamma_{R\,[60–90]}$, between $I\gamma_{L\,[30–60]}$ and $I\gamma_{L\,[60–90]}$, or between $I\gamma_{MOV\,[30–60]}$ and $I\gamma_{MOV\,[60–90]}$.

The gamma index values were also calculated by grouping the subjects by manual laterality (right-handed (R), left-handed (L), and ambidextrous (A)) and the differences (*t* test) were calculated between $I\gamma_R$ and $I\gamma_L$ in group R (statistical significance was not calculated in groups L and A due to the small sample size) (Table 4).

Table 4 shows too the classification of the differences in gamma indices ($I\gamma_{DIF}$) in the various frequency ranges and manual laterality groups (L, A, R).

In the various frequency ranges, $I\gamma_L > I\gamma_R$ in group L, $I\gamma_L \approx I\gamma_R$ in group A, and $I\gamma_R > I\gamma_L$ in group R.

The correlation (Pearson, using r values) was calculated between the various parameters in the three frequency bands, producing the following findings:

1. Subject age did not correlate with any other parameter.
2. EMG parameters: EMG signal onset latency (EMG_{LAT}) and amplitude (EMG_{PAR}) did not correlate with any other parameter. However, a positive and significant correlation was found between the EMG_{LAT} of the right- and left-hand movements, $r = .834$ ($p < .0001$).
3. The amplitude of the evoked response (ERP_{AMP}) did not correlate with any other parameter. However, a positive and significant correlation was found between the ERP_{AMP} of the right- and left-hand movements, $r = .961$ ($p < .0001$).
4. The mean PSD values (γ_B, γ_R, γ_L and γ_{MOV}) did not correlate with any other parameter. However, a positive and significant correlation was found between γ_R and γ_L, $r \geq .898$ ($p < .0001$) (minimum value obtained between the three frequency ranges).

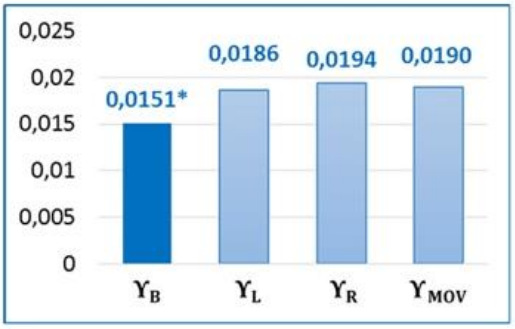

[30-60] Hz	T test
ϒB - ϒR	P < 0,001
ϒB - ϒL	P < 0,001
ϒB - ϒMOV	P < 0,001
ϒR - ϒL	No significant

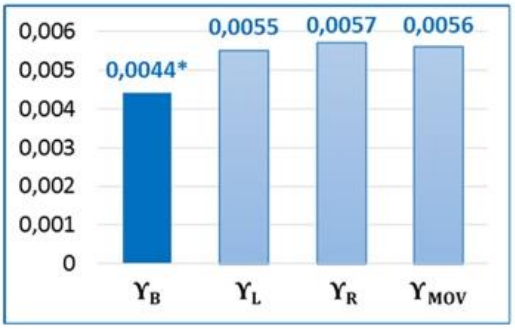

[60-90] Hz	T test
ϒB - ϒR	P = 0,003
ϒB - ϒL	P < 0,001
ϒB - ϒMOV	P < 0,001
ϒR - ϒL	No significant

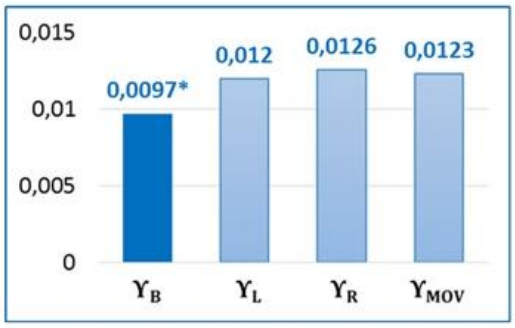

[30-90] Hz	T test
ϒB - ϒR	P < 0,001
ϒB - ϒL	P < 0,001
ϒB - ϒMOV	P < 0,001
ϒR - ϒL	No significant

Figure 4 — Y axis (PSD values of the GBA in μV^2). *Significant difference between basal GBA and motor GBA; no significant difference between γ_R and γ_L.

5. A positive and significant correlation was also found between γ_B and γ_R with $r \geq .850$ ($p < .0001$), and between γ_B and γ_L with $r \geq .914$ ($p < .0001$) (minimum value obtained between the three frequency ranges).
6. The gamma index (Iγ) did not correlate with any other parameter. However, a positive and significant correlation was found between Iγ_R and Iγ_L with $r \geq .408$ ($p < .05$) (minimum value obtained between the three frequency ranges).
7. Manual laterality (EHI scores) did not correlate with any other parameter except the difference in gamma indices (Iγ_{DIF}). Table 5 shows the correlation values between Iγ_{DIF} and the manual laterality values for the various frequency ranges (see example in Figure 6).

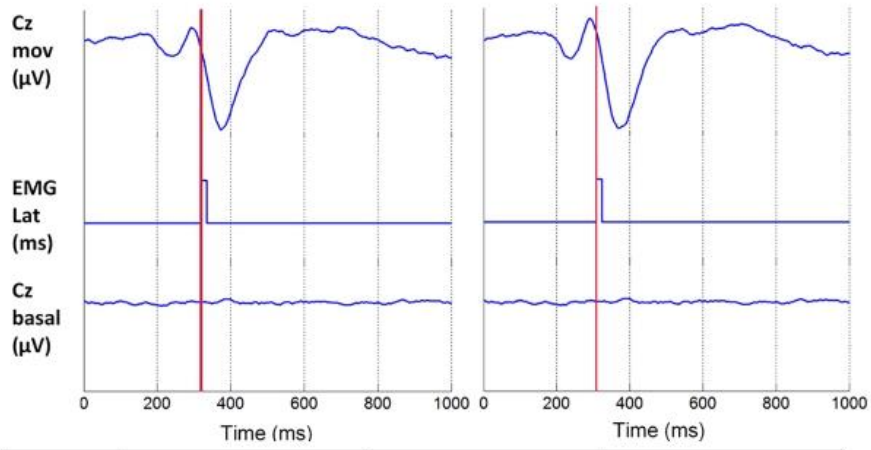

f (Hz)	IY_L	IY_{MOV}	IY_R
[30-60]	**1,2216** (1,1568 – 1,2864)	**1,2663** (1,1923 – 1,3403)	**1,3111** (1,2022 – 1,4199)
[60-90]	**1,2424** (1,1116 – 1,3732)	**1,2723** (1,1509 – 1,3937)	**1,3022** (1,1532 – 1,4511)
[30-90]	**1,2238** (1,1557 – 1,2918)	**1,2653** (1,1936 – 1,3369)	**1,3069** (1,2054 – 1,4082)

Figure 5 — Upper section: ERP graphs (Left and Right hand) obtained from the EEG Cz channel, based on the grand average (25 subjects) for the motor (Cz Mov) and basal (Cz Basal) tasks. The vertical lines indicate the average EMG activity onset latency (EMG_{LAT} (ms)). Lower section: Table showing average values (grand average of the 25 subjects) of the ERS ($I\gamma_R$, $I\gamma_L$ and $I\gamma_{MOV}$) for the three frequency ranges, expressed as: [mean (CI 95%)].

Table 4 Iγ and $I\gamma_{DIF}$ Classified by Manual Laterality Groups (L, A, R) and by Frequency Bands

f (Hz)	Iγ	L (*n* = 3)	A (*n* = 3)	R (*n* = 19)	$I\gamma_{DIF}$ L (*n* = 3)	$I\gamma_{DIF}$ A (*n* = 3)	$I\gamma_{DIF}$ R (*n* = 19)
[30–60]	$I\gamma_R$	1.1885	1.2174	1.3438*	-0.11 (< 0)	-0.07 (≈ 0)	0.14 (> 0)
	$I\gamma_L$	1.2963	1.2925	1.1987			
[60–90]	$I\gamma_R$	1.1948	1.1866	1.3373***	-0.35 (< 0)	-0.20 (< 0)	0.16 (> 0)
	$I\gamma_L$	1.5516	1.3933	1.1698			
[30–90]	$I\gamma_R$	1.1872	1.2131	1.3405**	-0.16 (< 0)	-0.10 (≈ 0)	0.15 (> 0)
	$I\gamma_L$	1.3426	1.3112	1.1912			

Note. Gamma index values ($I\gamma_R$, $I\gamma_L$) in the group R show that $I\gamma_R > I\gamma_L$ with tendency toward statistical significance ($p = .052$). Classification of the subtraction $I\gamma_{DIF} = (I\gamma_R — I\gamma_L)$ considering $I\gamma_{DIF} \leq |0.1|$ as (≈ 0). For each group, n = no. of subjects.

*$p = .035$

**Except in the 60–90 Hz band ($p = .130$).

***Confidence intervals are not expressed due to the small sample size.

Table 5 Pearson Correlation (r values) Between $I\gamma_{DIF}$ and Manual Laterality (EHI Scores)

f (Hz)	r ($I\gamma_{DIF}$, EHI)	Sig. (bilateral)
[30–60]	0.558	$p = .0037$*
[60–90]	0.632	$p = .0006$**
[30–90]	0.647	$p = .0004$**

Note. Correlation is significant (2 tails), *$p < .005$, **$p < .001$.

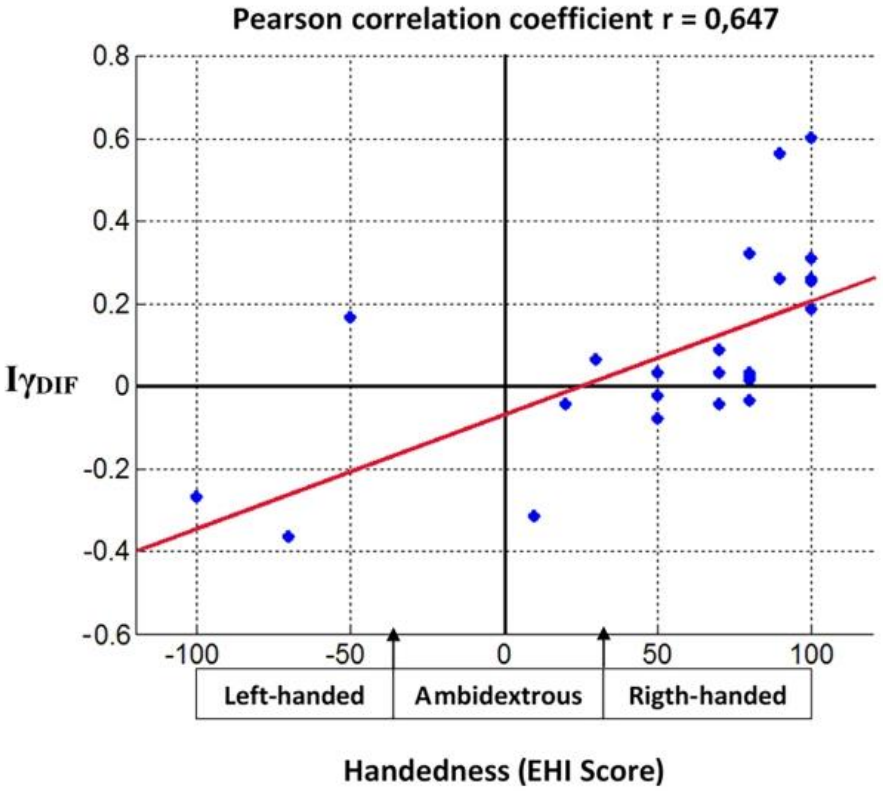

Figure 6 — Example of Pearson correlation between $I\gamma_{DIF}$ and the manual laterality score (EHI) for the 30–90 Hz frequency range, ($r = .647$, $p < .001$).

Discussion

Electrocorticography (ECoG) studies have confirmed that voluntary movements similar to those performed in this experiment generate GBA in somatosensory and motor areas (Crone, Miglioretti, Gordon, & Lesser, 1998). Therefore, it may be accepted that the GBA recorded in our motor experiment also originates from these same cortical areas.

Obtaining gamma-band signals from EEG surface recordings is technically challenging because of the gamma oscillations' reduced amplitude (< 1μV) and because the noise produced by muscle artifacts occurs in the same range of frequencies. Therefore, it is believed that the changes obtained in the 30–100 Hz range in electric scalp recordings (surface EEG) are almost completely attributable to EMG artifacts (Whitham et al., 2008). Only when recording the output of central EEG electrodes in the 30–45 Hz frequency band is EMG artifact occurrence low enough to allow detection of GBA in the form of significant changes in the EEG (Whitham et al., 2008).

In this paper, only data from the Cz channel was used, as it is the electrode that is most free of EMG artifacts (Fitzgibbon et al., 2013; Whitham et al., 2008). In addition, the following four facts suggest that the signal obtained in this analysis is genuine GBA oscillation and not EMG noise.

- *One*. If the signal obtained were mostly EMG noise, it would be evident predominantly, and would have greatest amplitude, in the high frequency band (60–90 Hz) and, to a lesser extent, in the low frequency band (30–60 Hz) because the EMG signal in the 30–45 Hz range is lower (Whitham et al., 2008). According to this hypothesis, Iγmov (60–90 Hz) would be expected to be much greater than Iγmov (30–60 Hz). However, in our findings the signal obtained in the high frequency band (60–90 Hz) behaves the same as that obtained in the low frequency band (30–60 Hz) (no significant differences were found). In other words, the gamma index remains constant in all the frequencies analyzed (Iγmov ≈ 1.27) This indicates that, in our case, the EEG signal obtained in the 60–90 Hz band is as little contaminated with EMG noise as the one in the 30–60 Hz band. Consequently, we believe that the activity recorded is principally GBA.
- *Two*. There are no differences in EMG signal amplitude in movement of the right or left hands (Table 2, EMG_{PAR}) while there are differences between $I\gamma_R$ and $I\gamma_L$ (Table 4). If the signal obtained were due to EMG artifacts, $I\gamma_R$ and $I\gamma_L$ would also be symmetrical.
- *Three*. A positive and significant correlation also exists between the gamma index and manual laterality, specifically between $I\gamma_{DIF}$ and EHI (Table 5). Figure 6 shows that the more right-handed a subject is, the greater the subject's $I\gamma_{DIF}$ (the subject produces more GBA when moving the right hand than when moving the left hand); and the more left-handed the subject is, the lower the subject's $I\gamma_{DIF}$ (the subject produces more GBA when moving the left hand than when moving the right hand). If the signal recorded were due to EMG artifacts, this correlation would not exist, as the movement amplitude (EMG_{PAR}) is similar for both hands and the activity recorded (supposed mainly to be EMG) would be the same for both hands. Therefore, the $I\gamma_R$ would be the same as the $I\gamma_L$ for all subjects, irrespective of manual laterality.
- *Four:* Finally, it would be logical to think that the recorded signal is GBA and not EMG artifacts because it behaves in accordance with neurophysiology. In other words, the correlation between $I\gamma_{DIF}$ and EHI (Figure 6) can also be explained as an expression of cerebral plasticity (Pascual-Leone, Amedi, Fregni, & Merabet, 2005). The more right-handed the subject is, the greater

the area of the cerebral cortex used to move the right hand as compared with the left one, meaning that $I\gamma_R > I\gamma_L$. Vice versa, when the subject is more left-handed $I\gamma_R < I\gamma_L$.

Returning to the results of our experiment: Firstly, averaging the motor task's EEG signal obtained an evoked activity (time-locked response) in the form of ERP. This motor-event-related potential (Figures 2 and 5) is similar in morphology and amplitude to those produced in similar motor experiments (Shibasaki, Barrett, Halliday, & Halliday, 1980; Shibata et al., 1999; Rinehart, Tonge, Bradshaw, Iansek, Enticott, & Johnson, 2006). This means that with our motor experiment design it is possible to obtain similar results to those produced by other published experiments.

In this motor experiment, the objective of attaining an ERP is not to analyze the parameters (ERP_{AMP}, EMG_{LAT}, etc.), but to ascertain whether the neuronal circuits involved in voluntary movement have been activated. Once we know that the motor task has activated these circuits, we extract and analyze the associated GBA, which in this case is the real objective of analysis.

Secondly, the ultimate objective is to obtain a simple numerical parameter that quantifies in percentage terms the ERS (increase in GBA) associated with the motor task. We have defined this ERS in terms of Iγ.

Iγ is an indirect indicator of the increase in GBA of the neurons involved in the movement (induced gamma oscillations), compared against the GBA generated during basal activity (spontaneous gamma oscillations). This Iγ is independent of the muscular force employed (EMG_{PAR}) and of subject age (no significant correlation exists with either of them).

Another significant parameter is the difference between the gamma indices ($I\gamma_{DIF}$), which gives us an idea of the predominance of GBA according to the subject's manual laterality. Thus, we found that in right-handed subjects ($I\gamma_R$—$I\gamma_L$) was > 0, while in left-handed subjects ($I\gamma_R$—$I\gamma_L$) was < 0 and in ambidextrous subjects ($I\gamma_R$—$I\gamma_L$) was closer to 0 (Table 4).

Numerous papers describe obtaining and quantifying GBA in motor areas. We can't compare these data obtained invasively using methods such as intracerebral recordings (Szurhaj, Bourriez, Kahane, Chauvel, Mauguière, & Derambure, 2005) and ECoG (Crone et al., 1998; Aoki, Fetz, Shupe, Lettich, & Ojemann, 1999; Ohara et al., 2000; Pfurtscheller, Graimann, Huggins, Levine, & Schuh, 2003; Miller, Schalk, Fetz, den Nijs, Ojemann, & Rao, 2010) with our results, because they record activity very close to or directly in the cerebral cortex and so avoid signal attenuation by biological tissue (meninges, bone and scalp) and have a high signal-to-noise ratio (SNR). These obtain high ERS values (ERS > 100%).

Neither we can't compare data obtained using MEG (Cheyne, Bells, Ferrari, Gaetz, & Bostan, 2008; Waldert et al., 2008; Cheyne, & Ferrari, 2013) because it records a magnetic signal that suffers little attenuation by biological tissue. It obtains variable ERS values (ERS ≈ 30–150%).

Therefore we only can compare our results with others obtained noninvasively using EEG (Shibata et al., 1999; Ball et al., 2008; Pfurtscheller, & Neuper, 1992; Pfurtscheller, Neuper, & Kalcher, 1993; Darvas, Scherer, Ojemann, Rao, Miller, & Sorensen, 2010; Demandt, Mehring, Vogt, Schulze-Bonhage, Aertsen, & Ball, 2012; Smith, Weaver, Grabowski, Rao, & Darvas, 2014) and MEG (Cheyne, Bells, Ferrari, Gaetz, & Bostan, 2008; Waldert et al., 2008; Cheyne, & Ferrari, 2013).

Very few papers have proposed using EEG to study GBA in relation to movement in humans and, due to the difficulty of recording GBA, these papers' findings are less clear, reporting values of ERS ≈ 10–20% (Shibata et al., 1999; Ball et al., 2008). Our EEG study is comparable to these latter ones and, quantitatively, we have obtained similar results with mean values of Iγ ≈ 1.27 in the various frequency ranges (Figure 5, Iγmov), which indicate ERS ≈ 27% (27% increase in motor GBA over basal GBA).

We have focused our analysis on the 30–90 Hz frequency band, though in our results we have expressed it in two frequency ranges, low GBA (30–60 Hz) and high GBA (60–90 Hz), as each has a different neurophysiological substrate (Crone et al., 1998). These different neurophysiological mechanisms may have significant diagnostic value in future clinical applications as well as in the research of the different networks involved in the motor control. Specifically high gamma-band activity is involved in cortical activity during rest or the performance of motor tasks during movement planning (Cheyne, & Ferrari, 2013).

Conclusions

In summary, a simplified GBA-analysis model applicable in clinical practice is proposed (Figure 7):

A conventional EEG is used to take two recordings of cerebral activity, one at rest and another when performing a simple motor task. Both recordings are analyzed using spectral power analysis to obtain the GBA. Averaging the data by frequency obtains the mean PSD value. Using the basal (γ_B) and motor (γ_{MOV}) GBA values, the ERS is calculated and defined as gamma index (Iγ), which is the motor area activity parameter that we propose for clinical use.

This parameter, Iγ, may offer a useful way of indirectly ascertaining operation of activated motor circuits from a clinical standpoint.

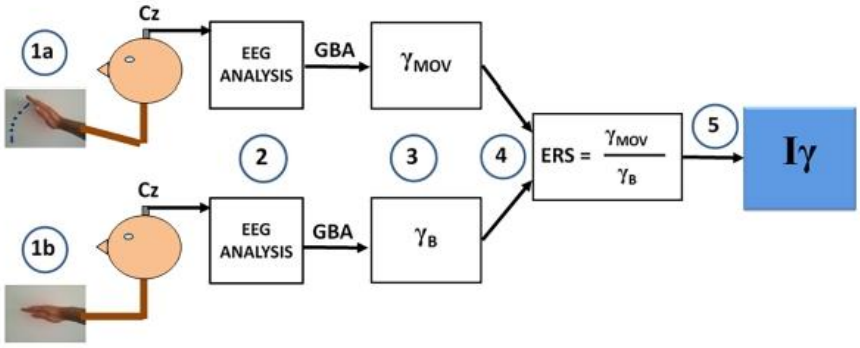

Figure 7 — Simplified model for clinical use. 1a) Motor task. 1b) Basal activity. 2) Acquisition and analysis of the EEG signal (power spectral analysis). 3) Obtaining of basal GBA (γ_B) and motor GBA (γ_{MOV}). 4) Calculation of the ERS. 5) Final parameter for clinical use (Iγ).

In some cortical diseases (vascular pathology traumatic and degenerative lesions) there are a damage of the excitatory pyramidal neurons and the GABAergic inhibitory interneurons responsible for gamma oscillations (GBA), therefore we guess that our method could be useful to assessment of the pathology of motor areas and as follow up in rehabilitation processes.

Another possible contribution by this method could be assessment of manual laterality in subjects based on the differences in cerebral activation when moving one hand or the other. This is because cerebral plasticity (Pascual-Leone et al., 2005) means that better results for Iγ will be obtained by moving the hand used most frequently to perform routine tasks.

Likewise, we believe that this method could enable the assessment of motor capacity, physical training and manual laterality in sport medicine.

Limitations and Drawbacks

Recording GBA using conventional EEG produces a low SNR, making acquisition in clinical practice difficult and not always possible. In fact, in our study 6 of the 31 participants (19.35%) were excluded because of the artifacts produced during the EEG recording.

An alternative way of obtaining the GBA noninvasively would be to acquire it by MEG, which would notably improve the SNR. However, MEG is a highly expensive technique and access to it in hospitals and health centers is very limited, meaning clinical use is not viable at present.

Our sample is very small and not uniformly distributed by age (rank: 18–47) or manual laterality (19 right-handed subjects, 3 left-handed subjects, and 3 ambidextrous subjects). It would be necessary to include older subjects and to balance the numbers of left-handed and ambidextrous subjects.

Our methodology could be improved in future studies as follows:

- Instruct subjects to close their eyes during the experiment (using an auditory stimulus or making continual hand movements without a cue) to avoid frequently produced blinking artifacts.
- Make the test more comfortable for subjects by reducing total recording time (by cutting the length of each trial) and by using a single EEG cable (Cz channel) rather than the cap with all the channels, etc.
- Simplify the analysis software to make it faster and more manageable.
- Use more complex mathematical signal-analysis methods that could improve the results (Iγ) of the study.

Finally, given the small sample size, the data obtained in this experiment could be confirmed by future studies with larger samples.

Acknowledgments

All the volunteers who participated in the study and contributors in the Department of Electronics at the University of Alcalá de Henares. The Rivas family (NSC Electromedicina), for its altruistic help and effective technical support. Michael Wibral, Cerisa Stawowsky, Georg-Friedrich Paasch and the team at the MEG Laboratory at the Max Planck Institut

in Frankfurt, for their guidance and patience. In memoriam, Felipe Quesney MD, PhD (Division of EEG and Clinical Neurophysiology, Montreal Neurological Institute, McGill University, Quebec, Canada), for always believing in the gamma band. To the Doctor Pedro Amo Merino, MD. The authors declared no potential conflicts of interest with respect to the research, authorship, and/or publication of this article. This research has been supported by Spain's Ministerio de Ciencia e Innovación under the "Advanced analysis of multifocal ERG and visual evoked potentials applied to the diagnosis of optic neuropathies" project (ref. TEC2011-26066).

References

Aoki, F., Fetz, E.E., Shupe, L., Lettich, E., & Ojemann, G.A. (1999). Increased gamma-range activity in human sensorimotor cortex during performance of visuomotor tasks. *Clinical Neurophysiology, 110*(3), 524–537. PubMed doi:10.1016/S1388-2457(98)00064-9

Ball, T., Demandt, E., Mutschler, I., Neitzel, E., Mehring, C., Vogt, K., . . . Schulze-Bonhage, A. (2008). Movement related activity in the high gamma range of the human EEG. *NeuroImage, 41*(2), 302–310. PubMed doi:10.1016/j.neuroimage.2008.02.032

Cardin, J.A., Carlen, M., Meletis, K., Knoblich, U., Zhang, F., Deisseroth, K., . . . Moore, C.I. (2009). Driving fast-spiking cells induces gamma rhythm and controls sensory responses. *Nature, 459*(7247), 663–667. PubMed doi:10.1038/nature08002

Cheyne, D., Bells, S., Ferrari, P., Gaetz, W., & Bostan, A.C. (2008). Self-paced movements induce high-frequency gamma oscillations in primary motor cortex. *NeuroImage, 42*(1), 332–342. PubMed doi:10.1016/j.neuroimage.2008.04.178

Cheyne, D., & Ferrari, P. (2013). MEG studies of motor cortex gamma oscillations: evidence for a gamma 'fingerprint' in the brain? *Frontiers in Human Neuroscience, 7,* 575. PubMed doi:10.3389/fnhum.2013.00575

Crone, N.E., Miglioretti, D.L., Gordon, B., & Lesser, R.P. (1998). Functional mapping of human sensorimotor cortex with electrocorticographic spectral analysis. II. Event-related synchronization in the gamma band. *Brain, 121*(Pt 12), 2301–2315. PubMed doi:10.1093/brain/121.12.2301

Darvas, F., Scherer, R., Ojemann, J.G., Rao, R.P., Miller, K.J., & Sorensen, L.B. (2010). High gamma mapping using EEG. *NeuroImage, 49*(1), 930–938. PubMed doi:10.1016/j.neuroimage.2009.08.041

Demandt, E., Mehring, C., Vogt, K., Schulze-Bonhage, A., Aertsen, A., & Ball, T. (2012). Reaching movement onset- and end-related characteristics of EEG spectral power modulations. *Frontiers in Neuroscience, 6,* 65. PubMed doi:10.3389/fnins.2012.00065

Fitzgibbon, S.P., Lewis, T.W., Powers, D.M.W., Whitham, E.W., Willoughby, J.O., & Pope, K.J. (2013). Surface Laplacian of central scalp electrical signals is insensitive to muscle contamination. *IEEE Transactions on Biomedical Engineering, 60*(1), 4–9. PubMed doi:10.1109/TBME.2012.2195662

Fries, P. (2009). Neuronal gamma-band synchronization as a fundamental process in cortical computation. *Annual Review of Neuroscience, 32,* 209–224. PubMed doi:10.1146/annurev.neuro.051508.135603

Herrmann, C.S., & Demiralp, T. (2005). Human EEG gamma oscillations in neuropsychiatric disorders. *Clinical Neurophysiology, 116*(12), 2719–2733. PubMed doi:10.1016/j.clinph.2005.07.007

Hirase, H., Iwai, Y., Takata, N., Shinohara, Y., & Mishima, T. (2014). Volume transmission signalling via astrocytes. *Philosophical Transactions of the Royal Society of London. Series B, Biological Sciences, 369*(1654), 20130604. PubMed doi:10.1098/rstb.2013.0604

Jia, X., & Kohn, A. (2011). Gamma rhythms in the brain. *PLoS Biology, 9*(4), e1001045. PubMed doi:10.1371/journal.pbio.1001045

Miller, K.J., Schalk, G., Fetz, E.E., den Nijs, M., Ojemann, J.G., & Rao, R.P. (2010). Cortical activity during motor execution, motor imagery, and imagery-based online feedback. *Proceedings of the National Academy of Sciences of the United States of America, 107*(9), 4430–4435. PubMed doi:10.1073/pnas.0913697107

Ohara, S., Ikeda, A., Kunieda, T., Yazawa, S., Baba, K., Nagamine, T., . . . Shibasaki, H. (2000). Movement-related change of electrocorticographic activity in human supplementary motor area proper. *Brain, 123*(Pt 6), 1203–1215. PubMed doi:10.1093/brain/123.6.1203

Oldfield, R.C. (1971). The assessment and analysis of handedness: the Edinburgh inventory. *Neuropsychologia, 9*(1), 97–113. PubMed doi:10.1016/0028-3932(71)90067-4

Oostenveld R, Fries P, Maris E, Schoffelen JM. FieldTrip: Open source software for advanced analysis of MEG, EEG, and invasive electrophysiological data. *Comput Intell Neurosci.* 2011;2011:156869.

Pascual-Leone, A., Amedi, A., Fregni, F., & Merabet, L.B. (2005). The plastic human brain cortex. *Annual Review of Neuroscience, 28,* 377–401. PubMed doi:10.1146/annurev.neuro.27.070203.144216

Pfurtscheller, G., Graimann, B., Huggins, J.E., Levine, S.P., & Schuh, L.A. (2003). Spatiotemporal patterns of beta desynchronization and gamma synchronization in corticographic data during self-paced movement. *Clinical Neurophysiology, 114*(7), 1226–1236. PubMed doi:10.1016/S1388-2457(03)00067-1

Pfurtscheller, G., & Lopez da Silva, F.H. (2011). EEG Event-Related Desynchronization (ERD) and Event-Related Synchronization (ERS). In D.L. Schomer & F.H. Lopes da Silva (Eds.), *Niedermeyer's Electroencephalography: Basic Principles, Clinical Applications, and Related Fields* (6th ed., pp. 935). Philadelphia: Lippincott Williams & Wilkins.

Pfurtscheller, G., & Lopes da Silva, F.H. (1999). Event-related EEG/MEG synchronization and desynchronization: basic principles. *Clinical Neurophysiology, 110*(11), 1842–1857. PubMed doi:10.1016/S1388-2457(99)00141-8

Pfurtscheller, G., & Neuper, C. (1992). Simultaneous EEG 10 Hz desynchronization and 40 Hz synchronization during finger movements. *Neuroreport, 3*(12), 1057–1060. PubMed doi:10.1097/00001756-199212000-00006

Pfurtscheller, G., Neuper, C., & Kalcher, J. (1993). 40-Hz oscillations during motor behavior in man. *Neuroscience Letters, 164*(1–2), 179–182. PubMed doi:10.1016/0304-3940(93)90886-P

Rinehart, N.J., Tonge, B.J., Bradshaw, J.L., Iansek, R., Enticott, P.G., & Johnson, K.A. (2006). Movement-related potentials in high-functioning autism and Asperger's disorder. *Developmental Medicine and Child Neurology, 48*(4), 272–277. PubMed doi:10.1017/S0012162206000594

Shibasaki, H., Barrett, G., Halliday, E., & Halliday, A.M. (1980). Components of the movement-related cortical potential and their scalp topography. *Electroencephalography and Clinical Neurophysiology, 49*(3–4), 213–226. PubMed doi:10.1016/0013-4694(80)90216-3

Shibata, T., Shimoyama, I., Ito, T., Abla, D., Iwasa, H., Koseki, K., . . . Nakajima, Y. (1999). Attention changes the peak latency of the visual gamma-band oscillation of the EEG. *Neuroreport, 10*(6), 1167–1170. PubMed doi:10.1097/00001756-199904260-00002

Smith, M.M., Weaver, K.E., Grabowski, T.J., Rao, R.P., & Darvas, F. (2014). Non-invasive detection of high gamma band activity during motor imagery. *Frontiers in Human Neuroscience, 8,* 817. PubMed doi:10.3389/fnhum.2014.00817

Szurhaj, W., Bourriez, J.L., Kahane, P., Chauvel, P., Mauguière, F., & Derambure, P. (2005). Intracerebral study of gamma rhythm reactivity in the sensorimotor cortex. *The European Journal of Neuroscience, 21*(5), 1223–1235. PubMed doi:10.1111/j.1460-9568.2005.03966.x

Tallon-Baudry, C., & Bertrand, O. (1999). Oscillatory gamma activity in humans and its role in object representation. *Trends in Cognitive Sciences, 3*(4), 151–162. PubMed doi:10.1016/S1364-6613(99)01299-1

Tan, H.R., Lana, L., & Uhlhaas, P.J. (2013). High-frequency neural oscillations and visual processing deficits in schizophrenia. *Frontiers in Psychology, 4,* 621. PubMed doi:10.3389/fpsyg.2013.00621

Uhlhaas, P.J., Haenschel, C., Nikolić, D., & Singer, W. (2008). The role of oscillations and synchrony in cortical networks and their putative relevance for the pathophysiology of schizophrenia. *Schizophrenia Bulletin, 34*(5), 927–943. PubMed doi:10.1093/schbul/sbn062

Uhlhaas, P.J., Pipa, G., Neuenschwander, S., Wibral, M., & Singer, W. (2011). A new look at gamma? High- (>60 Hz) γ-band activity in cortical networks: function, mechanisms and impairment. *Progress in Biophysics and Molecular Biology, 105*(1–2), 14–28. PubMed doi:10.1016/j.pbiomolbio.2010.10.004

Uhlhaas, P.J., & Singer, W. (2013). High-frequency oscillations and the neurobiology of schizophrenia. *Dialogues in Clinical Neuroscience, 15*(3), 301–313. PubMed

Waldert, S., Preissl, H., Demandt, E., Braun, C., Birbaumer, N., Aertsen, A., & Mehring, C. (2008). Hand movement direction decoded from MEG and EEG. *The Journal of Neuroscience, 28*(4), 1000–1008. PubMed doi:10.1523/JNEUROSCI.5171-07.2008

Whitham, E.M., Lewis, T., Pope, K.J., Fitzgibbon, S.P., Clark, C.R., & Loveless, S. (2008). DeLosAngeles D, Wallace AK, Broberg M, Willoughby JO. Thinking activates EMG in scalp electrical recordings. *Clinical Neurophysiology, 119*(5), 1166–1175. PubMed doi:10.1016/j.clinph.2008.01.024

8.2.2 Analysis of Gamma-Band Activity from Human EEG Using Empirical Mode Decomposition

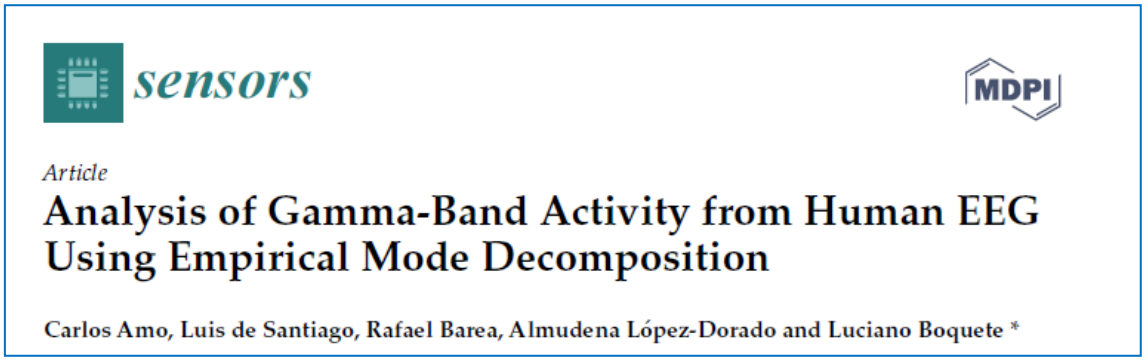

sensors

MDPI

Article

Analysis of Gamma-Band Activity from Human EEG Using Empirical Mode Decomposition

Carlos Amo, Luis de Santiago, Rafael Barea, Almudena López-Dorado and Luciano Boquete *

sensors

MDPI

Article

Analysis of Gamma-Band Activity from Human EEG Using Empirical Mode Decomposition

Carlos Amo, Luis de Santiago, Rafael Barea, Almudena López-Dorado and Luciano Boquete *

Departamento de Electrónica, Grupo de Ingeniería Biomédica, Universidad de Alcalá, Alcalá de Henares 28801, Spain; carlos.amo@edu.uah.es (C.A.); luis.desantiago@uah.es (L.d.S.); rafael.barea@uah.es (R.B.); almudena.lopez@uah.es (A.L.-D.)

* Correspondence: luciano.boquete@uah.es; Tel.: +34-918-856-572

Academic Editor: Wee Ser

Received: 2 February 2017; Accepted: 26 April 2017; Published: 29 April 2017

Abstract: The purpose of this paper is to determine whether gamma-band activity detection is improved when a filter, based on empirical mode decomposition (EMD), is added to the pre-processing block of single-channel electroencephalography (EEG) signals. EMD decomposes the original signal into a finite number of intrinsic mode functions (IMFs). EEGs from 25 control subjects were registered in basal and motor activity (hand movements) using only one EEG channel. Over the basic signal, IMF signals are computed. Gamma-band activity is computed using power spectrum density in the 30–60 Hz range. Event-related synchronization (ERS) was defined as the ratio of motor and basal activity. To evaluate the performance of the new EMD based method, ERS was computed from the basic and IMF signals. The ERS obtained using IMFs improves, from 31.00% to 73.86%, on the original ERS for the right hand, and from 22.17% to 47.69% for the left hand. As EEG processing is improved, the clinical applications of gamma-band activity will expand.

Keywords: electroencephalography; gamma-band activity; motor area; motor tasks; empirical mode decomposition; event-related synchronization; power spectral density

1. Introduction

1.1. Electroencephalogram (EEG)

An electroencephalogram (EEG) represents the electrical activity of the brain, recorded by placing several electrodes on the scalp. This activity is generated by the dendrites of the neurons adjacent to the cortical surface. The EEG frequency range is classified into neural oscillatory patterns: delta (1–4 Hz), theta (4–8 Hz), alpha (8–12 Hz), beta (15–30 Hz), and gamma-band oscillations (>30 Hz) [1].

One of the acknowledged issues with EEG is its low amplitude (on the order of microvolts) and high noise. Muscular artifacts, eye movements, and cardiac pulse are the principal sources of contamination in EEG recordings [2]. Semiautomatic detection of artifacts (eye blinks, muscle contraction, etc.) methods improve the quality of analysis results of EEG signals [3–5]. Signal processing methods, such as extraction of power spectral density (PSD) [6], wavelet analysis [7], independent component analysis (ICA) [8], and local mean decomposition [9], are used to improve recording quality and to analyze data. In most cases, automatic classification methods are implemented [10–13].

EEG is used extensively in neuroscience, cognitive science, cognitive psychology, neurolinguistics, and psychophysiological research. This is in addition to its more traditional place in clinical assessments or consciousness research [8].

The typical frequency range employed for the diagnosis of various brain conditions are low frequency bands (delta, theta, and alpha). Recently, new horizons have been explored by extracting

and analyzing high frequency (>30 Hz) components of EEG signals, applied to clinical assessments in diseases such as schizophrenia, visual processing deficits, and motor cortex dysfunctions. Robust results have been obtained using PSD computing in the frequency (>30 Hz) band [6,14,15].

Multichannel EEG systems are commonly employed to obtain high spatial resolutions. However, the setup process is time-consuming (attaching the electrodes to the scalp, adjusting the skin–electrode impedance value by adding gel). In addition, the system is uncomfortable and limits the movements of subjects. In ambulatory [2] or in portable-wearable applications, single-channel EEG systems are the best choice as they preserve brain activity very well, while also being easy to use. In recent years, acquisition and measurement techniques have been increasingly deployed in monochannel systems: dry electrodes, hardware systems, or new processing algorithms [16–18]. EEG monochannel systems are broadly used in several applications, such as brain computer interfaces [19], sleep studies [20,21], indicators of hypoxia [22], etc.

1.2. Gamma Activity

Gamma-band activity (GBA) comprises an EEG frequency range, from 30 to 200 Hz, and is distributed widely throughout cerebral structures. GBA participates in various cerebral functions, such as perception, attention, memory, consciousness, synaptic plasticity, and motor control [23].

Within the gamma-band frequency range, it is possible to differentiate between low gamma-band oscillations (30–60 Hz) and high gamma-band oscillations (60–200 Hz) [24].

Some electrophysiological studies have shown that gamma-band activity in the frequency range of 30 to 90 Hz can be recorded from a wide range of brain regions during rest or the performance of motor tasks [25,26].

During sensory, cognitive, and motor processes, two types of changes may be produced via electrical activity in the cerebral cortex. The first, evoked activity, is associated with stimulus and is time and phase locked. This evoked activity can be extracted from background activity in EEGs using linear methods, such as averaging. The second change is induced activity, associated with stimulus, and is time locked but not phase locked. Induced activity can only be extracted from background activity in EEGs using non-linear methods, such as power spectral analysis [27]. These non-linear methods use time–frequency transformations (e.g., Morlet wavelets or short-time Fourier transforms) on each individual trial prior to averaging across all trials [28].

Gamma bands were reported with visual stimulation and in movement or motor tasks [8]. The typical method to quantify induced GBA is comprised of the following steps: (a) band pass filtering and artifact rejection; (b) computing the power spectral density for a selected frequency range; and (c) quantifying the variations in GBA that are induced by a motor task (motor GBA) in relation to basal cortical activity (basal GBA) [29]. The decreases or increases in motor GBA, in relation to the basal level, are known as event-related desynchronization (ERD) and event-related synchronization (ERS), respectively [30]. The interpretation of ERD and ERS in the gamma band is related to a binding of sensory information and sensorimotor integration.

Gamma band activity is typically registered with a high number of electrodes: 128 [31] for the study of neural oscillations and event-related potentials in the sound-induced flash illusion in schizophrenia; 64 [32] for the assessment of tonic muscle pain; 32 [33] for multisensory processing deficits in patients with schizophrenia; or 30 [34] for computing sensory-evoked and event-related gamma coherences in Alzheimer's disease. This implies a long duration for the placement of electrodes and adjusting contact impedance. Complex signal processing methods must be used to reduce the noise and amplify components (band pass filters, artifact rejection, ICA, wavelets). Analyses are based on power spectral density computing in the band of interest using time-frequency analyses.

1.3. Empirical Mode Decomposition (EMD)

Since its presentation by Huan et al. in 1998 [8], EMD has been applied to study the non-linear and non-stationary properties of time series in areas such as geophysical studies [35], image analysis [36],

thermal profiles analysis [37], and power quality analysis [38]. EMD has demonstrated itself to be a reliable and effective method in the processing of different biomedical signals, such as EEGs [9], electromyography [39], visual evoked potentials [40], de-noising of ECG signals [11], and EEG artifact removal [2].

Few works have used EMD to study neural oscillatory pattern activity associated with tasks. In Reference [41], EMD was applied as a frequency filter to separate different frequency bands. In Reference [42], EMD was computed to obtain mu and beta rhythms in assessing motor imagery movements. Theta oscillation was selected using EMD in Reference [43]. In Reference [44], the authors demonstrated a better localization of time-varying frequency components of mu and beta rhythms during motor imagery using the EMD algorithm. In their following work [45], they used an extension of the algorithm of EMD, named multivariate EMD (MEMD), to circumvent the problem of cross-channel interdependence in a 64-channel setup. In this work, the gamma rhythm, decomposed using MEMD, showed a high correlation with the eventual movement accuracy.

1.4. Study Objectives

The main goal of this work was to investigate whether EMD monochannel EEG signal decomposition increased the detection of gamma-band activity of motor tasks. The original EMD method was applied as only one channel was used. This eliminated cross-channel interdependencies, avoiding the uniqueness problem [45]. As EEG processing was improved, the clinical applications of GBA were extended.

Because gamma activity is associated with a cognitive task-induced brain, the subjects of the experiment were induced to generate gamma band activity.

2. Materials and Methods

The study protocol was approved by the Ethics Committee of the Universidad de Alcalá (Madrid, Spain). Subjects participating in the study were required to sign an informed consent form prior to the start of the experiment.

2.1. Sample

The sample for this experiment was comprised of 31 subjects, six of whom were excluded during data analysis due to the presence of a high number of artifacts in their EEG recordings (blinking, muscle artifacts, etc.). All sample subjects were healthy, and none of the subjects were taking drugs or had a record of alcohol or drug abuse or dependency.

The final sample was comprised of 9 females and 16 males (mean age = 25.16; range = 18–47). The subjects were classified by manual laterality, according to the Edinburgh Handedness Inventory (EHI) [46], identifying 19 right-handed subjects (mean EHI = 79.47), 3 left-handed subjects (mean EHI = −73.33), and 3 ambidextrous subjects (mean EHI = 20.00).

The recording procedures were explained in detail in a previous publication [29]. Briefly, the experiment was comprised of two parts. In the first part (basal experiment), the subjects kept their eyes open and their gaze fixed on the center of a computer screen. A total of 18 min of basal activity was recorded. The objective of this first phase was to obtain basal GBA (spontaneous gamma oscillations) from the EEG trace.

In the second phase (motor experiment), the subjects performed a simple motor task immediately after receiving an on-screen cue, thereby obtaining motor GBA, induced by that movement (induced gamma oscillations), from the EEG trace. The task consisted of rapidly bending the wrist upwards and then briefly relaxing (rather than voluntarily flexing it). This task was performed for both hands and was organized into trials of 2 s of duration. Each trial started with the display of the cue in the center of the computer screen. This was followed by a white screen that remained in place until the start of the next trial. The cue was the order to start the motor task. The motor experiment comprised five

runs of 100 trials per hand. Runs alternated between the right and left hands to prevent muscle fatigue. Total motor task duration was approximately 40 min.

2.2. Data Acquisition

The equipment used in this experiment comprised a 32-channel Micromed EEG (Handy EEG SD32) and SystemPlus Evolution (Micromed SpA, Treviso, Italy) acquisition software. The recordings were obtained using a 22-bit sigma-delta A/D converter, with a sampling frequency (Fs) of 2048 Hz, an antialiasing band-pass filter set at 0.15–537.53 Hz, and a notch filter (50 Hz). Electrode impedances were kept below 10 kΩ to ensure that background noise in the acquired signal was <0.5 μV. The number of channels employed were, three for EEG, two for electrooculogram (EOG), and two for electromyogram (EMG). EEG (C3, C4, and Cz) was continuously recorded using an elastic cap, fitted with Ag/AgCl-positioned electrodes, as per the 10/20 system. FPz and Pz were the reference and ground electrodes, respectively. To monitor horizontal and vertical eye movement, the EOG signal was obtained via two electrodes, one placed above the outer canthus of the right eye and the other placed below the outer canthus of the left eye. The EMG signal was obtained via two surface electrodes (one active electrode and one reference electrode) located on each forearm, above the extensor carpi radialis longus muscle.

During all recordings, the laboratory lights were turned off and rechargeable batteries were used in the acquisition equipment to minimize potential AC induction at 50 Hz in the EEG power cables [47].

2.3. Data Analysis

The EEG, EMG, and EOG signals were analyzed, offline, using MATLAB 2016b (The MathWorks Inc., Natick, MA, USA) and FieldTrip [48], and the data were processed in European Data Format (EDF). The EEG signal measured on the Cz channel was analyzed. Figure 1 shows, block-by-block, the ERS computations.

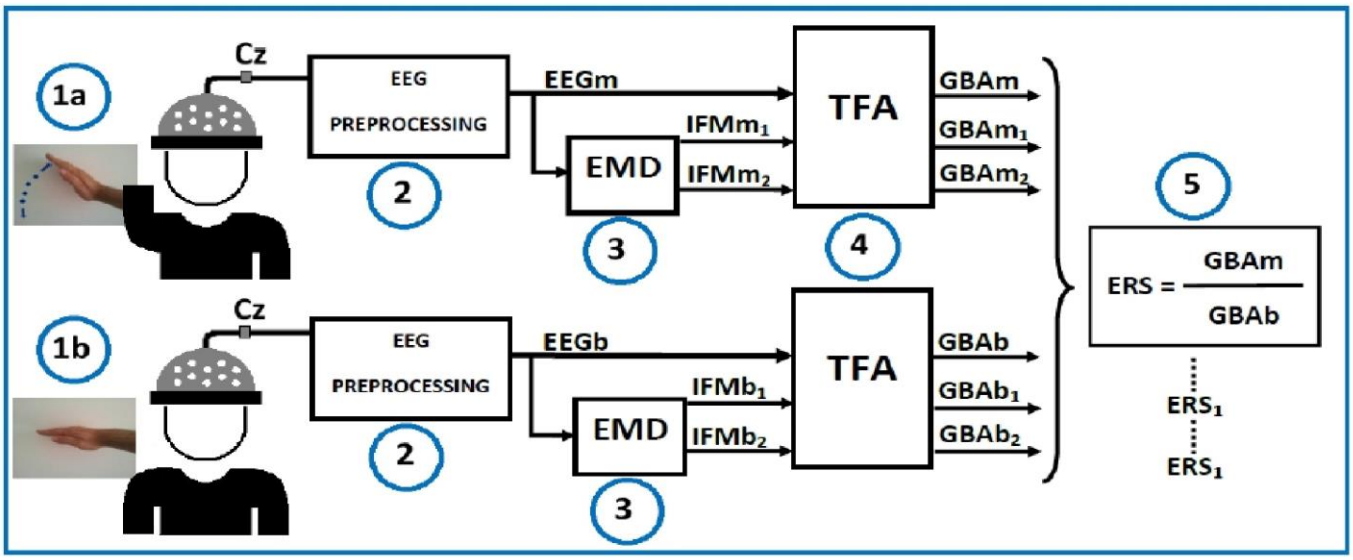

Figure 1. Simplified model of the event-related synchronization (ERS) calculation. Cz (electrode Cz from electroencephalogram (EEG) 10–20 system). (1a) Motor task; (1b) Basal activity; (2) Acquisition and analysis of the EEG signal (pre-processing); (3) Empirical Mode Decomposition (EMD) analysis of the EEG signal; (4) Time-frequency analysis (TFA) to obtain Gamma-band activity (GBA); (5) Calculation of the ERS.

The EEG pre-processing comprised a filter and artifact rejection stages. The signal was band-pass filtered (1–100 Hz) and narrow-band notch filtered (49–51 Hz eliminated band). Then, each trial was

visually inspected using the FieldTrip ft_RejectVisual function to eliminate amplitude jumps, eye blinks, and muscle movements that were not previously eliminated using automatic analysis (FieldTrip ft_RejectArtifact). Next, the linear trend error (FieldTrip ft_Detrend) was eliminated. The output of the EEG pre-processing block was noted as $x(t)$.

2.4. EMD Analysis of the EEG Signal

EMD decomposes a non-periodic and non-stationary signal into a finite number of intrinsic mode functions (IMFs). The IMFs must satisfy two conditions: (1) the number of extremes and the number of zero crossings are equal, or differ by no more than one, in the whole dataset; and (2) the mean value of the envelope defined by the local maximum and the envelope defined by the local minimum is zero at any point (IMFs are nearly periodic functions with zero mean). The original signal ($x(t)$) can be expressed as the sum of a finite number of IMFs and a residual

$$x(t) = \sum_{j=1}^{N} \mathrm{IMF}_j + r_N(t), \quad (1)$$

where N denotes the total number of IMFs, $\mathrm{IMF_j}$ is the jth intrinsic mode function, and r_N is the residue selecting N IMFs. EMD was applied to the $x(t)$ signal following four steps: (i) Find all extreme points (maxima and minima) of $x(t)$; (ii) generate the upper and lower envelopes (UE and LE, respectively) by interpolation of the maxima and minima with a cubic spline; (ii) compute the mean: $\mathrm{M}(t) = (\mathrm{UE} + \mathrm{LE})/2$; and (iv) subtract the mean from the original signal: $c(t) = x(t) - M(t)$.

This process is iterated until the resulting signal c(t) complies with the criteria of an intrinsic mode function. Then, IMF1 = $c(t)$ and the residue $r_1(t) = x(t) - c(t)$ is the new input signal for step (i), described above, ($x(t) = r_1(t)$).

The number of extreme points decreases as the number of previous loop iterations increases. This algorithm stops when: (1) $r(t)$ contains one extreme (maximum or minimum); (2) the computed IMF or the residual are too small; or (3) when five IMFs are computed.

The performance of Empirical Mode Decomposition is similar to that of a bank filter, where each IMF is bandwidth limited and can be identified as one of the frequency bands used in research and clinical practice. The only condition is that the sample frequency must be nearly five times that of the highest frequency of interest [49].

The EMD method estimates high-frequency modes first, since it fits envelopes through local minima and maxima. In Reference [50], the authors demonstrated that IMF1 represents the gamma band neuronal oscillation (>30 Hz), IMF2 represents beta band oscillation (13–30 Hz), IMF3 reflects the alpha band oscillation (8–13 Hz), IMF4 reflects the delta band oscillation (3.5–8 Hz) and IMFs 5 and 6 represent the theta band oscillation (0.5–3.5 Hz). Other works, such as References [51,52], also support the idea that IMF1 reflects the gamma band in EEG signals. Selecting the first IMF is comparable to a high-pass filtering based on Fourier methods. Unlike Fourier filtering, EMD does not remove components below an arbitrary cut-off frequency, so the gamma-band main contributions may vary between IMF1 and IMF2 [40]. An example of an EEG signal decomposed into IMF1 and IMF2 is shown in Figure 2 (with their corresponding frequency spectrums).

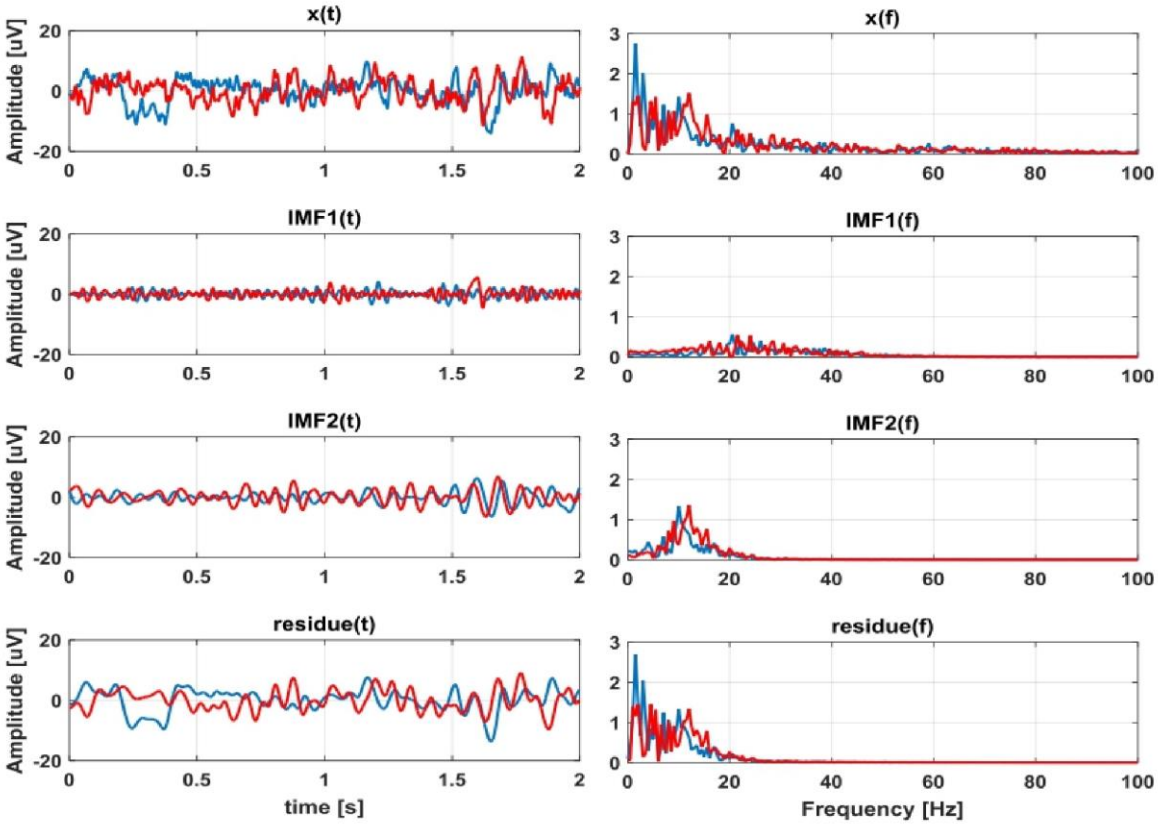

Figure 2. Example of electroencephalogram (EEG) signal decomposed into Intrinsic Mode Functions (IMF) IMF1, IMF2, and a residue. The left side is the time domain and the right side is the frequency domain. The red line depicts the basal activity, and the blue line is the motor activity (μV = micro Volts).

2.5. Calculation of TFA-GBA

The induced and spontaneous GBA were obtained from signals $x(t)$, IMF1(t), and IMF2(t) as power spectral values and were estimated using a multi-taper fast Fourier transform (FFT) (FieldTrip ft_freqanalysis function). The time-frequency analysis (TFA) computed the mean PSD value (in μV^2) in the frequency band (30–60 Hz). PSD reflected the amplitude of the neuronal oscillations, calculated using the time-frequency transformations [6]. GBA parameters were calculated for each individual trial and were averaged for each hand. An overall average was calculated for all subjects. Table 1 shows the parameters obtained in each experiment.

Table 1. Experimental parameters.

Experiment	Gamma Oscillations	Waveform *	TFA Output μV^2	Processing Method
Basal (b) activity	Spontaneous	$x(t)$ = EEGb	GBAb	Typical
		IMFb1	$GBAb_1$	Based on IMF1
		IMFb1	$GBAb_2$	Based on IMF2
Motor (m) activity	Induced	$x(t)$ = EEGm	GBAm	Typical
		IMFm1	$GBAm_1$	Based on IMF1
		IMFm2	$GBAm_2$	Based on IMF2

* As defined in Figure 1.

Once the basal GBA and motor GBA values were obtained for the right and left hands, ERS was defined by normalizing the values in relation to basal gamma activity and were presented as a

percentage. This established the ERS as Equation (2) for the original signal $x(t)$, as Equation (3) for the signal IMF1 (t), and as Equation (4) for the signal IMF2 (t).

$$\mathrm{ERS}(\%) = \frac{\mathrm{GBAm} - \mathrm{GBAb}}{\mathrm{GBAb}} \times 100, \quad (2)$$

$$ERS1(\%) = \frac{\mathrm{GBAm1} - \mathrm{GBAb1}}{\mathrm{GBAb1}} \times 100, \quad (3)$$

$$ERS2(\%) = \frac{\mathrm{GBAm2} - \mathrm{GBAb2}}{\mathrm{GBAb2}} \times 100, \quad (4)$$

Negatives values of ERS were obtained when the basal activity was higher than the motor activity. These ERS parameters were calculated for each hand of each subject. The total average was calculated for all subjects.

2.6. Statistical Analyses

All statistical analyses were performed using the SPSS 22.0 program (SPSS Inc., Chicago, IL, USA). Data were tested using the Kolmogorov and Smirnov methods to determine whether they followed a Gaussian distribution. The data sampled from the Gaussian distribution were compared using the paired Student's t-test, and non-Gaussian data were compared using the Wilcoxon test (non-parametric). Results are expressed as the mean and confidence interval (CI 95%). The significance value for the differences was set at $p < 0.05$.

3. Results

Table 2 shows the values (the total average for the 25 subjects) for the PSD of the basal GBA (GBAb, $GBAb_1$, and GBA_2) for the calculated frequency band.

Table 2. Average basal Gamma-band activity (GBA) values (Power Spectrum Density (PSD) in μV^2), expressed as the mean (CI 95%).

GBAb	$GBAb_1$	$GBAb_2$
0.0151 (0.0121–0.0180)	0.0059 (0.0045–0.0072)	0.0072 (0.0058–0.0086)

Table 3 shows the values (the total average for the 25 subjects) for the PSD of the motor GBA (GBAm, GBAm1, and GBAm2) for both hands.

Table 3. Average motor GBA values (PSD in μV^2), expressed as the mean (CI 95%).

Case	Left Hand	Right Hand
GBAm	0.0186 (0.0146–0.0225)	0.0194 (0.0156–0.0232)
GBAm1	0.0081 (0.0064–0.0098)	0.0088 (0.0071–0.0105)
GBAm2	0.0082 (0.0063–0.0100)	0.0083 (0.0063–0.0104)

The ERS values obtained from the original pre-processing signal ($x(t)$) were compared with ERS1 and ERS2, obtained from the EMD method (IMF1 (t), IMF2 (t)). Table 4 shows these values for each subject of the study.

Table 4. Study subjects detailed for each case. Bold results are the highest results for each subject.

		Right Hand			Left Hand		
		Typical	Based on IMFs		Typical	Based on IMFs	
Subject	Laterality *	ERS^{RH} *	$ERS1^{RH}$ *	$ERS2^{RH}$ *	ERS^{LH} *	$ERS1^{LH}$ *	$ERS2^{LH}$ *
1	A	30.7%	54.6%	3.5%	57.5%	67.6%	43.0%
2	R	32.0%	48.6%	22.6%	3.9%	5.4%	3.8%
3	R	13.0%	16.7%	6.7%	7.2%	13.3%	−3.3%
4	R	35.6%	15.6%	61.3%	17.8%	9.4%	33.3%
5	R	95.4%	291.7%	1.7%	23.1%	88.9%	3.4%
6	R	68.5%	429.4%	−19.3%	41.3%	294.1%	−23.8%
7	R	1.0%	−2.0%	5.4%	2.0%	0.0%	2.7%
8	R	25.3%	40.8%	17.0%	24.7%	46.0%	10.2%
9	R	9.4%	37.9%	−16.4%	17.2%	44.8%	−7.3%
10	L	1.7%	−2.0%	7.4%	23.3%	24.0%	25.9%
11	R	23.0%	47.4%	1.1%	18.4%	32.2%	7.0%
12	L	30.3%	35.8%	22.3%	59.1%	68.4%	46.2%
13	R	20.2%	25.8%	13.0%	22.2%	23.2%	19.3%
14	R	38.0%	59.7%	24.2%	34.1%	56.8%	19.7%
15	R	11.0%	29.1%	−1.0%	14.3%	35.6%	3.8%
16	R	27.8%	41.1%	15.8%	26.4%	32.6%	20.4%
17	L	24.6%	35.7%	13.0%	6.4%	14.9%	−0.5%
18	R	92.3%	296.8%	−10.4%	19.2%	65.0%	−4.3%
19	R	60.3%	26.0%	104.0%	38.2%	28.6%	52.7%
20	R	1.4%	51.8%	−19.3%	5.0%	49.5%	−14.3%
21	R	1.6%	−0.8%	7.8%	2.5%	−1.4%	9.0%
22	A	13.4%	89.6%	−10.8%	5.8%	76.0%	−15.9%
23	R	32.9%	19.6%	47.2%	22.7%	26.4%	21.2%
24	R	64.7%	146.5%	18.1%	37.1%	76.6%	13.4%
25	A	21.1%	11.1%	33.4%	24.4%	14.0%	36.5%

* RH = Right Hand, LH = Left Hand. Laterality: A = Ambidextrous, R = Right-handed, L = Left-handed.

When the data were analyzed subject by subject, in 18 of the 25 cases, the best method was IMF1 for both hands. In six subjects (4, 7, 10, 19, 21, and 25), IMF2 was the best method for both hands, and for one subject (23) the best method was different for each hand.

Higher values of ERS were found in the right hand in right-handed subjects. This is because the more right-handed the subject is, the greater the area of the cerebral cortex used to move the right hand as compared with the left hand [29]. The same applies for ERS values in the left hand in left-handed subjects. For example, subject number 12 is left-handed and $ERS1^{RH}$ * = 35.8% < $ERS1^{LH}$ * = 68.4% and subject number 6 is right-handed and $ERS1^{RH}$ * = 429.4% > $ERS1^{LH}$ * = 294.1%.

Figure 3 and Table 5 present the average and the statistic ERS values. As a result of the pre-processing of EEG signals using IMFs, the GBA detection was improved for both the right and left hands: ERS1 > ERS ($p < 0.05$) and ERS1 > ERS2 ($p < 0.05$). ERS1 improves from 31.00% to 73.86% of the original ERS results for the right hand and from 22.17% to 47.69% of the original results of the left hand. The grand average value of ERS2 is significantly lower than that of ERS in both hands (ERS < ERS2, $p < 0.05$). As many of the subjects were right-handed (19 of 25), the highest average values were obtained for the right hand compared to the left hand for the typical method (ERS^{RH} = 31.0% > ERS^{LH} = 22.17%) for ERS1 ($ERS1^{RH}$ = 73.86% > $ERS1^{LH}$ = 47.69%) and for ERS2 ($ERS2^{RH}$ = 13.93% > $ERS2^{LH}$ = 12.09%).

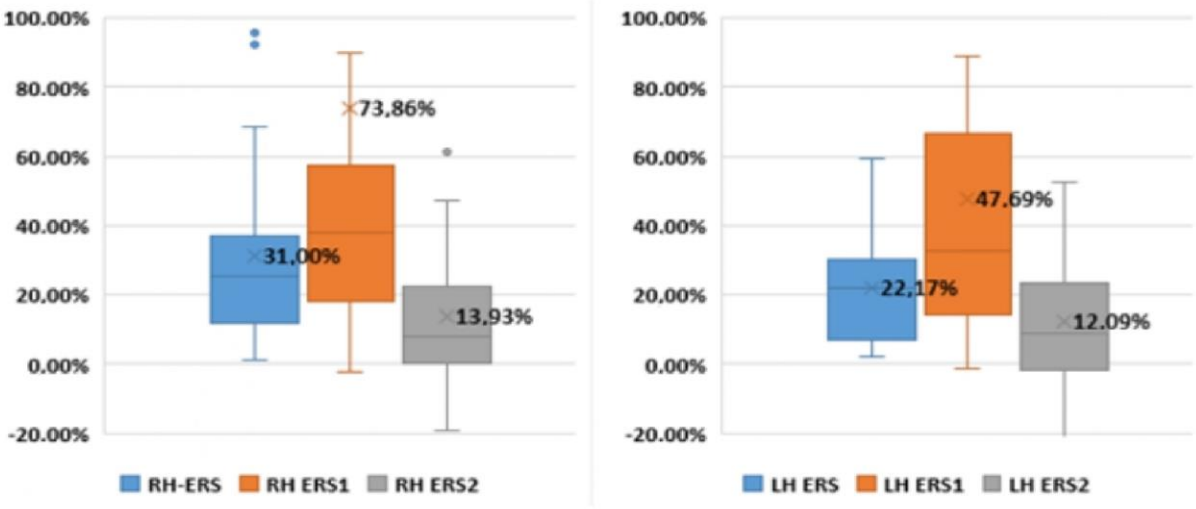

Figure 3. ERS values. RH = Right Hand, LH = Left Hand. To a better visualization, high outlier values have been removed.

Table 5. ERS values.

Hand		N	TEST	*p*
Right hand	ERS and ERS1	25	T-Student	0.023
	ERS and ERS2	25	T-Student	0.021
	ERS1 and ERS2	25	T-Student	0.020
Left hand	ERS and ERS1	25	T-Student	0.001
	ERS and ERS2 *	25	Wilcoxon	0.006
	ERS1 and ERS2 *	25	Wilcoxon	0.002

* ERS2 data follows a non-Gaussian distribution.

4. Discussion

The purpose of this paper was to apply an EMD method to EEG signal processing and to evaluate whether the obtained IMFs improved the analysis of GBA using only one channel. This method is based on filtering the EEG signal using empirical model decomposition (EMD), after artifact rejection, and before obtaining the PSD values (Figure 1, step 3). The performance of this new method (band pass and notch filter + artifact rejection + EMD decomposition + TFA) was evaluated via comparison with the typical method (band pass and notch filter + artifact rejection + TFA).

The method with the highest GBA values (computed as motor/basal PSD ratio, ERS) was considered the best method for use in clinical purposes. ERS1 improves, from 31.00% to 73.86%, the results of the original ERS for the right hand, and from 22.17% to 47.69% of the original results for the left hand. Significantly higher values were obtained when IMF1 was used rather than those of the typical method for both the right (ERS = 31.00%, ERS1 = 73.86%, $p < 0.05$) and left hands (ERS = 22.17%, ERS1 = 47.69%, $p < 0.05$). However, significantly lower values were obtained when IMF2 was used, as opposed to those of the typical method, for right (ERS = 31.00%, ERS2 = 13.93%, $p < 0.05$) and left hands (ERS = 22.17%, ERS2 = 12.09%, $p < 0.05$). In all cases (subjects and hands), the EMD method (ERS1 or ERS2) values were higher than the ERS values.

These results demonstrated that using EMD in pre-processing enhanced GBA detection and ERS computation. The decomposition, based on direct extraction of the signal energy in IMFs, is particularly helpful for non-stationary signal evaluation compared to those used in GBA and ERS. Better computation of ERS allows researchers to achieve better quantification of changes in the activity of local interactions between main neurons and interneurons, which control the frequency components

of the in-progress EEG. The use of EMD in the process of quantifying gamma-band activity could be transduced in an improvement of the diagnosis of functional deficits in patients with cerebrovascular disorders and Parkinson's disease [30].

The differences between ERS1 (obtained from IMF1) and ERS2 (obtained from IMF2) can be explained if EMD is interpreted as an adaptive filter [53]. The extracted IMFs are in decreasing order of frequency. The gamma-band can be considered "high EEG frequencies", so it makes sense that the first components of the EMD decompositions are associated with GBA. The EMD decomposition is intrinsic to the frequency components of the signal registered, thus, in subjects with high frequency components (above 60 Hz), IMF1 will be above the range and IMF2 will suit the gamma band under consideration (30 to 60 Hz). As an example, Figure 4 shows the PSD waveforms and ERS waveform for subject 1 (S1) in the 30–60 Hz band. In this case, it is clear that GBAb2 is higher below the 30 Hz frequency limit. The relationship between IMF1 and GBA has been found in previous works [50–52].

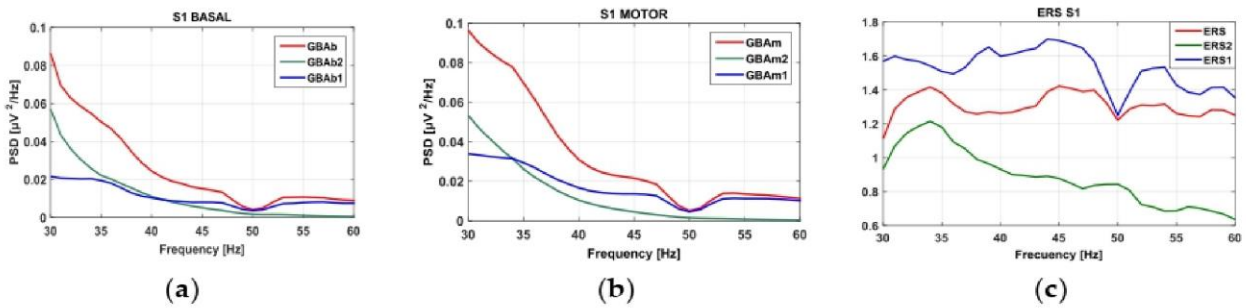

Figure 4. GBA signals from the right hand of subject S1: (**a**) Basal activity spectrum; (**b**) motor activity spectrum; (**c**) ERS spectrum.

The ERS values obtained using the original method agree with the results obtained in previous works: ERS ≈ 10–20% [54,55]. More recent studies [56] observed an increase in gamma-band activity in different tasks (emotional stimuli, face recognition, and motor control) using invasive techniques, such as electrocorticography. In our case, researchers obtained satisfactory results using a non-invasive technique.

From a neurophysiological point of view, it is important to remark that FPz has been selected as the reference because it is a midline electrode; thus, it is minimally contaminated by muscle artifacts [57]. One known problem of taking this point as reference is that the measured levels of GBA are low when Cz (active) minus FPz (reference) is computed. However, in this work, researchers compared the ratio between the motor activity and basal activity, so both parameters are equally affected by this fact, and the final ratio is unaltered.

EEG datasets obtained from setups with high numbers of EEG channels comprise a high dataset dimension, and this directly increases the computational complexity of performing further signal processing methods [58]; which further increases the time required to prepare the test. In this case, minimum complexity was been achieved using only one electrode.

5. Conclusions

As new methods to process and filter EEG signals are developed, the detection of gamma-band activity in motor tasks is improved. This study described how IMFs are effective in assessing GBA as a complement to Fourier-based methods. The ratio of motor and basal activity obtained using IMFs improved, from 31.00% to 73.86% of the original value, for the right hand, and 22.17% to 47.69% for the left. The new method can improve the study of cerebral motor areas and the assessment of neural diseases (vascular, traumatic, and degenerative pathologies). Complexity and testing time in clinical practice can be reduced because only one EEG channel is used.

Acknowledgments: This research was partially supported by Universidad de Alcalá grant: "Diagnóstico precoz de neuropatías ópticas mediante análisis de registros de potenciales evocados visuales multifocales" UAH GC2016-004 and ISCIII grant RETICS RD16/0008/0020.

Author Contributions: Designed the experiments: C.A. and L.B. Performed the experiments: C.A. Analyzed the data: L.d.S. and C.A. Developed analysis tools: L.d.S. and A.L.-D. Wrote the paper: L.d.S., C.A., and L.B. Supervised and managed the project: L.B. and R.B.

Conflicts of Interest: The authors declare no conflicts of interest. The founding sponsors had no role in the design of the study; in the collection, analyses, or interpretation of data; in the writing of the manuscript, and in the decision to publish the results.

References

1. Lally, N.; Mullins, P.G.; Roberts, M.V.; Price, D.; Gruber, T.; Haenschel, C. Glutamatergic correlates of gamma-band oscillatory activity during cognition: A concurrent ER-MRS and EEG study. *Neuroimage* **2014**, *85*, 823–833. [CrossRef] [PubMed]
2. Chen, X.; Liu, A.; Peng, H.; Ward, R. A Preliminary Study of Muscular Artifact Cancellation in Single-Channel EEG. *Sensors* **2014**, *14*, 18370–18389. [CrossRef] [PubMed]
3. Bhardwaj, S.; Jadhav, P.; Adapa, B.; Acharyya, A.; Naik, G.R. Online and automated reliable system design to remove blink and muscle artefact in EEG. In Proceedings of the 2015 37th Annual International Conference of the IEEE Engineering in Medicine and Biology Society (EMBC), Milan, Italy, 25–29 August 2015; pp. 6784–6787.
4. Kwon, Y.; Kim, K.I.; Tompkin, J.; Kim, J.H.; Theobalt, C. Efficient Learning of Image Super-Resolution and Compression Artifact Removal with Semi-Local Gaussian Processes. *IEEE Trans. Pattern Anal. Mach. Intell.* **2015**, *37*, 1792–1805. [CrossRef] [PubMed]
5. Feis, R.A.; Smith, S.M.; Filippini, N.; Douaud, G.; Dopper, E.G.; Heise, V.; Trachtenberg, A.J.; van Swieten, J.C.; van Buchem, M.A.; Rombouts, S.A.; et al. ICA-based artifact removal diminishes scan site differences in multi-center resting-state fMRI. *Front. Neurosci.* **2015**, *9*. [CrossRef] [PubMed]
6. Uhlhaas, P.J.; Singer, W. High-frequency oscillations and the neurobiology of schizophrenia. *Dialogues Clin. Neurosci.* **2013**, *15*, 301–313. [PubMed]
7. Sharma, R.; Pachori, R.B. Classification of epileptic seizures in EEG signals based on phase space representation of intrinsic mode functions. *Expert Syst. Appl.* **2015**, *42*, 1106–1117. [CrossRef]
8. Urigüen, J.A.; Garcia-Zapirain, B. EEG artifact removal—State-of-the-art and guidelines. *J. Neural Eng.* **2015**, *12*, 31001. [CrossRef] [PubMed]
9. Guo, Y.; Naik, G.R. Hung Nguyen Single channel blind source separation based local mean decomposition for Biomedical applications. In Proceedings of the 2013 35th Annual International Conference of the IEEE Engineering in Medicine and Biology Society (EMBC), Osaka, Japan, 3–7 July 2013; pp. 6812–6815.
10. Shin, Y.; Lee, S.; Ahn, M.; Cho, H.; Jun, S.C.; Lee, H.-N. Noise robustness analysis of sparse representation based classification method for non-stationary EEG signal classification. *Biomed. Signal Process. Control* **2015**, *21*, 8–18. [CrossRef]
11. Li, M.; Chen, W.; Zhang, T. Classification of epilepsy EEG signals using DWT-based envelope analysis and neural network ensemble. *Biomed. Signal Process. Control* **2017**, *31*, 357–365. [CrossRef]
12. Zhang, X.; Li, J.; Liu, Y.; Zhang, Z.; Wang, Z.; Luo, D.; Zhou, X.; Zhu, M.; Salman, W.; Hu, G.; et al. Design of a Fatigue Detection System for High-Speed Trains Based on Driver Vigilance Using a Wireless Wearable EEG. *Sensors* **2017**, *17*, 486. [CrossRef] [PubMed]
13. Chai, R.; Naik, G.; Nguyen, T.N.; Ling, S.; Tran, Y.; Craig, A.; Nguyen, H. Driver Fatigue Classification with Independent Component by Entropy Rate Bound Minimization Analysis in an EEG-based System. *IEEE J. Biomed. Health Inform.* **2016**. [CrossRef] [PubMed]
14. Ramyead, A.; Studerus, E.; Kometer, M.; Uttinger, M.; Gschwandtner, U.; Fuhr, P.; Riecher-Rössler, A. Prediction of psychosis using neural oscillations and machine learning in neuroleptic-naïve at-risk patients. *World J. Biol. Psych.* **2016**, *17*, 285–295. [CrossRef] [PubMed]
15. Ramyead, A.; Studerus, E.; Kometer, M.; Heitz, U.; Gschwandtner, U.; Fuhr, P.; Riecher-Rössler, A. Neural oscillations in antipsychotic-naïve patients with a first psychotic episode. *World J. Biol. Psych.* **2016**, *17*, 296–307. [CrossRef] [PubMed]

16. Zhang, Z.; Li, H.; Mandic, D. Blind source separation and artefact cancellation for single channel bioelectrical signal. In Proceedings of the 2016 IEEE 13th International Conference on Wearable and Implantable Body Sensor Networks (BSN), San Francisco, CA, USA, 14–17 June 2016; IEEE: New York, NY, USA, 2016; pp. 177–182.
17. Chen, X.; Liu, A.; Chiang, J.; Wang, Z.J.; McKeown, M.J.; Ward, R.K. Removing Muscle Artifacts from EEG Data: Multichannel or Single-Channel Techniques? *IEEE Sens. J.* **2016**, *16*, 1986–1997. [CrossRef]
18. Maddirala, A.; Shaik, R.A. Removal of EOG Artifacts from Single Channel EEG Signals Using Combined Singular Spectrum Analysis and Adaptive Noise Canceler. *IEEE Sens. J.* **2016**, *16*, 8279–8287. [CrossRef]
19. Minguillon, J.; Lopez-Gordo, M.A.; Pelayo, F. Trends in EEG-BCI for daily-life: Requirements for artifact removal. *Biomed. Signal Process. Control* **2017**, *31*, 407–418. [CrossRef]
20. Lucey, B.P.; Mcleland, J.S.; Toedebusch, C.D.; Boyd, J.; Morris, J.C.; Landsness, E.C.; Yamada, K.; Holtzman, D.M. Comparison of a single-channel EEG sleep study to polysomnography. *J. Sleep Res.* **2016**, *25*, 625–635. [CrossRef] [PubMed]
21. Da Silveira, T.L.; Kozakevicius, A.J.; Rodrigues, C.R. Single-channel EEG sleep stage classification based on a streamlined set of statistical features in wavelet domain. *Med. Biol. Eng. Comput.* **2017**, *55*, 343–352. [CrossRef] [PubMed]
22. Zhang, T.; Wang, Y.; Li, G. Effect of intermittent hypoxic training on hypoxia tolerance based on single-channel EEG. *Neurosci. Lett.* **2016**, *617*, 39–45. [CrossRef] [PubMed]
23. Uhlhaas, P.J.; Haenschel, C.; Nikolić, D.; Singer, W. The role of oscillations and synchrony in cortical networks and their putative relevance for the pathophysiology of schizophrenia. *Schizophr. Bull.* **2008**, *34*, 927–943. [CrossRef] [PubMed]
24. Uhlhaas, P.J.; Pipa, G.; Neuenschwander, S.; Wibral, M.; Singer, W. A new look at gamma? High- (>60 Hz) γ-band activity in cortical networks: Function, mechanisms and impairment. *Prog. Biophys. Mol. Biol.* **2011**, *105*, 14–28. [CrossRef] [PubMed]
25. Cheyne, D.; Bells, S.; Ferrari, P.; Gaetz, W.; Bostan, A.C. Self-paced movements induce high-frequency gamma oscillations in primary motor cortex. *Neuroimage* **2008**, *42*, 332–342. [CrossRef] [PubMed]
26. Cheyne, D.; Ferrari, P. MEG studies of motor cortex gamma oscillations: Evidence for a gamma "fingerprint" in the brain? *Front. Hum. Neurosci.* **2013**, *7*, 575. [CrossRef] [PubMed]
27. Pfurtscheller, G. EEG event-related desynchronization (ERD) and synchronization (ERS). *Electroencephalogr. Clin. Neurophysiol.* **1997**, *103*, 26. [CrossRef]
28. Tan, H.-R.M.; Lana, L.; Uhlhaas, P.J. High-frequency neural oscillations and visual processing deficits in schizophrenia. *Front. Psychol.* **2013**, *4*, 621. [CrossRef] [PubMed]
29. Amo, C.; del Castillo, M.O.; Barea, R.; de Santiago, L.; Martínez-Arribas, A.; Amo-López, P.; Boquete, L. Induced Gamma-Band Activity During Voluntary Movement: EEG Analysis for Clinical Purposes. *Motor Control* **2016**, *20*, 409–428. [CrossRef] [PubMed]
30. Pfurtscheller, G.; Lopes da Silva, F.H. Event-related EEG/MEG synchronization and desynchronization: Basic principles. *Clin. Neurophysiol.* **1999**, *110*, 1842–1857. [CrossRef]
31. Minzenberg, M.J.; Yoon, J.H.; Cheng, Y.; Carter, C.S. Sustained Modafinil Treatment Effects on Control-Related Gamma Oscillatory Power in Schizophrenia. *Neuropsychopharmacology* **2016**, *41*, 1231–1240. [CrossRef] [PubMed]
32. Li, L.; Liu, X.; Cai, C.; Yang, Y.; Li, D.; Xiao, L.; Xiong, D.; Hu, L.; Qiu, Y. Changes of gamma-band oscillatory activity to tonic muscle pain. *Neurosci. Lett.* **2016**, *627*, 126–131. [CrossRef] [PubMed]
33. Karch, S.; Loy, F.; Krause, D.; Schwarz, S.; Kiesewetter, J.; Segmiller, F.; Chrobok, A.I.; Keeser, D.; Pogarell, O. Increased Event-Related Potentials and Alpha-, Beta-, and Gamma-Activity Associated with Intentional Actions. *Front. Psychol.* **2016**, *7*. [CrossRef] [PubMed]
34. Başar, E.; Femir, B.; Emek-Savaş, D.D.; Güntekin, B.; Yener, G.G. Increased long distance event-related gamma band connectivity in Alzheimer's disease. *NeuroImage Clin.* **2017**, *14*, 580–590. [CrossRef] [PubMed]
35. Huang, N.E.; Wu, Z. A review on Hilbert-Huang transform: Method and its applications to geophysical studies. *Rev. Geophys.* **2008**, *46*. [CrossRef]
36. Nunes, J.; Bouaoune, Y.; Delechelle, E.; Niang, O.; Bunel, P. Image analysis by bidimensional empirical mode decomposition. *Image Vis. Comput.* **2003**, *21*, 1019–1026. [CrossRef]
37. Subhani, S.K.; Suresh, B.; Ghali, V.S. Empirical mode decomposition approach for defect detection in non-stationary thermal wave imaging. *NDT E Int.* **2016**, *81*, 39–45. [CrossRef]

38. Camarena-Martinez, D.; Valtierra-Rodriguez, M.; Perez-Ramirez, C.A.; Amezquita-Sanchez, J.P.; de Jesus Romero-Troncoso, R.; Garcia-Perez, A. Novel Downsampling Empirical Mode Decomposition Approach for Power Quality Analysis. *IEEE Trans. Ind. Electron.* **2016**, *63*, 2369–2378. [CrossRef]
39. Naik, G.R.; Selvan, S.E.; Nguyen, H.T. Single-Channel EMG Classification with Ensemble-Empirical-Mode-Decomposition-Based ICA for Diagnosing Neuromuscular Disorders. *IEEE Trans. Neural Syst. Rehabil. Eng.* **2016**, *24*, 734–743. [CrossRef] [PubMed]
40. Liang, H.; Bressler, S.L.; Buffalo, E.; Desimone, R.; Fries, P. Empirical mode decomposition of field potentials from macaque V4 in visual spatial attention. *Biol. Cybern.* **2005**, *92*, 380–392. [CrossRef] [PubMed]
41. Noshadi, S.; Abootalebi, V.; Sadeghi, M.T.; Shahvazian, M.S. Selection of an efficient feature space for EEG-based mental task discrimination. *Biocybern. Biomed. Eng.* **2014**, *34*, 159–168. [CrossRef]
42. Bashar, S.K.; Bhuiyan, M.I.H. Classification of motor imagery movements using multivariate empirical mode decomposition and short time Fourier transform based hybrid method. *Eng. Sci. Technol. Int. J.* **2016**, *19*, 1457–1464. [CrossRef]
43. Chang, C.-F.; Liang, W.-K.; Lai, C.-L.; Hung, D.L.; Juan, C.-H. Theta Oscillation Reveals the Temporal Involvement of Different Attentional Networks in Contingent Reorienting. *Front. Hum. Neurosci.* **2016**, *10*. [CrossRef] [PubMed]
44. Cheolsoo, P.; Looney, D.; Kidmose, P.; Ungstrup, M.; Mandic, D.P. Time-Frequency Analysis of EEG Asymmetry Using Bivariate Empirical Mode Decomposition. *IEEE Trans. Neural Syst. Rehabil. Eng.* **2011**, *19*, 366–373. [CrossRef] [PubMed]
45. Park, C.; Plank, M.; Snider, J.; Kim, S.; Huang, H.C.; Gepshtein, S.; Coleman, T.P.; Poizner, H. EEG Gamma Band Oscillations Differentiate the Planning of Spatially Directed Movements of the Arm Versus Eye: Multivariate Empirical Mode Decomposition Analysis. *IEEE Trans. Neural Syst. Rehabil. Eng.* **2014**, *22*, 1083–1096. [CrossRef] [PubMed]
46. Oldfield, R.C. The assessment and analysis of handedness: The Edinburgh inventory. *Neuropsychologia* **1971**, *9*, 97–113. [CrossRef]
47. Herrmann, C.; Demiralp, T. Human EEG gamma oscillations in neuropsychiatric disorders. *Clin. Neurophysiol.* **2005**, *116*, 2719–2733. [CrossRef] [PubMed]
48. Oostenveld, R.; Fries, P.; Maris, E.; Schoffelen, J.-M. FieldTrip: Open source software for advanced analysis of MEG, EEG, and invasive electrophysiological data. *Comput. Intell. Neurosci.* **2011**, *2011*, 156869. [CrossRef] [PubMed]
49. Huang, N.E.; Shen, Z.; Long, S.R.; Wu, M.C.; Shih, H.H.; Zheng, Q.; Yen, N.-C.; Tung, C.C.; Liu, H.H. The empirical mode decomposition and the Hilbert spectrum for nonlinear and non-stationary time series analysis. *Proc. R. Soc. A Math. Phys. Eng. Sci.* **1998**, *454*, 903–995. [CrossRef]
50. Tsai, F.-F.; Fan, S.-Z.; Lin, Y.-S.; Huang, N.E.; Yeh, J.-R. Investigating Power Density and the Degree of Nonlinearity in Intrinsic Components of Anesthesia EEG by the Hilbert-Huang Transform: An Example Using Ketamine and Alfentanil. *PLoS ONE* **2016**, *11*, e0168108. [CrossRef] [PubMed]
51. Liang, H.; Bressler, S.L.; Desimone, R.; Fries, P. Empirical mode decomposition: A method for analyzing neural data. *Neurocomputing* **2005**, *65*, 801–807. [CrossRef]
52. Hsu, C.-H.; Lee, C.-Y.; Liang, W.-K. An improved method for measuring mismatch negativity using ensemble empirical mode decomposition. *J. Neurosci. Methods* **2016**, *264*, 78–85. [CrossRef] [PubMed]
53. Flandrin, P.; Rilling, G.; Goncalves, P. Empirical Mode Decomposition as a Filter Bank. *IEEE Signal Process. Lett.* **2004**, *11*, 112–114. [CrossRef]
54. Shibata, T.; Shimoyama, I.; Ito, T.; Abla, D.; Iwasa, H.; Koseki, K.; Yamanouchi, N.; Sato, T.; Nakajima, Y. Attention changes the peak latency of the visual gamma-band oscillation of the EEG. *Neuroreport* **1999**, *10*, 1167–1170. [CrossRef] [PubMed]
55. Ball, T.; Demandt, E.; Mutschler, I.; Neitzel, E.; Mehring, C.; Vogt, K.; Aertsen, A.; Schulze-Bonhage, A. Movement related activity in the high gamma range of the human EEG. *Neuroimage* **2008**, *41*, 302–310. [CrossRef] [PubMed]
56. Babiloni, C.; Del Percio, C.; Vecchio, F.; Sebastiano, F.; Di Gennaro, G.; Quarato, P.P.; Morace, R.; Pavone, L.; Soricelli, A.; Noce, G.; et al. Alpha, beta and gamma electrocorticographic rhythms in somatosensory, motor, premotor and prefrontal cortical areas differ in movement execution and observation in humans. *Clin. Neurophysiol.* **2016**, *127*, 641–654. [CrossRef] [PubMed]

57. Fitzgibbon, S.P.; Lewis, T.W.; Powers, D.M.; Whitham, E.W.; Willoughby, J.O.; Pope, K.J. Surface Laplacian of central scalp electrical signals is insensitive to muscle contamination. *IEEE Trans. Biomed. Eng.* **2013**, *60*, 4–9. [CrossRef] [PubMed]
58. Chai, R.; Tran, Y.; Naik, G.R.; Nguyen, T.N.; Ling, S.H.; Craig, A.; Nguyen, H.T. Classification of EEG based-mental fatigue using principal component analysis and Bayesian neural network. In Proceedings of the 2016 38th Annual International Conference of the IEEE Engineering in Medicine and Biology Society (EMBC), Orlando, FL, USA, 16–20 August 2016; pp. 4654–4657.

8.2.3 Induced gamma band activity from EEG as a posible index of training-related brarin plasticity in motor tasks

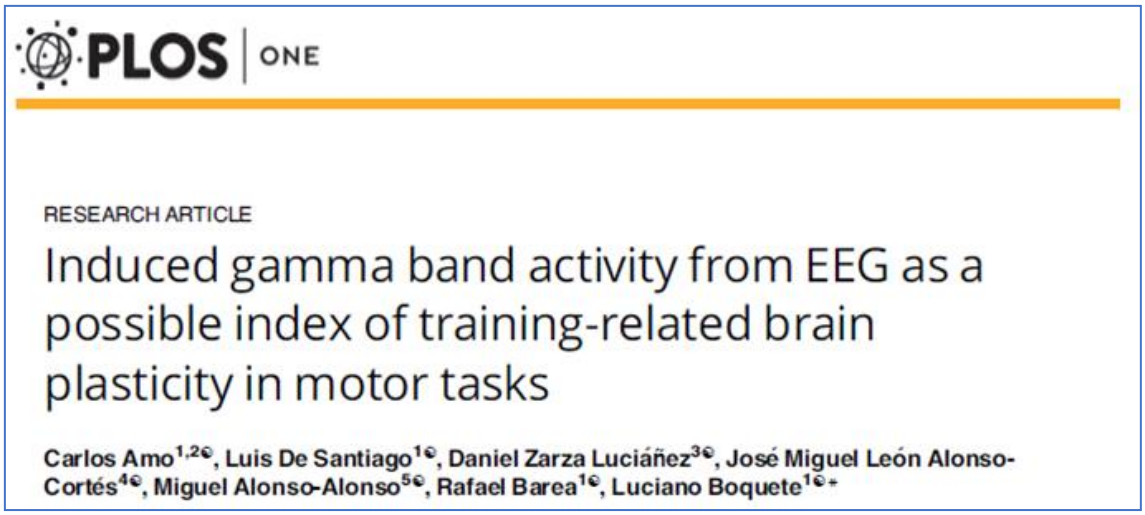

PLOS ONE

RESEARCH ARTICLE

Induced gamma band activity from EEG as a possible index of training-related brain plasticity in motor tasks

Carlos Amo[1,2☯], Luis De Santiago[1☯], Daniel Zarza Luciáñez[3☯], José Miguel León Alonso-Cortés[4☯], Miguel Alonso-Alonso[5☯], Rafael Barea[1☯], Luciano Boquete[1☯*]

PLOS ONE

RESEARCH ARTICLE

Induced gamma band activity from EEG as a possible index of training-related brain plasticity in motor tasks

Carlos Amo[1,2☯], Luis De Santiago[1☯], Daniel Zarza Luciáñez[3☯], José Miguel León Alonso-Cortés[4☯], Miguel Alonso-Alonso[5☯], Rafael Barea[1☯], Luciano Boquete[1☯*]

1 Department of Electronics, Universidad de Alcalá, Alcalá de Henares, Spain, **2** Research Department—Clinical Neurophysiology, Ecnis-Sigma SL, Madrid, Spain, **3** Department of Clinical Neurophysiology, Hospital Nisa Pardo de Aravaca, Madrid, Spain, **4** Department of Clinical Neurophysiology, Complejo Asistencial Universitario de Palencia, Hospital Río Carrión, Palencia, Spain, **5** Laboratory of Bariatric and Nutritional Neuroscience, Center for the Study of Nutrition Medicine, Beth Israel Deaconess Medical Center, Harvard Medical School Boston, MA, United States of America

☯ These authors contributed equally to this work.
* luciano.boquete@uah.es

Citation: Amo C, De Santiago L, Zarza Luciáñez D, León Alonso-Cortés JM, Alonso-Alonso M, Barea R, et al. (2017) Induced gamma band activity from EEG as a possible index of training-related brain plasticity in motor tasks. PLoS ONE 12(10): e0186008. https://doi.org/10.1371/journal.pone.0186008

Editor: Tifei Yuan, Nanjing Normal University, CHINA

Received: June 22, 2017

Accepted: September 22, 2017

Published: October 5, 2017

Data Availability Statement: All relevant data are within the paper and its Supporting Information files.

Funding: This research was partially supported by Universidad de Alcalá grant: "Diagnóstico precoz de neuropatías ópticas mediante análisis de registros de potenciales evocados visuales multifocales" UAH GC2016-004 and ISCIII grant RETICS RD16/0008/0020 to LB. The funders had no role in study design, data collection and

Abstract

The aim of this study was proposing gamma band activity (GBA) as an index of training-related brain plasticity in the motor cortex. Sixteen controls underwent an experimental session where electroencephalography (EEG) activity was recorded at baseline (resting) and during a motor task (hand movements). GBA was obtained from the EEG data at baseline and during the task. Index of plasticity (IP) was defined as the relationship between GBA at the end of the motor task (GBA_{M_FIN}), divided by GBA at the beginning of the task (GBA_{M_INI}) for movements of both hands. There was a significant increase in GBA at the end of the task, compared to the initial GBA for the motor task ($GBA_{M\_FIN} > GBA_{M\_INI}$). No differences were found at baseline ($GBA_{B\_FIN} \approx GBA_{B\_INI}$). Individual IP values had a positive ($r = 0.624$) and significant correlation with subject's handedness. Due to plastic changes, GBA could indirectly but objectively reveal changes in cerebral activity related to physical training. This method could be used as a future diagnostic test in the follow-up of patients undergoing rehabilitation. It could also have potential applications in the fields of sports medicine.

Introduction

Plasticity is an intrinsic property of the human brain that enables it to adapt to variations in the physical environment, physiologic changes and new experiences. Plastic changes occur by modifying pre-existing neuronal connections through changes in cortico-cortical and cortico-sub-cortical networks in response to new afferent impulses or efferent demands. This way, the initial modifications changed-mediated at molecular and cellular level can be followed by the establishment of new connections through dendritic growth and arborisation [1].

One of the founding fathers in the study of brain plasticity, Santiago Ramón y Cajal, already argued in his book, *Textura del Sistema Nervioso* [2], that the ability to modify behavior must

analysis, decision to publish, or preparation of the manuscript. There was no additional external funding received for this study.

Competing interests: The authors have declared that no competing interests exist.

have an anatomical basis in the brain and thus, he extended the notion of plasticity to a neural substrate. In this book he proposed, as an example, the skills of a pianist which require many years of mental and physical practice.

With the acquisition of new abilities, the brain changes initially through the reinforcement of the established neuronal networks and, subsequently, with the generation of new circuits. These plastic changes imply an increase in the activated cortical areas. The phenomenon is well illustrated in the following motor experiment [3]. During five days of practice, a group of healthy volunteers were trained to play a specific musical sequence with the five fingers of one hand. With this training it was possible to significantly improve the ability to perform the sequence and decrease the number of errors. Motor cortical areas were mapped through focal transcranial magnetic stimulation (TMS) that can be used to treat and measure the nervous system [4,5]. This technique confirms a significant increase of the cortical representation of the extensor and flexor muscles of the fingers of the used hand. The same results were obtained with the mental practice of the same motor sequence of the fingers (imagined movement).

Physiological changes produced by plasticity can be long-lasting. For example, it has been confirmed that after several years of training, the representation of the motor cortical areas is very different for the fingers of the right and left hand of professional violinists [6]. It is also observed in sports practice that physical training causes plastic modulation of neuronal circuits [7].

An objective way of quantifying plastic changes due to motor training could be measuring the activity of cortical networks involved during the voluntary movement. This variation of the cortical activity has been described in several experiments with electroencephalography (EEG) as an event-related synchronization (ERS) in the frequencies of the gamma band (>30 Hz) [8–10].

Gamma band activity (GBA) is widely distributed in all cerebral structures, as well as in the retina and olfactory tract. It is generated by GABA, glutamate and acetylcholine neurotransmitters and has been linked to key brain functions such as perception, attention, memory, consciousness, synaptic plasticity and motor control [11].

The aim of this study is to describe a new EEG-based method to quantify the effects of motor training by measuring plastic changes in the brain cortex, specifically via GBA related to motor activity. The measure of these plastic changes could serve as a quantitative biomarker to motor cerebral disorders and for evaluation in rehabilitation therapies or in sport medicine.

As repeated activity of a specific movement is known to lead to new interconnections, implying a higher number or neurons [1], we hypothesized that:

1. Due to plastic changes, the power of GBA would be significantly higher at the end of a motor task (more neurons involved in the movement) than at the beginning (fewer neurons involved in the movement).
2. An index of plasticity (IP) would best represent these changes. This index would be defined as the ratio between the GBA at the end of a motor task and the GBA at the beginning ($IP = GBA_{M\_FIN} / GBA_{M\_INI}$).

Material and methods

This study was approved by the Ethics Committee of the University of Alcalá (Madrid, Spain). Informed written consent was obtained from all participants prior to any study procedure.

Sample

A total of 16 subjects took part in the experiment (6 females, 10 males) with a mean age of 27.12 years (range: 20–47). All subjects were healthy, with no previous known medical,

psychiatric or neurological disease, including head injury, epilepsy, past history of alcoholism or drug abuse. Only medication-free subjects were allowed to take part in the study.

Experimental procedures

Participants sat on a comfortable chair facing a computer monitor placed 0.8 m away from their head. Forearms were in resting position on a table and with hand palms facing down.

The experiment consisted of two parts (baseline and motor experiment), conducted in a single session for each subject.

During the baseline part of the experiment, subjects remained with eyes open staring at a black dot displayed at the center of a white screen. A total of 18 minutes of baseline activity were acquired, divided in 3 parts (6 minutes) with a resting period between them of approximately one minute. The purpose of this first part was to obtain baseline GBA (spontaneous gamma oscillations) of the EEG.

In the second part (motor experiment), participants performed a motor task immediately after a signal (cue) was displayed on the screen. The task consisted in a quick extension of the wrist followed by a light relaxation. Subjects practiced this exercise previously in a training session (repeating 10 times the motor task with each hand: the cue was displayed on the screen and the subject moved the hand). The purpose of this second part was to obtain the movement-related GBA (induced gamma oscillations) of the EEG.

The motor task was performed in trials of two seconds that started at t = 0 seconds with the cue being displayed at the center of the screen for 150 ms, followed by a white screen which remained until the beginning of the next trial (t = 2 s).

The complete motor experiment consisted of 500 trials (500 extensions of the wrist) for each hand divided in 5 runs. Each run consists of 100 consecutive trials. Right and left hand runs were alternated in order to prevent from muscle fatigue. The total duration of the motor experiment was approximately 40 minutes.

Throughout the experiment (baseline and motor), subjects remained starring at a fixed dot on the screen to control for variability in eye movements and they were instructed to avoid blinking, swallowing or any other movements apart from the one required with the hand.

At the end of the experimental sessions participants were asked to fill in the Edinburgh Handedness Inventory scale (EHI), to determine manual laterality [12]. The final sample was composed by 11 right-handed, 2 left-handed and 3 ambidextrous subjects.

Data acquisition

EEG was acquired with a 32-channel Micromed system, model Handy EEG SD32 and the acquisition software *System Plus Evolution* (Micromed SpA, Treviso, Italy). We used an A/D sigma-delta converter with 22 bits of resolution, sampling frequency 2048 Hz, band pass filters 0.15–537.53 Hz, a notch filter of 50 Hz and electrode impedances < 10 kΩ.

We used three EEG channels (Cz, FPz and Pz), two channels of Electrooculogram (EOG) and four channels of Electromyogram (EMG). EEG was recorded using Ag/AgCl electrodes located according to the 10/20 system. Cz was the active electrode; FPz and Pz were reference and ground electrodes respectively. EOG was recorded to monitor the ocular vertical-horizontal movements with an electrode placed over the external ocular edge of the right eye and the other one placed under the external ocular edge of the left eye. EMG was obtained through two surface electrodes (active plus reference) placed above each of the forearms over the extensor *carpi radialis longus* muscle.

During recordings the lights of the laboratory were turned off and we used batteries for the acquisition equipment and for the computer with the purpose of reducing as much as possible

the induction of the alternating signal to 50 Hz in the wires of EEG. A more detailed description of the experimental methodology and procedures can be found in a recent publication [10].

Data analysis

The EEG, EMG and EOG signals were analyzed offline using *Matlab 2009b* (The Math Works Inc. Natick, MA, USA) and *FieldTrip* [13] and the data were processed in European Data Format.

The signal of the baseline part of the experiment (acquired without triggers) was divided into segments of the same duration as for the trials of the motor experiment (2 seconds) in order to compare them. The signal of the motor experiment was divided according to the 2 seconds trials based on the triggers corresponding to each cue.

EEG signal was high-pass filtered (1 Hz) to remove baseline drift and low-pass filtered (100 Hz). In addition, a 49-51Hz notch filter has been implemented to minimize power line interference. Butterworth method (fourth-order, zero phase shift) has been used to implement the filters.

Using the *ft_RejectArtifact* and the *ft_RejectVisual* functions of FieldTrip, EMG and EOG artifacts were discarded applying the function's standard parameters and the corresponding EMG (30–100 Hz) and EOG (1–70 Hz) filters. The linear trend error was eliminated using the *ft_Detrend* function.

After these processing steps, we obtained the following parameters from EMG and EEG (free of artifacts), average value for each subject and for all of them (grand average).

EMG parameters. Mean amplitude (EMG_{MEAN}) and maximum amplitude (EMG_{MAX}) were calculated in each trial. Also the peak-average ratio (EMG_{PAR}) was defined as: $\mathbf{EMG_{PAR}} = \frac{\mathbf{EMG_{MAX}}}{\mathbf{EMG_{MEAN}}}$.

Calculation of GBA. The GBA was obtained from the spectral power values for the frequency band 30–60 Hz and was calculated with multi taper Fast Fourier Transform (FFT), using the *ft_freqanalysis* function. Results were expressed as the average value of the power spectral density (PSD) in μV^2.

For each subject, we calculated the PSD separately for each trial and the average of all trials of the baseline and motor task.

Based on the average values of the PSD, the following parameters were defined:

- Baseline GBA (GBA_B): the PSD during the baseline experiment, representing the spontaneous gamma oscillations.
- Motor GBA (GBA_M): the PSD during the motor task of the right (GBA_{MR}) or left (GBA_{ML}) hand, representing the induced gamma oscillations.

Calculation of the ERS (event related synchronization) from GBA. ERS was defined by normalizing the GBA_M values with respect to GBA_B:

- ERS during motor activity of the right hand: $ERS_R = \frac{GBA_{MR}}{GBA_B}$
- ERS during the motor activity of the left hand: $ERS_L = \frac{GBA_{ML}}{GBA_B}$

Calculation of the motor task intervals. With the purpose of comparing the GBA at the beginning and end of the motor task, three groups of trials (free of artifacts) were defined:

- initial [GBA_{M_INI} = 100 first trials of the motor task],

Table 1. IP definitions for each case.

Basal	Motor		
Increase of GBA_B	Right IP	Left IP	IP difference between sides
$\Delta GBA_B = \frac{GBA_{B\_FIN}}{GBA_{B\_INI}}$	$IP_R = \frac{GBA_{MR\_FIN}}{GBA_{MR\_INI}}$	$IP_L = \frac{GBA_{ML\_FIN}}{GBA_{ML\_INI}}$	$IP_R - IP_L$

https://doi.org/10.1371/journal.pone.0186008.t001

- middle [GBA_{M_MID} = 100 trials in the middle of the motor task],
- final [GBA_{M_FIN} = 100 last trials of the motor task].

The different groups of GBA_M are identified with letters "R" for the right hand (GBA_{MR_INI}, GBA_{MR_MID}, GBA_{MR_FIN}) and "L" for the left one (GBA_{ML_INI}. . .).

Calculation of the index of plasticity (IP). Table 1 shows the IP definitions for basal and motor parameters.

The variation of basal activity cannot be considered as a plastic change so is not defined as IP. The variation or increase of the basal activity is defined as ΔGBA_B and does not imply functional changes. In order to calculate ΔGBA_B (Table 1), the average values of the initial and final periods of the baseline experiment (GBA_{B_INI} and GBA_{B_FIN}) are obtained. These initial and final periods of the baseline experiment are equivalent and can be compared to the ones in the motor task.

IP was defined as the relationship between the GBA at the end of the motor task (GBA_{M_FIN}) divided by the GBA at the beginning of the same motor task (GBA_{M_INI}) for movements of both hands. The IP index difference was defined with the purpose of verifying if there were differences according to the manual laterality of each subject. Fig 1 shows the procedures to calculate the IP_R (which is the same for the IP_L and for ΔGBA_B).

Statistical analysis

All statistical analyses were performed using the SPSS 21.0 statistical package software (SPSS Inc. Chicago, Illinois, USA). Student's t test (t test) was used to compare the averages and Pearson's linear correlation was used to compare quantitative variables. The Gaussian distribution assumption was tested using the Kolmogorov–Smirnov test.

The results are expressed as average and confidence interval (CI 95%). The significance value for the differences was set at $p < 0.05$.

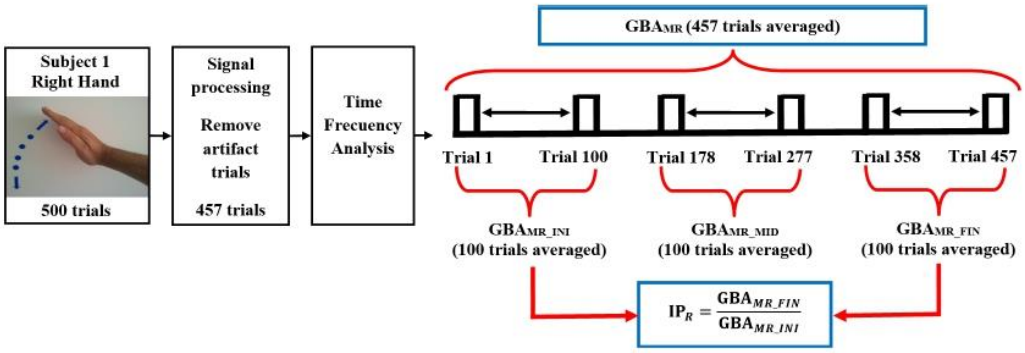

Fig 1. Example of the procedure used for the calculation of IP_R (subject 1, right hand). In this example 457 of the 500 trials of the motor task were obtained free of artifact. The GBA_{MR} value expressed as μV^2 is obtained through the time-frequency analysis of the valid trials (457). For the calculation of the IP_R, the average value of the last 100 valid trials is obtained (GBA_{MR_FIN}) and it is divided by the average value of the first 100 valid trials (GBA_{MR_INI}). The IP has no units. GBA = Gamma band activity, IP = Index of plasticity, MR = Motor Right, INI = Initial, MID = Middle, FIN = Final.

https://doi.org/10.1371/journal.pone.0186008.g001

Results

We present the results based on the steps taken to test the study hypotheses.

First step: Obtain the GBA values

Fig 2 shows the GBA values of the baseline part of the experiment (GBA_B) were compared with the ones from the motor part of the experiment (GBA_{MR} and GBA_{ML}). We also compared values of the right (GBA_{MR}) and left (GBA_{ML}) hand. The average values (16 subjects) of GBA are the following (Mean (CI 95%)): $GBA_B = 0.0154$ (0.0119–0.0189), $GBA_{MR} = 0.0191$ (0.0144–0.0237) and $GBA_{ML} = 0.0193$ (0.0141–0.0243). There was a significant increase ($p < 0.001$) of the GBA of both hands in movement with respect to the GBA at rest ($GBA_{MR} > GBA_B$ and $GBA_{ML} > GBA_B$). No significant differences were found between both hands ($GBA_{MR} \approx GBA_{ML}$, $p = 0.799$).

Second step: Obtain the ERS values

The average values (16 subjects) for right and left hand of the ERS are the following (Mean (CI 95%)): $ERS_R = 1.2365$ (1.1467–1.3161) and $ERS_L = 1.2486$ (1.1402–1.3212).

The increase (ERS) of the motor GBA over the basal GBA expressed as % is:

$$ERS_{R(\%)} = \frac{GBA_{MR}}{GBA_B} = 23.65\%$$

$$ERS_{L(\%)} = \frac{GBA_{ML}}{GBA_B} = 24.86\%$$

There was no significant difference between ERS_R and ERS_L.

Third step: Prove that there is no correlation between the EMG amplitude and the GBA during movement

Table 2 provides the average values of the EMG amplitude expressed as EMG_{PAR} and the GBA during movement (GBA_{MR}, GBA_{ML}), for both hands.

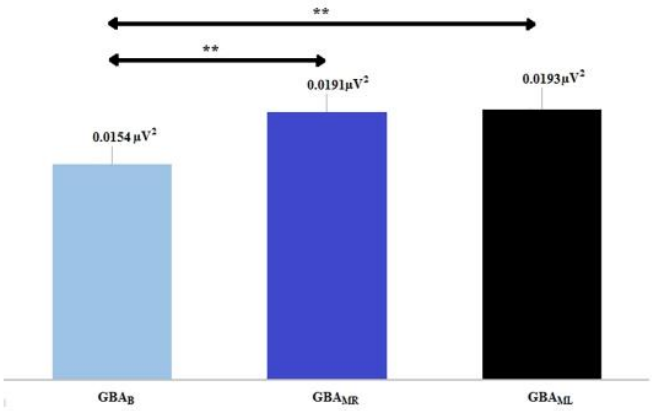

Fig 2. Average values of the GBA (PSD in μV^2) at rest and during the movement of both hands. It is observed that $GBA_{MR} > GBA_B$ and $GBA_{ML} > GBA_B$. There are no significant differences between the movements of both hands ($GBA_{MR} \approx GBA_{ML}$). GBA = Gamma Band Activity, B = Basal, MR = Motor Right, ML = Motor Left. Asterisks indicate highly statistically significant difference ($p<0.01$).

https://doi.org/10.1371/journal.pone.0186008.g002

Table 2. EMG_{PAR} and GBA values (average and CI 95%).

	Left hand	Right hand
EMG_{PAR} (μV/μV)	**11.8** (10.9–12.8)	**12.3** (10.5–14.1)
GBA ($μV^2$)	GBA_{ML} =	GBA_{MR} =
	0.0191 (0.0144–0.0237)	**0.0193** (0.0141–0.0243)

EMG = Electromyogram, GBA = Gamma Band Activity, ML = Motor Left, MR = Motor Right.

https://doi.org/10.1371/journal.pone.0186008.t002

There were no significant correlations between both parameters in both hands, right ($EMG_{PAR\ right}$, GBA_{MR}; r = -0.043, p = 0.874) and left ($EMG_{PAR\ left}$, GBA_{ML}; r = 0.271, p = 0.310), indicating that the GBA obtained during the motor task was independent from the amplitude (EMG) of the performed movement.

Fourth step: Calculation of the GBA for the three intervals of the motor task and calculation of the index of plasticity

Here we expected to prove that the GBA_B did not increase over time while the GBA_{MR} and GBA_{ML} increased with movement repetition (training). In order to do that, the average values of the GBA were calculated for each of the intervals of the experiment (initial, middle and final) which were previously defined. Baseline activity was also divided into intervals equivalent to the ones of the motor task in order to compare them. The average values (16 subjects) of GBA of each interval are shown in Table 3.

There was a significant increase of the final activity compared to the initial activity for the motor task ($GBA_{MR\_FIN} > GBA_{MR\_INI}$ (p = 0.044) and $GBA_{ML\_FIN} > GBA_{ML\_INI}$ (p = 0.042)) while there was no significant difference for the baseline activity ($GBA_{B\_FIN} > GBA_{B\_INI}$, not significant, p = 0.086).

Fig 3 shows the average values of the GBA were also calculated by intervals only for right-handed subjects (n = 11: 7 males, 4 females). We did not calculate that for ambidextrous (n = 3) or for left-handed subjects (n = 2) due to the limited sample.

Based on the GBA values by intervals, the indices of plasticity were calculated for the movements of both hands (IP_R, IP_L) and the variation of the final baseline activity with respect to the initial one (ΔGBA_B). The variation of the baseline activity is considered only to demonstrate that it does not undergo significant changes over time and to compare it to the plasticity indices (IP_R, IP_L).

Table 4 shows the plasticity indices for the total sample (n = 16) and for the sample of right-handed subjects (n = 11). Significant differences were found between the ΔGBA_B and both plasticity index (ΔGBA_B vs. IP_R, p = 0.04 and ΔGBA_B vs. IP_L, p = 0.03). No significant differences were found between both plasticity index (IP_R vs. IP_L, p = 0.77).

Table 3. GBA values: Basal, right and left in the different intervals of the experiment.

	Interval		
	Initial	**Middle**	**Final**
GBA_B ($μV^2$)	0.0152	0.0156	0.0155
GBA_{MR} ($μV^2$)	0.0179	0.0195	0.0203
GBA_{ML} ($μV^2$)	0.0172	0.0195	0.0215

Total sample (16 subjects). GBA = Gamma Band Activity
MR = Motor Right, ML = Motor Left.

https://doi.org/10.1371/journal.pone.0186008.t003

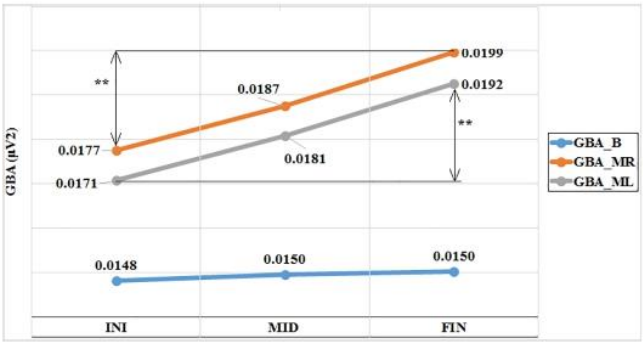

Fig 3. Average values of the GBA (PSD in μV^2) at rest and during the movement of both hands. The values are represented according to the time intervals (initial, middle, final) for the right-handed subjects (n = 11). GBA = Gamma Band Activity, B = Basal, MR = Motor Right, ML = Motor Left, INI = Initial, MID = Middle, FIN = Final. Asterisks indicate statistically significant difference.

https://doi.org/10.1371/journal.pone.0186008.g003

Fifth step: Test the coherence of the results with the neurophysiology

Fig 4 shows the correlation between IP, determined by the difference of indices (IP_R–IP_L) and manual laterality (r = 0.624, p = 0.01). The regression line shows a significant relationship between manual laterality (EHI) and the indices difference (IP_R–IP_L).

Discussion

The purpose of this study was to describe a method to quantify the effects of the voluntary movements (motor task) on the motor cortex through the quantification of increases of the GBA. The knowledge and the evaluation of these cortical plastic changes could be applied in the clinical practice.

We found GBA changes during repeated practice of a specific movement. There was a significant increase in GBA at the end of the task, compared to the initial GBA for the motor task ($GBA_{M\_FIN} > GBA_{M\_INI}$) ($p < 0.05$). No differences were found at baseline ($GBA_{B\_FIN} \approx GBA_{B\_INI}$).

In previous experiments with magnetoencephalography (MEG), it has been verified that the same motor task used in this study, causes activation of the motor cortical network (primary and supplementary motor areas) with both voluntary and imagined movement [14,15].

Our findings suggest that evaluation of training-induced changes in GBA and IP can improve the assessment of brain activity. In this work, these changes have been related with voluntary movement.

In order to quantify training-related brain plastic changes, it would be necessary to quantify the changes in the activated cortical areas before and during an intervention. This cortical measure can be performed by means of different neuroimaging and neurophysiology

Table 4. IP_R, IP_I and ΔGBA_B values for the total sample and for the right-handed subjects.

	Total sample (n = 16)	Right-handed (n = 11)
ΔGBA_B	1.0168	1.0176
IP_R	1.1144	1.1075
IP_L	1.2442	1.1218

GBA = Gamma Band Activity, IP = Index of Plasticity, R = Right, L = Left.

https://doi.org/10.1371/journal.pone.0186008.t004

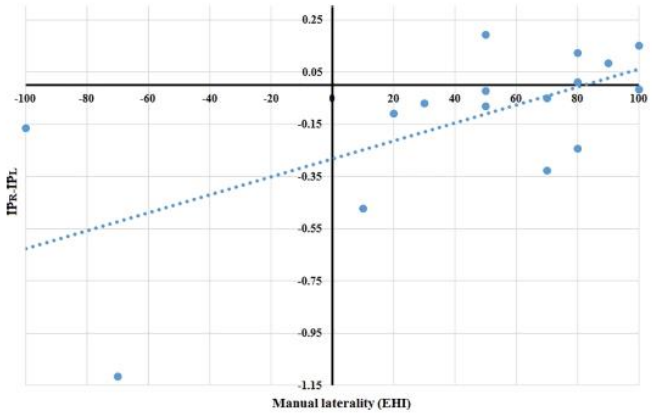

Fig 4. Correlation between the manual laterality (Edinburgh Handedness Inventory (EHI)) and the difference of indices (IP_R–IP_L). Total sample 16 subjects. IP = Index of plasticity, R = Right, L = Left.

https://doi.org/10.1371/journal.pone.0186008.g004

techniques; EEG, MEG, positron emission tomography (PET), TMS and functional magnetic resonance imaging (fMRI) [1,3,6,7,16,17]. All of these techniques provide an approximate and indirect measure of the activated cerebral areas although the only real and direct measure of the activated cerebral areas (gamma activity) during movement would be electrocorticography (ECoG). The problem of ECoG is the high invasivity [18].

Studies performed with conventional EEG to quantify the effects of exercise on the brain are easier, but they only measure changes in the power spectrum of the different frequency bands of the EEG [19–21]. A more approximate measure with EEG would be the quantification of cortical motor activity with ERS, but it could only measure the activity increase during exercise in relation to baseline activity [8]. This measure would be more closely related to cortical excitability than with the size of the cortical area involved.

However, this experiment could indirectly measure plastic changes by comparing the gamma activity of the EEG at the beginning (GBA_{M_INI}) with the gamma activity at the end of the repeated exercise (GBA_{M_FIN}). Specifically, we defined an Index of Plasticity, $IP = \frac{GBA_{M\_FIN}}{GBA_{M\_INI}}$, which should be > 1 according to the initial hypothesis $GBA_{M\_FIN} > GBA_{M\_INI}$. We could also define IP based on ERS:

If $ERS_{FIN} = \frac{GBA_{M\_FIN}}{GBA_B}$ and $ERS_{INI} = \frac{GBA_{M\_INI}}{GBA_B}$ then:

$$IP = \frac{ERS_{FIN}}{ERS_{INI}} = \frac{GBA_{M\_FIN}/GBA_B}{GBA_{M\_INI}/GBA_B} = \frac{GBA_{M\_FIN} \times GBA_B}{GBA_B \times GBA_{M\_INI}} = \frac{GBA_{M\_FIN}}{GBA_{M\_INI}}$$

Thus, the parameter IP described in this paper quantifies the activation of new areas and their progress over time with the repetition of the exercise, that is, plastic changes.

One important question is whether these training-induced GBA changes are related to a greater number of cortical motor areas involved in a specific motor task, in other words, if the proposed IP is indeed measuring plasticity.

In ECoG studies, the activated areas during movement have been compared with the increases of the GBA, demonstrating that ERS values change with the different motor tasks and with the different activated areas, consequently, it can be approximately assumed that for the same motor task, the greater the underlying area, the higher the value of ERS [8].

Therefore, the IP mathematically defined by changes of the ERS, would indicate an approximate measure of plasticity. Cortical area maps obtained with other techniques as TMS, fMRI, ECoG, etc.) could be carried out to confirm this fact.

To demonstrate that this experiment measure the proposed IP, we tested the initial hypotheses following different steps through the obtained results:

- The first step was to prove that the GBA during movement is significantly higher than the baseline GBA. Fig 2 shows a significant increase of the GBA with the movement with respect to baseline GBA ($GBA_{MR} > GBA_B$ and $GBA_{ML} > GBA_B$ ($p < 0.01$ in both hands)). This first step proved that the described task produced a quantifiable and significant GBA, what implies that the activation of the motor cortex can be measured.
- The second step consisted in calculating the ERS values: $ERS_R = 23.65\%$ and $ERS_L = 24.86\%$. These ERS values were in the same range as the others reported in previous studies with motor tasks similar to the one used in the current study, which obtained ERS values ≈ 10–30% [10,22–24].
- In the third step we proved that there was no significant correlation between the movement intensity of the hand (EMG_{PAR}) and the GBA_M. This means that the activation of the motor cortex (GBA_M) was measured independently from the amplitude of EMG (EMG_{PAR}) obtained during the motor task. This result is in line with other similar experiment in which the amplitude, duration and frequency of oscillations were not related to movement parameters [25].
- The fourth step corresponded to the calculation of the IP. Fig 3 demonstrated that the GBA_B does not increase over time ($GBA_{B\_FIN} > GBA_{B\_INI}$ (not significant)), while the GBA_{MR} and GBA_{ML} increase with the repetition of the movement ($GBA_{MR\_FIN} > GBA_{MR\_INI}$ ($p < 0.05$) and $GBA_{ML\_FIN} > GBA_{ML\_INI}$ ($p < 0.05$)).
- The fifth step provides evidence for the coherence of results with neurophysiology. As shown in Table 4, we observed an IP_R and IP_L asymmetry (not significant) in the total sample (n = 16), possibly because the sample is heterogeneous. However, if only the right-handed subjects (n = 11) were considering, IP_R and IP_L values were similar.
  The relation of the IP with manual laterality could be established; the (Pearson) correlation between manual laterality (EHI) and the indices difference (IP_R–IP_L) was positive (r = 0.624) and significant (p = 0.01) (Fig 4). Despite the negative value (IP_R–IP_L) presented by some of the right-handed subjects, the general trend showed by the regression line is coherent with the neurophysiology because the more right-handed the subject is, more brain cortex recruits when the right motor task progresses, and vice versa. The more left-handed the subject is, the more recruitment of brain cortex is observed as the left motor task progresses.

Based on the 5 steps stated above, we proved our study hypotheses. Due to plastic changes, GBA power is significantly higher at the end of a motor task than at the beginning. This method obtains GBA by means of the EEG and defines the IP; our results are significant and coherent with neurophysiology.

The methodology we describe here is an objective measure of the GBA that could be used as an approximate and indirect measure of the neuronal plasticity. Other methods based on neuroimaging and neurophysiology like the MEG, PET, TMS and fMRI could be more direct, but they are not as accessible due to their complexity and high cost, and they would not be very practical in sports medicine or in routine clinical practice.

Our study has limitations. The plastic capacity of the brain could be measure indirectly with the method presented in this paper. It is not possible to establish a direct comparison with other previous studies because there are not publications which describe a measure of brain plasticity similar to the IP described here. In this study we evaluated GBA changes induced by exercise which implies activation changes of different cerebral areas, while in

previous research described functional changes (MEG, FMRI, TMS, and PET) [6,7,16,17] or focused only on the power spectrum of the EEG [19–21]. As a second limitation, the sample that we used was very small and it was not homogeneously distributed in manual laterality (11 right-handed, 2 left-handed and 3 ambidextrous subjects). It would be necessary to introduce more subjects and balance the number of left-handed and ambidextrous subjects. Regarding the method, it could be improved and simplified in further studies taking into account the following:

- Conduct the experiment with closed eyes, using an auditory stimulus or making a constant movement of the hands without cue, in order to avoid the frequent blinking artifact.
- Make the test more comfortable for the subject, reducing the total recording time (shorting the time of each trial).

Finally, our study did not evaluate longitudinal changes beyond what was found in a brief session of training. Future studies should evaluate changes in IP over longer periods of time and in larger sample sizes. Other interesting cases to study are to compare results between gender (male/females) or between different age groups (young/old).

Conclusions

In this study we describe a method that could evaluate training-related plastic changes. The described method is applicable on a daily basis by using a simple task using the EEG which is a low cost technique and widely available. A simple numeric parameter, the IP, is proposed, which could indirectly but objectively measure the changes caused by the physical training in each individual.

This method could be used as a future diagnostic test in the follow-up of patients undergoing rehabilitation, assessing the recovery of their neurological disability after a stroke or brain injury. It could also have potential applications in the fields of sports medicine.

Supporting information

S1 Table. Parameters value of each subject of the sample. EHI = Edinburgh Handedness Inventory, GBA = Gamma Band Activity, B = Basal, MR = Motor Right, ML = Motor Left, ERS = Event Related Synchronization, INI = Initial, MED = Middle, FIN = Final, ΔGBAB = variation of the basal activity, IP = Index of plasticity, EMG = Electromyogram, PAR = Peak Average Ratio.
(XLSX)

Acknowledgments

We thank all the volunteers who participated in the study in the Department of Electronics at the University of Alcalá.

We also thank Michael Wibral, Cerisa Stawowsky, Georg-Friedrich Paasch and the team at the MEG Lab at the Max Planck Institut in Frankfurt, for their teaching.

Author Contributions

Conceptualization: Carlos Amo, Miguel Alonso-Alonso.

Formal analysis: Miguel Alonso-Alonso.

Funding acquisition: Luciano Boquete.

Investigation: Luis De Santiago, Daniel Zarza Luciáñez, José Miguel León Alonso-Cortés, Miguel Alonso-Alonso.

Methodology: Carlos Amo, Daniel Zarza Luciáñez, José Miguel León Alonso-Cortés, Miguel Alonso-Alonso.

Project administration: Carlos Amo.

Resources: José Miguel León Alonso-Cortés.

Software: Luis De Santiago, Rafael Barea.

Supervision: Luis De Santiago, Luciano Boquete.

Validation: Luis De Santiago, Luciano Boquete.

Visualization: Luis De Santiago, Daniel Zarza Luciáñez, Luciano Boquete.

Writing – original draft: Carlos Amo, Luis De Santiago, Luciano Boquete.

Writing – review & editing: Carlos Amo, Luis De Santiago, Luciano Boquete.

References

1. Pascual-Leone A, Amedi A, Fregni F, Merabet LB. The plastic human brain cortex. Annu Rev Neurosci. 2005; 28: 377–401. https://doi.org/10.1146/annurev.neuro.27.070203.144216 PMID: 16022601
2. Ramón y Cajal S. La Textura del Sistema Nervioso del Hombre y los Vertebrados. Imprenta y Libreria de Nicolás Moya, editor. Madrid; 1899.
3. Pascual-Leone A, Nguyet D, Cohen LG, Brasil-Neto JP, Cammarota A, Hallett M. Modulation of muscle responses evoked by transcranial magnetic stimulation during the acquisition of new fine motor skills. J Neurophysiol. 1995; 74: 1037–45. PMID: 7500130
4. Shen Y, Cao X, Shan C, Dai W, Yuan T-F. Heroin Addiction Impairs Human Cortical Plasticity. Biol Psychiatry. Elsevier; 2017; 81: e49–e50. https://doi.org/10.1016/j.biopsych.2016.06.013 PMID: 27567311
5. Huang X, Chen Y-Y, Shen Y, Cao X, Li A, Liu Q, et al. Methamphetamine abuse impairs motor cortical plasticity and function. Mol Psychiatry. The Author(s); 2017; 22: 1274–1281. https://doi.org/10.1038/mp.2017.143 PMID: 28831198
6. Elbert T, Pantev C, Wienbruch C, Rockstroh B, Taub E. Increased Cortical Representation of the Fingers of the Left Hand in String Players. Science (80-). 1995; 270: 305–307. https://doi.org/10.1126/science.270.5234.305 PMID: 7569982
7. Debarnot U, Sperduti M, Di Rienzo F, Guillot A. Experts bodies, experts minds: How physical and mental training shape the brain. Front Hum Neurosci. 2014; 8: 280. https://doi.org/10.3389/fnhum.2014.00280 PMID: 24847236
8. Pfurtscheller G, Lopes da Silva FH. Event-related EEG/MEG synchronization and desynchronization: basic principles. Clin Neurophysiol. 1999; 110: 1842–1857. https://doi.org/10.1016/S1388-2457(99)00141-8 PMID: 10576479
9. Tallon-Baudry, Bertrand, Tallon-Baudry C, Bertrand O. Oscillatory gamma activity in humans and its role in object representation. Trends Cogn Sci. 1999; 3: 151–162. 10322469 PMID: 10322469
10. Amo C, del Castillo MO, Barea R, de Santiago L, Martínez-Arribas A, Amo-López P, et al. Induced Gamma-Band Activity During Voluntary Movement: EEG Analysis for Clinical Purposes. Motor Control. 2016; 20: 409–428. https://doi.org/10.1123/mc.2015-0010 PMID: 26284500
11. Uhlhaas PJ, Haenschel C, Nikolic D, Singer W, Nikolić D, Singer W. The Role of Oscillations and Synchrony in Cortical Networks and Their Putative Relevance for the Pathophysiology of Schizophrenia. Schizophr Bull. 2008; 34: 927–943. https://doi.org/10.1093/schbul/sbn062 PMID: 18562344
12. Oldfield RC. The assessment and analysis of handedness: the Edinburgh inventory. Neuropsychologia. 1971; 9: 97–113. PMID: 5146491
13. Oostenveld R, Fries P, Maris E, Schoffelen J-M. FieldTrip: Open source software for advanced analysis of MEG, EEG, and invasive electrophysiological data. Comput Intell Neurosci. 2011; 2011: 156869. https://doi.org/10.1155/2011/156869 PMID: 21253357
14. Amo C, Criado JR, Otis SM. Magnetoencephalogram recording from secondary motor areas during imagined movements. Arq Neuropsiquiatr. 2006; 64: 394–397. https://doi.org/10.1590/S0004-282X2006000300008 PMID: 16917607

15. Amo C, Boyajian RA, Romine JS, Otis SM. High-Resolution Magnetoencephalographic Functional Mapping of the Cortical Network Mediating Intentional Movement. Am J Phys Med Rehabil. 2007; 86: 304–309. https://doi.org/10.1097/PHM.0b013e3180383c0d PMID: 17413544

16. Rossini PM, Altamura C, Ferreri F, Melgari J-M, Tecchio F, Tombini M, et al. Neuroimaging experimental studies on brain plasticity in recovery from stroke. Eura Medicophys. 2007; 43: 241–54. PMID: 17589415

17. Kami A, Meyer G, Jezzard P, Adams MM, Turner R, Ungerleider LG. Functional MRI evidence for adult motor cortex plasticity during motor skill learning. Nature. 1995; 377: 155–158. https://doi.org/10.1038/377155a0 PMID: 7675082

18. Boninger ML, Wechsler LR, Stein J. Robotics, Stem Cells, and Brain-Computer Interfaces in Rehabilitation and Recovery from Stroke. Am J Phys Med Rehabil. 2014; 93: S145–S154. https://doi.org/10.1097/PHM.0000000000000128 PMID: 25313662

19. Etnier JL, Landers DM. Brain function and exercise. Current perspectives. Sports Med. 1995; 19: 81–5. PMID: 7747005

20. Lardon MT, Polich J. EEG changes from long-term physical exercise. Biol Psychol. 1996; 44: 19–30. https://doi.org/10.1016/S0301-0511(96)05198-8 PMID: 8906355

21. Ermutlu N, Yücesir I, Eskikurt G, Temel T, İşoğlu-Alkaç Ü. Brain electrical activities of dancers and fast ball sports athletes are different. Cogn Neurodyn. Springer Netherlands; 2015; 9: 257–263. https://doi.org/10.1007/s11571-014-9320-2 PMID: 25834650

22. Herrmann C, Demiralp T. Human EEG gamma oscillations in neuropsychiatric disorders. Clin Neurophysiol. 2005; 116: 2719–2733. https://doi.org/10.1016/j.clinph.2005.07.007 PMID: 16253555

23. Shibata T, Shimoyama I, Ito T, Abla D, Iwasa H, Koseki K, et al. Event-related dynamics of the gamma-band oscillation in the human brain: information processing during a GO/NOGO hand movement task. Neurosci Res. 1999; 33: 215–222. https://doi.org/10.1016/S0168-0102(99)00003-6 PMID: 10211765

24. Ball T, Demandt E, Mutschler I, Neitzel E, Mehring C, Vogt K, et al. Movement related activity in the high gamma range of the human EEG. Neuroimage. 2008; 41: 302–10. https://doi.org/10.1016/j.neuroimage.2008.02.032 PMID: 18424182

25. Murthy VN, Fetz EE. Coherent 25- to 35-Hz oscillations in the sensorimotor cortex of awake behaving monkeys. Proc Natl Acad Sci U S A. National Academy of Sciences; 1992; 89: 5670–4. https://doi.org/10.1073/PNAS.89.12.5670 PMID: 1608977

8.2.4 Induced Gamma-Band Activity during Actual and Imaginary Movements: EEG Analysis

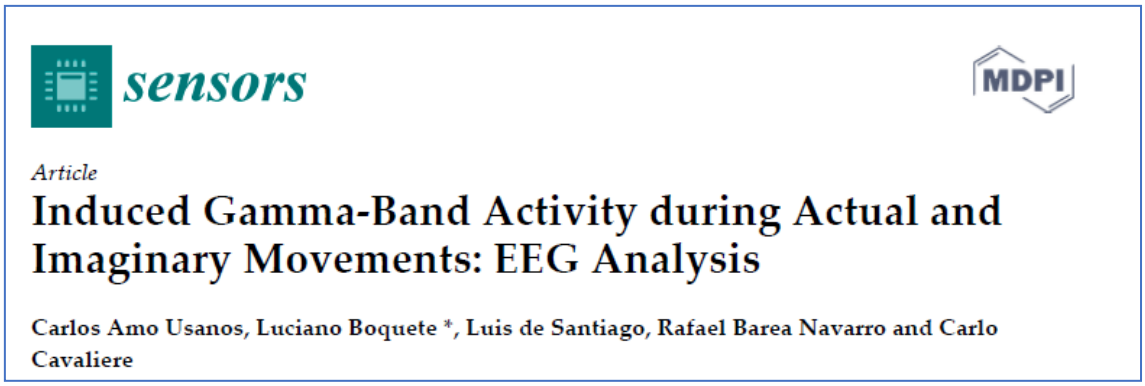

sensors

MDPI

Article

Induced Gamma-Band Activity during Actual and Imaginary Movements: EEG Analysis

Carlos Amo Usanos, Luciano Boquete *, Luis de Santiago, Rafael Barea Navarro and Carlo Cavaliere

sensors

MDPI

Article

Induced Gamma-Band Activity during Actual and Imaginary Movements: EEG Analysis

Carlos Amo Usanos, Luciano Boquete *, Luis de Santiago, Rafael Barea Navarro and Carlo Cavaliere

Biomedical Engineering Group. Department of Electronics, Universidad de Alcalá. Plaza de San Diego, s/n 28801 Alcalá de Henares, Spain
*Correspondence: luciano.boquete@uah.es

Received: 9 February 2020; Accepted: 10 March 2020; Published: 11 March 2020

Abstract: The purpose of this paper is to record and analyze induced gamma-band activity (GBA) (30–60 Hz) in cerebral motor areas during imaginary movement and to compare it quantitatively with activity recorded in the same areas during actual movement using a simplified electroencephalogram (EEG). Brain activity (basal activity, imaginary motor task and actual motor task) is obtained from 12 healthy volunteer subjects using an EEG (Cz channel). GBA is analyzed using the mean power spectral density (PSD) value. Event-related synchronization (ERS) is calculated from the PSD values of the basal GBA (GBAb), the GBA of the imaginary movement (GBAim) and the GBA of the actual movement (GBAac). The mean GBAim and GBAac values for the right and left hands are significantly higher than the GBAb value ($p = 0.007$). No significant difference is detected between mean GBA values during the imaginary and actual movement ($p = 0.242$). The mean ERS values for the imaginary movement (ERSimM (%) = 23.52) and for the actual movement (ERSacM = 27.47) do not present any significant difference ($p = 0.117$). We demonstrated that ERS could provide a useful way of indirectly checking the function of neuronal motor circuits activated by voluntary movement, both imaginary and actual. These results, as a proof of concept, could be applied to physiology studies, brain–computer interfaces, and diagnosis of cognitive or motor pathologies.

Keywords: electroencephalography; gamma-band activity; motor areas; imaginary motor tasks; actual motor tasks; event-related synchronization; power spectral density.

1. Introduction

The synchronization of neuronal firing in the 20–200 Hz range is known as gamma-band activity (GBA) and can be divided into two bands, low (30–60 Hz) and high (60–200 Hz) [1,2]. GBA is generated in most brain structures, at a retinal level, and in the olfactory system. The principal neurotransmitters involved in its generation are glutamate (excitatory), acetylcholine and gamma-aminobutyric acid (inhibitory); GBA is linked to cerebral functions such as perception, attention, memory, consciousness, synaptic plasticity and motor control [3].

Neurophysiological studies have documented that in subjects at rest or performing motor tasks GBA in the 30–90 Hz frequency range appears in extensive areas of the brain [4]. Furthermore, movement-related GBA has been proposed as the integrator of sensory and motor processes during movement preparation and control [5].

GBA in voluntary movement (actual or imaginary) can be evaluated using intracranial electrodes [6] or electrocorticography (ECoG) [7–11]. These invasive methods, however, are largely inapplicable in standard clinical practice.

Several papers describe GBA recorded using non-invasive, low-cost and easily accessible methods such as conventional surface electroencephalograms (EEGs). The evaluation of activity in

the gamma band using EEG records for actual, but not imaginary movements, was investigated in [12–17].

Motor imagery may be defined as a dynamic state during which representations of a given motor act are internally rehearsed in working memory without any motor output [18]. In this mental task subjects are instructed to imagine themselves moving without performing that movement so without muscle activation. The available evidence indicates that actual and imaginary movements share a substantial overlap of common functional circuits [19].

Previous papers describe the analysis of the GBA obtained during an imaginary movement from EEG recordings employing invasive methods (ECoG) [11,20].

Advances in obtaining GBA non-invasively during imaginary movement using conventional EEGs are presented in Table 1. These papers analyze various frequency intervals, use differing imaginary movement paradigms and employ a high number of EEG channels.

Table 1. Studies analyzing GBA non-invasively during imaginary movement using conventional EEGs.

Authors	Number of Subjects	Channels	Frequency Range	Imagined Movement	Main Conclusions
Khan and Sepulveda, (2010) [21]	5	64	32–48 Hz	Wrist: extension, flexion, pronation, and supination.	An average recognition rate of approximately 89% was achieved in four movement types between the left and right wrists.
Kiroi et al., (2012) [22]	8	14	31–45 Hz 55–70 Hz	Flexion or oscillatory movement of the arm at the elbow, clenching of the hand.	Increase in activation levels, particularly in the central areas of the cortex.
Smith et al., (2014) [23]	10	54	70–150 Hz	Finger movement imagery.	Significant power increase was observed during motor imagery.
Korik et al., (2018) [24]	12	41	28–40 Hz	Imagined 3D limb movement.	The power spectral density contributes to the encoding of movement-related information during arm movement.
Lazurenko et al., (2018) [25]	24	17	30–48 Hz and 52–70 Hz	Imaginary hand, leg, and tongue movements.	Sensorimotor and associative areas of both hemispheres were actively involved in imaginary and actual movements.
Veslin et al., (2019) [26]	12	14	35–45	Right and left elbow movements.	Similar activity was obtained in the gamma band during the preparation and execution of both actual and imaginary movements.

Acquiring the EEG signal in the gamma band is problematic. The EEG signal is generally contaminated by interferences from physiological signals (electrocardiogram (ECG), electromyogram (EMG), electrooculogram (EOG), etc.) and non-physiological artifacts (power line noise, electronic devices, etc.) [27]. Moreover, due to the $1/f^n$ nature of the EEG spectra, the decrease in power with the increase in frequency [28] makes it more difficult to obtain responses in the gamma band than in other lower EEG frequencies.

Multichannel EEG systems make it possible to obtain spatial resolutions and apply signal separation algorithms, such as Independent Component Analysis (ICA) [29], so as to obtain responses in the gamma band. However, the setup process is tedious (attaching the electrodes, adjusting the impedance) and participants find the system uncomfortable. In recent years, research has been conducted into use of monochannel EEG systems in brain–computer interfaces (BCI´s) [30] (analyzed band: 0.5–10 Hz), [31] (steady-state visual evoked potentials), sleep studies [32,33], etc. However, to our knowledge, a single-channel system for detecting activity in the gamma band has not been implemented in imaginary movements.

The authors of this paper hypothesize that it is possible to analyze EEG activity in the gamma band during both actual and imaginary movements using a simple and quantifiable method easily applicable in daily practice.

Possible applications of a system with these characteristics may be the implementation of BCIs or in the study of diseases that affect cognitive or motor functions.

The advantage of a BCI can be focused on the implementation of a communication system [34], real-time control of peripherals as robots [35–37] or emotion recognition, among other. Many of the current BCI based on the detection of EEG imaginary movements (for a review [38]) analyze the alpha/beta EEG band, usually using several channels. The success of motor imagery BCI in translational applications is established in three learning pillars: at the machine, subject, and application level [39]. Some BCI´s multichannel works that analyze the gamma band can be referenced: [40] (19 EEG channels) [41] (21 channels), or [42] (128 channels).

Cognitive [43] and motor [44] functions affect the activity of the gamma band; consequently, a single-channel EEG system may be interesting for clinical use in the study of Alzheimer's disease [45,46], depression [47], schizophrenia [48], etc. and also in some cortical diseases (traumatic vascular pathology and degenerative lesions).

The primary purpose of this paper is to obtain and analyze gamma activity in the 30–60 Hz frequency range caused by motor activity using a simplified EEG recording taken while performing an imaginary and actual motor task. The secondary purpose is to compare that activity during the imaginary motor task with the GBA obtained during the actual motor task.

2. Material and Methods

2.1 Participants and Experiment Description

All subjects were over the age of 18, have been informed about the details of the investigation and signed the informed consent according to a protocol approved by the local ethics committees of the University of Alcalá (Spain) and compliant with the tenets of the Declaration of Helsinki.

The study cohort for this experiment comprised 12 subjects (3 females and 9 males; mean age = 28.7; range = 21–47). All sample subjects were healthy and free of medical, neurological (including craniocerebral trauma and epilepsy) and psychiatric disease. None of the subjects were taking medicinal products and none had a record of alcohol or drug abuse or dependency.

According to the Edinburgh Handedness Inventory [49] were identified 9 right-handed subjects, 2 left-handed subjects, and 1 ambidextrous subject.

Details of the methodology employed in the experiment and in acquisition and analysis of the data in the EEG recordings have been published previously [17]. In brief, each subject is seated facing a computer monitor. They are positioned at a distance of 0.8 m and rest their forearms on a table with the palms of their hands facing downward. The experiment comprises 3 steps:

1. Basal recording. Participants keep their eyes fixed on the center of the screen (to prevent eye movement; they also try not to blink) and refrain from performing any motor or specific mental activity. A total of 18 minutes of basal activity are recorded, divided into 3 parts (each 6 minutes long) with a rest of approximately 1 minute between each. This step is the first performed by the participants.

2. Imaginary motor task. An on-screen cue triggers the imaginary motor task, thereby obtaining in the EEG trace the motor GBA induced by that imaginary movement. The imaginary task consists of simulating, without muscle activation, rapid extension of the wrist followed by brief relaxation. This phase lasts approximately 40 minutes.

3. Actual motor task. The subjects perform an actual motor task with the same characteristics and duration of imaginary motor task.

During the motor activities, the physical conditions for the participants were the same as in the basal stage, the only difference being that they performed the actual or imaginary activities. Each trial lasted 2 s and started (at t = 0 s) with display (for 150 ms) of the cue in the center of the computer monitor. This was followed by a white screen that remained in place until the start of the next trial (t = 2 s). The motor experiments comprised 5 runs per hand alternated between right and left to prevent mental and muscle fatigue and each run comprised 100 trials. For both the imaginary motor task and the actual motor task, the subjects practiced the exercise in a training session held before the experiment was conducted.

2.2. Data Acquisition

The EEG signals were acquired with a 32-channel Micromed EEG (Handy EEG SD32) and the SystemPlus Evolution (Micromed SpA, Treviso, Italy) software, using a 2048-Hz sampling frequency, band-pass filters from 0.15–537.53 Hz and a 50-Hz notch filter. Electrode impedance was below 10 kΩ. The experiment was performed in a conventional laboratory with lights turned off and rechargeable batteries were used in the acquisition equipment to minimize potential alternating current induction at 50 Hz in the EEG power cables [50].

The EEG (active electrodes (C3, C4, Cz), reference (FPz), earth (Pz)) was recorded in continuous mode using Ag/AgCl electrodes. The electrooculogram was recorded to monitor eye movements. The electromyogram was obtained using two surface electrodes (active and reference) above the extensor carpi radialis longus muscle to confirm the movement in the actual motor task and the lack of movement in the imaginary motor task.

2.3. Data Analysis

The electrophysiological data were analyzed using MATLAB R2017b (The MathWorks Inc. Natick, MA, USA) and FieldTrip [51].

For analysis of both the basal EEG and during the motor tasks, 2-second segments corresponding to the trials established in the experiment were used. Band-pass (1 Hz, 100 Hz) and notch filters (band eliminated: 49–51 Hz) were applied. FieldTrip functions were used to complete signal processing, obtaining an artifact-free signal that was averaged for each subject and each hand. Finally, all the subjects were averaged to produce a grand average.

The GBA was quantified as spectral power values for the frequency band (low gamma band: 30–60 Hz, according to the taxonomy defined in [1]) using a multitaper Fast-Fourier transform (FieldTrip ft_freqanalysis function).

To analyze the GBA, only the Cz channel signals were used, as centrally channels were the least contaminated by movement and EMG artifacts [52]. Moreover, analyzing one of the central channels ensures that the implemented system does not depend on a subject's hand dominance since it is known that the answer during a motor imagery task differs according to handedness [53,54].

2.4. Calculation of the GBA

The results for the GBA were expressed as the mean power spectral density (PSD) value in μV^2. Based on the mean PSD values, the following parameters were defined:

- GBA during the basal experiment: GBAb.
- GBA during actual motor tasks: GBAac.
- GBA during imaginary motor tasks: GBAim.

The corresponding suffix was added to indicate right hand, left hand or mean of both (-R, -L, -M). For example: GBAacR indicates the GBA obtained from the actual movement of the right hand; GBAimL indicates the GBA obtained from the imaginary movement of the left hand; and GBAimM indicates the mean of the GBA obtained from the imaginary movement of the right and left hands.

2.5. Calculation of ERS for the GBA

Quantification of ERS in imaginary or actual movements was defined as a power increase relative to the basal state (GBAb). For this purpose, the GBA values of the motor tasks were normalized relative to the basal activity and expressed as a percentage [55]. For example, Equation (1) and (2) represent the ERS values for the means of both hands for the actual movement (ERSacM) and the imaginary movement (ERSimM).

$$\mathrm{ERSacM}(\%) = \frac{\mathrm{GBAacM} - \mathrm{GBAb}}{\mathrm{GBAb}} \times 100 \quad (1)$$

$$\mathrm{ERSimM}(\%) = \frac{\mathrm{GBAimM} - \mathrm{GBAb}}{\mathrm{GBAb}} \times 100 \quad (2)$$

Positive ERS values indicate a power increase in the activity compared to the basal situation. Both the GBA and the ERS were calculated for each trial and averaged for each hand. The corresponding suffix was added to indicate right hand, left hand or mean of both (-R, -L, -M). The grand average was then calculated for all the subjects. Finally, the mean ERS values for the actual movement (ERSacM) were compared with the mean values for the imaginary movement (ERSimM).

2.6. Statistical Analysis

Statistical tests were performed using the SPSS 25.0 software (SPSS Inc. Chicago, IL, USA). Normally distributed variables are expressed as mean ± standard deviation; non-normally distributed variables are reported as median (interquartile range [IQR]).

The normality of the results was assessed using the Shapiro–Wilk (W) test. The results were compared using the dependent t-test (paired-samples t-test) in normal distributions or the Wilcoxon signed-rank test (Z) in non-normal distributions. A p value below 0.05 was considered statistically significant.

3. Results

The results of the study are shown in the tables below as the mean of the values for the entire sample (12 subjects), for each hand and both hands.

First, the results for basal activity (GBAb) were obtained, followed by those for the imaginary motor task (GBAim) and those for the actual motor task (GBAac). The latter two results are expressed as right hand, left hand, and mean for both hands. Figure 1 shows the results obtained in a box plot format. All the GBA values obtained (Table 2) follow a normal distribution, except GBAimL ($W = 0.86$, $p = 0.049$). No significant differences were found between imaginary and actual activity in either the right hand ($p = 0.237$), the left hand ($p = 0.783$) or the mean ($p = 0.242$).

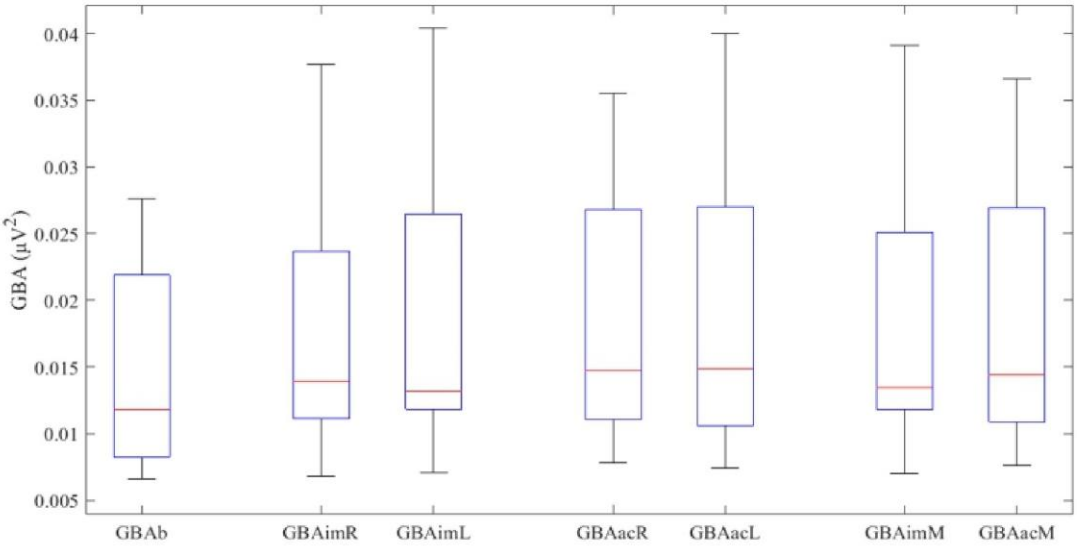

Figure 1 GBA values (μV²) obtained in the various experiments. The upper and lower box ends denote the first and third quartiles; the red line represents the median, and the whiskers represent 1.5 x interquartile range.

Table 2. Analysis of the GBA data obtained.

Action	GBA	μV²	Comparison of Means
Basal	GBAb*	0.0145 ± 0.0076	-----
Right Hand	GBAimR*	0.0175 ± 0.0098	t(11) = -1.251, p = 0.237
	GBAacR*	0.0185 ± 0.0097	
Left Hand	GBAimL	0.0131 (0.0159)	Z = 0.275, p = 0.783
	GBAacL*	0.0185 ± 0.0104	
Mean Values	GBAimM*	0.0180 ± 0.0101	t(11) = 1.236, p = 0.242
	GBAacM*	0.0185 ± 0.0099	

*Normal distribution, Shapiro–Wilk test ($p > 0.05$).

The basal GBA activity is significantly lower relative to the imaginary movement of the right hand ($t(11) = -3.127$, $p = 0.010$), the left hand ($Z = -3.059$, $p = 0.002$) and the mean ($t(11) = -3.321$, $p = 0.007$). We also found that the basal GBA is significantly lower relative to the actual movement of the right hand ($t(11) = -5.493$, $p = 0.0001$), the left hand ($t(11) = -3.752$, $p = 0.003$) and the mean ($t(11) = -4.965$, $p = 0.0001$).

Figure 2 represents the ERS values graphically. The ERSacL ($W = 0.895$, $p = 0.138$) and ERSacM ($W = 0.863$, $p = 0.054$) values follow a normal distribution; the other results do not meet the condition of normality ($p < 0.044$ in all cases).

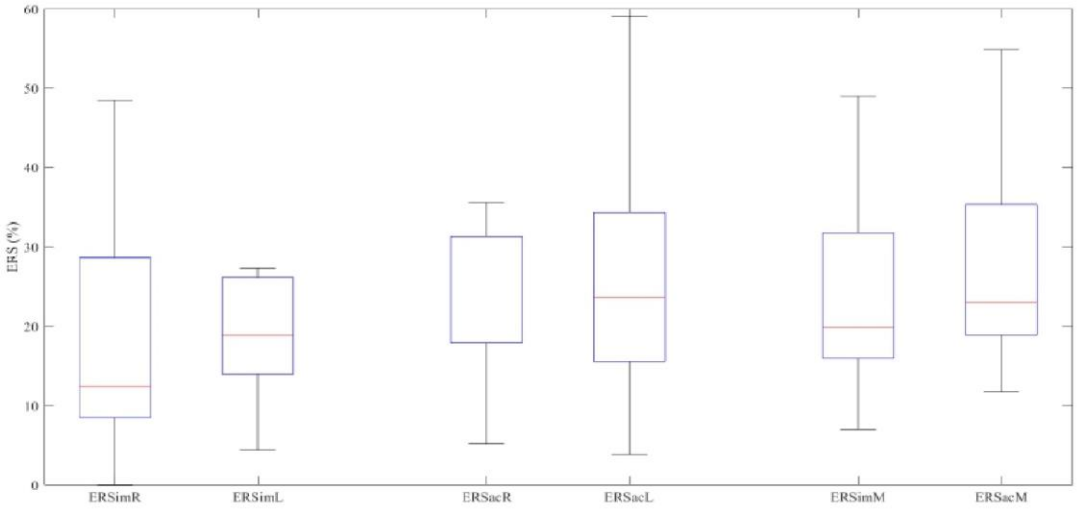

Figure 2. ERS values (%) in the various experiments.

The Wilcoxon signed-rank test finds no significant difference between the ERS values obtained in the imaginary movements and those obtained in the actual movements for either the right hand ($Z = -1.020$, $p = 0.308$), the left hand ($Z = 0.471$, $p = 0.638$) or the mean values ($Z = -1.569$, $p = 0.117$) (Table 3).

Table 3. Analysis of the ERS data obtained.

	ERS	ERS (%)	Comparison of Means Wilcoxon Signed-rank Test
Right Hand	ERSimR	12.435 (21.124)	$Z = -1.020$, $p = 0.308$
	ERSacR	28.850 (14.889)	
Left Hand	ERSimL	18.828 (13.578)	$Z = -0.471$, $p = 0.638$
	ERSacL*	26.972 ± 17.447	
Mean Values	ERSimM	15.983 (14.313)	$Z = -1.569$, $p = 0.117$
	ERSacM*	27.479 ± 13.256	

*Normal distribution, Shapiro–Wilk test ($p > 0.05$).

In the imaginary movements (ERS), there is no significant difference between right- and left-hand data distributions ($Z = -1.726$, $p = 0.084$). Neither is there any significant difference between the activity (ERS) for the right and left hands in the actual movements ($Z = -0.235$, $p = 0.814$).

In conclusion, our results indicate a significant increase in GBA, relative to basal activity, in both the actual movements and the imaginary movements for both hands. Furthermore, there is no significant difference between the imaginary and actual movements in both hands.

4. Discussion

The purpose of this paper has been to obtain and analyze the GBA in the cerebral motor areas by taking a monochannel EEG recording during an imaginary motor task and comparing that recording with the GBA obtained during an actual motor task. In this experiment, the basal GBA is

significantly lower than the GBA values obtained during the imaginary and actual movements. Furthermore, no significant differences ($p = 0.117$) are observed between the ERS values for the actual and imaginary movements (ERSimM ≈ ERSacM).

No previous papers analyze GBA using a combination of a single-channel (Cz) EEG and our stimulation and analysis frequency paradigm. Obtaining GBA during imaginary motor tasks using a conventional 64-channel EEG is described in [21], who analyze the 32–48 Hz EEG band, intending to discriminate wrist movement imagery. The purpose of the paper is to implement a brain–computer interface and it does not report ERS values. In a study by [22], greater GBA activity is observed during the imaginary movement than during the actual movement. This contrasts with our results, in which we found greater activity in the actual movement (ERSacM (%) = 27.479 ± 13.256, ERSimM (%) = 15.983 (14.313), with no significant difference). This contradiction may be due to the use of different types of movement, a different number of EEG channels and analysis of different gamma-band frequencies.

As is the case in our study, [23] observe significant increases in the power of the GBA during finger movement imagery. However, it does not report numerical values that would make it possible to compare results.

In [25] the authors observe that actual and imagery movements active sensorimotor and associative areas of both hemispheres, especially at 52–70 Hz band. They also found differences in activity between the actual movement and the imaginary movement in the frequencies analyzed (30–48 Hz: $p = 0.000$; 52–70 Hz: $p = 0.011$) in the temporal–parietal–occipital zone.

Works [24] and [26] likewise describe an increase, relative to basal activity, in the gamma band in both the imaginary movement and the actual movement. In addition, they do not find any difference in GBA between the actual movement and the imaginary movement. These papers, however, do not report overall numerical data for GBA since they focus on its anatomical location. In our case, the results express PSD values in the form of ERS to simplify their quantification for clinical purposes.

As regards the GBA obtained during imaginary movement using invasive methods [11,20], the results are not comparable with ours because in these previous studies they were obtained directly from the cerebral cortex (ECoG) without attenuation of the signal-to-noise ratio or the muscle artifacts found in a conventional EEG.

The GBA values we obtained during actual movement, however, are comparable with those of previous papers, the results of which are as follows: ERS ≈ 10–20 % [13,14] and ERS ≈ 20–30 % [17] and have values similar to ours (ERS ≈ 20–28 %).

Based on our study, it can be concluded that the ERS values for the imaginary and actual tasks do not show any significant difference (ERSimM ≈ ERSacM, ($p > 0.05$)). Activation of the same cortical areas during the actual and imaginary movements has been demonstrated in previous papers. The motor imagery belongs to the same category of processes involved in the programming and preparation of actual actions, the difference being that in this latter case, execution would be blocked at the corticospinal level. It can be assumed that the motor imagery shares the same neuronal mechanisms responsible for preparing and programming actual movements [18]. This hypothesis can be confirmed by experimentation e.g., using neuroimaging techniques to map cerebral activity during the imaginary movements, which reveals an activation pattern similar to that of execution of an actual action [56]. During the imaginary movement of the hand, there is an increase in the power of the gamma bands relative to the resting state (ERS), producing a significant overlap in spatial distribution (cortical areas) with the actual movement [11].

5. Conclusions

In this paper, we have developed a proof of concept that could confirm the viability of detecting gamma-band activity in imaginary and actual motor movements in environments compatible with clinical practice, doing so using a single EEG channel and without the need for a shielded chamber room.

Possible improvements to this experiment could include increasing the number of subjects and making the sample more homogeneous in terms of age and manual laterality (e.g., recruiting equal numbers of right-handed, left-handed, and ambidextrous subjects). It would also be beneficial to instruct subjects to close their eyes during the experiment and use an auditory stimulus or a non-cued paradigm (self-paced condition), making continual hand movements to avoid blinking artifacts.

At signal processing level, it would be convenient to implement some method for physiological artifact identification and removal in EEG registers (see [57] for a review). Consequently, it is intended to evaluate the detection capacity of GBA using artifact reduction techniques in single-channel acquisition systems, designed to eliminate some particular type of interference (e.g., ocular movements [58]) or more generalists ones [59].

This paper shows a proof of concept that explains the way to extract the gamma-band activity by a simple motor experiment (real or imaginary). It is not a method to discriminate between GBAim and GBAac, nor between the anatomical origin of the GBA (right or left hemisphere). However, this method could be used to create protocols applicable to BCI´s that can take advantage of both GBAim and GBAac, as in the distinction between imaginary movements of hands versus feet. Moreover, more variety of BCI codes could be created using the GBA signal obtained from both cerebral hemispheres.

If the results of this paper were confirmed in more exhaustive studies, gamma-band detection of imaginary movements could be used in the implementation of BCI´s, supporting the evaluation of cognitive functions in some cortical diseases (traumatic vascular pathology and degenerative lesions) or for use in assessing the pathology of motor areas, following up rehabilitation processes.

Author Contributions: Formal analysis, L.S. and C.C.; Funding acquisition, L.B.; Investigation, C.A.U., L.B. and R.B.N.; Methodology, C.A.U. and L.S.; Software, R.B.N. and C.C.; Supervision, L.B.; Validation, C.A.U.; Writing – original draft, L.S., R.B.N. and C.C.; Writing – review and editing, C.A.U. and L.B.

Funding: This research was supported by the Secretariat of State for Research, Development and Innovation [grant number DPI2017-88438-R (AEI/FEDER, EU), awarded to LB].

Conflicts of Interest: The authors declare no conflict of interest.

References

1. Uhlhaas, P.J.; Pipa, G.; Neuenschwander, S.; Wibral, M.; Singer, W. A new look at gamma? High- (>60 Hz) γ-band activity in cortical networks: Function, mechanisms and impairment. *Prog. Biophys. Mol. Biol.* **2011**, *105*, 14–28.
2. Combrisson, E.; Perrone-Bertolotti, M.; Soto, J.L.; Alamian, G.; Kahane, P.; Lachaux, J.-P.; Guillot, A.; Jerbi, K. From intentions to actions: Neural oscillations encode motor processes through phase, amplitude and phase-amplitude coupling. *Neuroimage* **2017**, *147*, 473–487.
3. Uhlhaas, P.J.; Haenschel, C.; Nikolić, D.; Singer, W. The role of oscillations and synchrony in cortical networks and their putative relevance for the pathophysiology of schizophrenia. *Schizophr. Bull.* **2008**, *34*, 927–943.
4. Cheyne, D.; Ferrari, P. MEG studies of motor cortex gamma oscillations: Evidence for a gamma "fingerprint" in the brain? *Front. Hum. Neurosci.* **2013**, *7*, doi: 10.3389/fnhum.2013.00575
5. Tallon-Baudry, C.; Bertrand, O. Oscillatory gamma activity in humans and its role in object representation. *Trends Cogn. Sci.* **1999**, *3*, 151–162.
6. Szurhaj, W.; Bourriez, J.-L.; Kahane, P.; Chauvel, P.; Mauguière, F.; Derambure, P. Intracerebral study of gamma rhythm reactivity in the sensorimotor cortex. *Eur. J. Neurosci.* **2005**, *21*, 1223–1235.
7. Crone, N.E.; Miglioretti, D.L.; Gordon, B.; Lesser, R.P. Functional mapping of human sensorimotor cortex with electrocorticographic spectral analysis. II. Event-related synchronization in the gamma band. *Brain* **1998**, *121*, 2301–2315.
8. Aoki, F.; Fetz, E.E.; Shupe, L.; Lettich, E.; Ojemann, G.A. Increased gamma-range activity in human sensorimotor cortex during performance of visuomotor tasks. *Clin. Neurophysiol.* **1999**, *110*, 524–537.
9. Ohara, S.; Ikeda, A.; Kunieda, T.; Yazawa, S.; Baba, K.; Nagamine, T.; Taki, W.; Hashimoto, N.; Mihara, T.; Shibasaki, H. Movement-related change of electrocorticographic activity in human supplementary motor area proper. *Brain* **2000**, *123*, 1203–1215.
10. Pfurtscheller, G.; Graimann, B.; Huggins, J.E.; Levine, S.P.; Schuh, L.A. Spatiotemporal patterns of beta desynchronization and gamma synchronization in corticographic data during self-paced movement. *Clin. Neurophysiol.* **2003**, *114*, 1226–1236.
11. Miller, K.J.; Schalk, G.; Fetz, E.E.; den Nijs, M.; Ojemann, J.G.; Rao, R.P.N. Cortical activity during motor execution, motor imagery, and imagery-based online feedback. *Proc. Natl. Acad. Sci. USA.* **2010**, *107*, 4430–4435.
12. Pfurtscheller, G.; Neuper, C. Simultaneous EEG 10 Hz desynchronization and 40 Hz synchronization during finger movements. *Neuroreport* **1992**, *3*, 1057–1060.
13. Shibata, T.; Shimoyama, I.; Ito, T.; Abla, D.; Iwasa, H.; Koseki, K.; Yamanouchi, N.; Sato, T.; Nakajima, Y. Event-related dynamics of the gamma-band oscillation in the human brain: information processing during a GO/NOGO hand movement task. *Neurosci. Res.* **1999**, *33*, 215–22.
14. Ball, T.; Demandt, E.; Mutschler, I.; Neitzel, E.; Mehring, C.; Vogt, K.; Aertsen, A.; Schulze-Bonhage, A. Movement related activity in the high gamma range of the human EEG. *Neuroimage* **2008**, *41*, 302–310.
15. Darvas, F.; Scherer, R.; Ojemann, J.G.; Rao, R.P.; Miller, K.J.; Sorensen, L.B. High gamma mapping using EEG. *Neuroimage* **2010**, *49*, 930–938.
16. Demandt, E.; Mehring, C.; Vogt, K.; Schulze-Bonhage, A.; Aertsen, A.; Ball, T. Reaching movement onset- and end-related characteristics of EEG spectral power modulations. *Front. Neurosci.* **2012**, *6*, doi:10.3389/fnins.2012.00065.
17. Amo, C.; Del Castillo, M.O.; Barea, R.; de Santiago, L.; Martínez-Arribas, A.; Amo-López, P.; Boquete, L.

Induced Gamma-Band Activity During Voluntary Movement: EEG Analysis for Clinical Purposes. *Motor Control* **2016**, *20*, 409–428.

18. Decety, J. The neurophysiological basis of motor imagery. *Behav. Brain Res.* **1996**, *77*, 45–52.
19. Hardwick, R.M.; Caspers, S.; Eickhoff, S.B.; Swinnen, S.P. Neural correlates of action: Comparing meta-analyses of imagery, observation, and execution. *Neurosci. Biobehav. Rev.* **2018**, *94*, 31–44.
20. Leuthardt, E.C.; Schalk, G.; Wolpaw, J.R.; Ojemann, J.G.; Moran, D.W. A brain-computer interface using electrocorticographic signals in humans. *J. Neural Eng.* **2004**, *1*, 63–71.
21. Khan, Y.U.; Sepulveda, F. Brain–computer interface for single-trial EEG classification for wrist movement imagery using spatial filtering in the gamma band. *IET Signal Process.* **2010**, *4*, 510–517.
22. Kiroi, V.N.; Vladimirskii, B.M.; Aslanyan, E. V.; Bakhtin, O.M.; Minyaeva, N.R. Electrographic Correlates of Actual and Imagined Movements: Spectral Analysis. *Neurosci. Behav. Physiol.* **2012**, *42*, 21–27.
23. Smith, M.M.; Weaver, K.E.; Grabowski, T.J.; Rao, R.P.N.; Darvas, F. Non-invasive detection of high gamma band activity during motor imagery. *Front. Hum. Neurosci.* **2014**, *8*, doi:10.3389/fnhum.2014.00817.
24. Korik, A.; Sosnik, R.; Siddique, N.; Coyle, D. Decoding Imagined 3D Hand Movement Trajectories From EEG: Evidence to Support the Use of Mu, Beta, and Low Gamma Oscillations. *Front. Neurosci.* **2018**, *12*, doi:org/10.3389/fnins.2018.00130
25. Lazurenko, D.M.; Kiroy, V.N.; Aslanyan, E. V.; Shepelev, I.E.; Bakhtin, O.M.; Minyaeva, N.R. Electrographic Properties of Movement-Related Potentials. *Neurosci. Behav. Physiol.* **2018**, *48*, 1078–1087.
26. Veslin, E.Y.; Dutra, M.S.; Bevilacqua, L.; Raptopoulos, L.S.C.; Andrade, W.S.; Pereira, A.S.; Fiorani, M.; Soares, J.G.M. Lower gamma band in the classification of left and right elbow movement in real and imaginary tasks. *J. Brazilian Soc. Mech. Sci. Eng.* **2019**, *41*, 91.
27. Nottage, J.F.; Horder, J. State-of-the-Art Analysis of High-Frequency (Gamma Range) Electroencephalography in Humans. *Neuropsychobiology* **2015**, *72*, 219–228.
28. Allegrini, P.; Menicucci, D.; Bedini, R.; Fronzoni, L.; Gemignani, A.; Grigolini, P.; West, B.J.; Paradisi, P. Spontaneous brain activity as a source of ideal 1/f noise. *Phys. Rev. E. Stat. Nonlin. Soft Matter Phys.* **2009**, *80*, doi:10.1103/PhysRevE.80.061914
29. Hyvärinen, A. Independent component analysis: recent advances. *Philos. Trans. A. Math. Phys. Eng. Sci.* **2013**, *371*, doi:10.1098/rsta.2011.0534
30. Ogino, M.; Kanoga, S.; Muto, M.; Mitsukura, Y. Analysis of Prefrontal Single-Channel EEG Data for Portable Auditory ERP-Based Brain–Computer Interfaces. *Front. Hum. Neurosci.* **2019**, doi: 10.3389/fnhum.2019.00250
31. Ajami, S.; Mahnam, A.; Abootalebi, V. Development of a practical high frequency brain–computer interface based on steady-state visual evoked potentials using a single channel of EEG. *Biocybern. Biomed. Eng.* **2018**, *38*, 106–114.
32. Lucey, B.P.; Mcleland, J.S.; Toedebusch, C.D.; Boyd, J.; Morris, J.C.; Landsness, E.C.; Yamada, K.; Holtzman, D.M. Comparison of a single-channel EEG sleep study to polysomnography. *J. Sleep Res.* **2016**, *25*, 625–635.
33. Michielli, N.; Acharya, U.R.; Molinari, F. Cascaded LSTM recurrent neural network for automated sleep stage classification using single-channel EEG signals. *Comput. Biol. Med.* **2019**, *106*, 71–81.
34. Han, C.-H.; Kim, Y.-W.; Kim, D.Y.; Kim, S.H.; Nenadic, Z.; Im, C.-H. Electroencephalography-based endogenous brain–computer interface for online communication with a completely locked-in patient. *J.*

Neuroeng. Rehabil. **2019**, *16*, 18.

35. Diez, P.F.; Torres Müller, S.M.; Mut, V.A.; Laciar, E.; Avila, E.; Bastos-Filho, T.F.; Sarcinelli-Filho, M. Commanding a robotic wheelchair with a high-frequency steady-state visual evoked potential based brain–computer interface. *Med. Eng. Phys.* **2013**, *35*, 1155–1164.
36. Edelman, B.J.; Meng, J.; Suma, D.; Zurn, C.; Nagarajan, E.; Baxter, B.S.; Cline, C.C.; He, B. Noninvasive neuroimaging enhances continuous neural tracking for robotic device control. *Sci. Robot.* **2019**, *4*, doi: 10.1126/scirobotics.aaw6844
37. Xu, Y.; Ding, C.; Shu, X.; Gui, K.; Bezsudnova, Y.; Sheng, X.; Zhang, D. Shared control of a robotic arm using non-invasive brain–computer interface and computer vision guidance. *Rob. Auton. Syst.* **2019**, *115*, 121–129.
38. Padfield, N.; Zabalza, J.; Zhao, H.; Masero, V.; Ren, J. EEG-Based Brain-Computer Interfaces Using Motor-Imagery: Techniques and Challenges. *Sensors* **2019**, *19*, doi:10.3390/s19061423
39. Perdikis, S.; Tonin, L.; Saeedi, S.; Schneider, C.; Millán, J. del R. The Cybathlon BCI race: Successful longitudinal mutual learning with two tetraplegic users. *PLOS Biol.* **2018**, *16*, doi:10.1371/journal.pbio.2003787
40. Ahn, M.; Ahn, S.; Hong, J.H.; Cho, H.; Kim, K.; Kim, B.S.; Chang, J.W.; Jun, S.C. Gamma band activity associated with BCI performance: simultaneous MEG/EEG study. *Front. Hum. Neurosci.* **2013**, *7*, doi:10.3389/fnhum.2013.00848
41. Szczuko, P. Real and imaginary motion classification based on rough set analysis of EEG signals for multimedia applications. *Multimed. Tools Appl.* **2017**, *76*, 25697–25711.
42. Van Benthem, K.D.; Cebulski, S.; Herdman, C.M.; Keillor, J. An EEG Brain–Computer Interface Approach for Classifying Vigilance States in Humans: A Gamma Band Focus Supports Low Misclassification Rates. *Int. J. Human–Computer Interact.* **2018**, *34*, 226–237.
43. Herrmann, C.S.; Munk, M.H.J.; Engel, A.K. Cognitive functions of gamma-band activity: memory match and utilization. *Trends Cogn. Sci.* **2004**, *8*, 347–355.
44. Nowak, M.; Zich, C.; Stagg, C.J. Motor Cortical Gamma Oscillations: What Have We Learnt and Where Are We Headed? *Curr. Behav. Neurosci. reports* **2018**, *5*, 136–142.
45. van Deursen, J.A.; Vuurman, E.F.P.M.; Verhey, F.R.J.; van Kranen-Mastenbroek, V.H.J.M.; Riedel, W.J. Increased EEG gamma band activity in Alzheimer's disease and mild cognitive impairment. *J. Neural Transm.* **2008**, *115*, 1301–1311.
46. Başar, E.; Femir, B.; Emek-Savaş, D.D.; Güntekin, B.; Yener, G.G. Increased long distance event-related gamma band connectivity in Alzheimer's disease. *NeuroImage Clin.* **2017**, *14*, 580–590.
47. Yamamoto, T.; Sugaya, N.; Siegle, G.J.; Kumano, H.; Shimada, H.; Machado, S.; Murillo-Rodriguez, E.; Rocha, N.B.; Nardi, A.E.; Takamura, M.; et al. Altered Gamma-Band Activity as a Potential Biomarker for the Recurrence of Major Depressive Disorder. *Front. Psychiatry* **2018**, *9*, doi:10.3389/fpsyt.2018.00691
48. Baradits, M.; Kakuszi, B.; Bálint, S.; Fullajtár, M.; Mód, L.; Bitter, I.; Czobor, P. Alterations in resting-state gamma activity in patients with schizophrenia: a high-density EEG study. *Eur. Arch. Psychiatry Clin. Neurosci.* **2019**, *269*, 429–437.
49. Oldfield, R.C. The assessment and analysis of handedness: the Edinburgh inventory. *Neuropsychologia* **1971**, *9*, 97–113.
50. Herrmann, C.S.; Demiralp, T. Human EEG gamma oscillations in neuropsychiatric disorders. *Clin. Neurophysiol.* **2005**, *116*, 2719–33.
51. Oostenveld, R.; Fries, P.; Maris, E.; Schoffelen, J.-M. FieldTrip: Open source software for advanced

analysis of MEG, EEG, and invasive electrophysiological data. *Comput. Intell. Neurosci.* **2011**, *2011*, doi:10.1155/2011/156869

52. Fitzgibbon, S.P.; Lewis, T.W.; Powers, D.M.W.; Whitham, E.W.; Willoughby, J.O.; Pope, K.J. Surface Laplacian of central scalp electrical signals is insensitive to muscle contamination. *IEEE Trans. Biomed. Eng.* **2013**, *60*, 4–9.
53. Willems, R.M.; Toni, I.; Hagoort, P.; Casasanto, D. Body-specific motor imagery of hand actions: neural evidence from right- and left-handers. *Front. Hum. Neurosci.* **2009**, *3*, doi:10.3389/neuro.09.039.2009
54. Zapała, D.; Zabielska-Mendyk, E.; Augustynowicz, P.; Cudo, A.; Jaśkiewicz, M.; Szewczyk, M.; Kopiś, N.; Francuz, P. The effects of handedness on sensorimotor rhythm desynchronization and motor-imagery BCI control. *Sci. Rep.* **2020**, *10*, doi:10.1038/s41598-020-59222-w
55. Pfurtscheller, G.; Lopes da Silva, F.H. Event-related EEG/MEG synchronization and desynchronization: basic principles. *Clin. Neurophysiol.* **1999**, *110*, 1842–1857.
56. Jeannerod, M.; Decety, J. Mental motor imagery: a window into the representational stages of action. *Curr. Opin. Neurobiol.* **1995**, *5*, 727–732.
57. Mannan, M.M.N.; Kamran, M.A.; Jeong, M.Y. Identification and Removal of Physiological Artifacts From Electroencephalogram Signals: A Review. *IEEE Access* **2018**, *6*, 30630–30652.
58. Saini, M.; Payal; Satija, U. An Effective and Robust Framework for Ocular Artifact Removal From Single-Channel EEG Signal Based on Variational Mode Decomposition. *IEEE Sens. J.* **2020**, *20*, 369–376.
59. Chavez, M.; Grosselin, F.; Bussalb, A.; De Vico Fallani, F.; Navarro-Sune, X. Surrogate-Based Artifact Removal From Single-Channel EEG. *IEEE Trans. Neural Syst. Rehabil. Eng.* **2018**, *26*, 540–550.